ALMA MATER STUDIORUM
UNIVERSITY OF BOLOGNA

Phylosophy Doctoral Program in Electronics, Computer Science and Telecommunications

Department of Electrical, Electronic, and Information Engineering
"Guglielmo Marconi"

Cicle XXV

Settore concorsuale: 09/F2 - TELECOMUNICAZIONI

Settore scientifico disciplinare: ING-INF/03 - TELECOMUNICAZIONI

SPECTRUM SENSING ALGORITHMS FOR COGNITIVE RADIO APPLICATIONS

Ph. D. Candidate:
ANDREA MARIANI

Advisors:
Prof. Dr.
MARCO CHIANI
Dr.
ANDREA GIORGETTI

Ph. D. Program Coordinator:
Prof. Dr.
ALESSANDRO
VANELLI-CORALLI

FINAL EXAM 2013

It works! It works!
I finally invented something that works!
Dr. Emmett Brown

ADC analog to digital converter

AWGN additive white Gaussian noise

CDF cumulative distribution function

c.d.f. cumulative distribution function

CR cognitive radio

DAA detect and avoid

DFT discrete Fourier transform

DVB-T digital video broadcasting – terrestrial

ECC European Community Commission

FCC Federal Communications Commission

FFT fast Fourier transform

GPS Global Positioning System

i.i.d. independent, identically distributed

IFFT inverse fast Fourier transform

MB multiband

MC multicarrier

MF matched filter

MI mutual information

MIMO multiple-input multiple-output

MRC maximal ratio combiner

MMSE minimum mean-square error

OFDM orthogonal frequency-division multiplexing

p.d.f. probability distribution function

PAM pulse amplitude modulation

PSD power spectral density

PSK phase shift keying

QAM quadrature amplitude modulation

QPSK quadrature phase shift keying

r.v. random variable

R.V. random vector

SNR signal-to-noise ratio

SS spread spectrum

TH time-hopping

ToA time-of-arrival

UWB ultrawide band

UWB Ultrawide band

WLAN wireless local area network

WMAN wireless metropolitan area network

WPAN wireless personal area network

WSN wireless sensor network

ML maximum likelihood

GLR generalized likelihood ratio

GLRT generalized likelihood ratio test

LLRT log-likelihood ratio test

LRT likelihood ratio test

P_{EM} probability of emulation, or false alarm

P_{MD} probability of missed detection

P_D probability of detection

P_{FA} probability of false alarm

ROC receiver operating characteristic

AGM arithmetic-geometric mean ratio test

AIC Akaike information criterion

BIC Bayesian information criterion

BWB bounded worse beaviour

CA-CFAR cell-averaging constant false alarm rate

CAIC consistent AIC

CAICF consistent AIC with Fisher information

CFAR constant false alarm rate

CDR constant detection rate

CP cyclic prefix

CPC cognitive pilot channel

CL centroid localization

CSCG circularly-symmetric complex Gaussian

d.o.f. degrees of freedom

DC distance based combining

DSM dynamic spectrum management

DSA dynamic spectrum access

DTV digital television

ECC European Communications Committee

ED energy detector

EDC efficient detection criterion

EGC equal gain combining

EME energy to minimum eigenvalue ratio

ENP estimated noise power

ERC European Research Council

ES-WCL energy based selection WCL

EU European Union

ExAIC exact AIC

ExBIC exact BIC

FIM Fisher information matrix

GLRT generalized likelihood ratio test

HC hard combining

HF hard fusion

ITC information theoretic criteria

K-L Kullback-Leibler

LR likelihood ratio

LS least square

MDL minimum description length

MET ratio of maximum eigenvalue to the trace

ML maximum likelihood

MTM multi taper method

MME maximum to minimum eigenvalues ratio

NP Neyman-Pearson

p.d.f. probability distribution function

OFCOM Office of Communications

OSA opportunistic spectrum access

OSF oversampling factor

PMSE programme making and special events

PU primary user

PWCL power based WCL

r.o.f. roll-off factor

RAN Regional Area Network

RMSE root mean square error

RWCL relative WCL

RSS received signal strength

SC soft combining

SCM sample covariance matrix

SCovM sample covariance matrix

SCorM sample correlation matrix

SDR software defined radio

SF soft fusion

SP sensing period

SS spectrum sensing

SSE signal subspace eigenvalues

SU secondary user

TOA time of arrival

TDOA time difference of arrival

TVBD TV Bands Device

TS-WCL two step WCL

WCL weighted centroid localization

WSD white space device

WSN wireless sensor network

WSS wideband spectrum sensing

Abstract

Future wireless communications systems are expected to be extremely dynamic, smart and capable to interact with the surrounding radio environment. To implement such advanced devices, cognitive radio (CR) is a promising paradigm, focusing on strategies for acquiring information and learning. The first task of a cognitive systems is spectrum sensing, that consists the analysis of the radio frequency spectrum. In particular, CR has been mainly studied in the context of opportunistic spectrum access, in which secondary devices are allowed to transmit avoiding harmful interference to higher priority systems, called primary users. Thus cognitive nodes must implement signal detection techniques to identify unused bands for transmission.

In the present work, we study different spectrum sensing algorithms, focusing on their statistical description and evaluation of the detection performance. Moving from traditional sensing approaches we consider the presence of practical impairments, such as parameter uncertainties, and analyze algorithm design. Far from the ambition of cover the broad spectrum of spectrum sensing, we aim at providing contributions to the main classes of sensing techniques, from basic energy detection, to cooperative eigenvalue based algorithms, to wideband approaches, touching also simple localization strategies for CR networks. In particular, in the context of energy detection we studied the practical design of the test, considering the case in which the unknown noise power is estimated at the receiver. This analysis allows to deepen the phenomenon of the SNR wall, providing the conditions for its existence. This work highlight that the presence of the SNR wall is determined by the accuracy of the noise power estimation process. In the context of the eigenvalue based detectors, that can be adopted by multiple sensors systems, we studied the practical situation in presence of unbalances in the noise power level at the receivers. In this context we studied the design of the decision threshold providing a statistical description of the tests based on a moment matching approach. Then, we shift the focus from single band detectors to wideband sensing, proposing a new approach based on information theoretic criteria to distinguish occupied from unoccupied frequency

bands. This technique is blind and, requiring no threshold setting, can be adopted even if the statistical distribution of the observed data in not known exactly. In the last part of the thesis we move from signal detection and analyze some simple cooperative localization techniques based on weighted centroid strategies.

Acknowledgement

This achievement would not have been possible without the help and support of many people, and this is an attempt to say thank you to them all.

First, I would like to thank my advisor, Prof. Marco Chiani. It has been an invaluable opportunity to have him as a mentor, for his guidance, his willingness, for pushing me to aim high, and teaching me the love for doing things well and passion for research. A special thank to my co-advisor Andrea Giorgetti, for his guidance, his support and for being an example in doing research and working hard. I would like to thank all the telecommunications group guys at the University of Bologna, Cesena campus, for making this a wonderful working place, starting from my Ph.D. fellows, Nico, for our friendship across the oceans, Simone, Vincenzo, Anna and Stefano, and also Matteo, Enrico and Prof. Davide Dardari. A special thank to Guido for all we shared in these intense ten years. I would like to thank Prof. Sithamparanathan Kandeepan, who allowed me to visit him at the Royal Melbourne Institute of Technology and for the fruitful research collaboration that we are carrying on. Thanks to whom made me feel welcome in Melbourne, to Ester and the guys from the St. Francis Youth Choir.

Un grazie a tutte quelle persone che mi hanno sostenuto e accompagnato in questi anni. Alla mia famiglia, ai miei genitori per tutti i doni e la pazienza, all' Eli che non la ritroviamo più il sabato mattina, a Lori che continua a lottare, a Tommy, Filo, gli zii e le nonne che mi seguono dall'alto. Al mio gruppo scout e in particolare al buon Giovanni Look-crazy e i ragazzi del clan Le Rapide di Montiano per la strada fatta insieme, al coro Musica Enchiriadis per la passione, il divertimento e per l'avermi fatto riscoprire la musica in una veste nuova. Un grazie particolare a Francesca per l'amicizia e lo stupirci insieme delle strade che continuiamo a percorrere, e a Mirko per l'esempio, per l'amore per le cose belle e per il consigliarmi le vere amicizie. Grazie a Benedetta per questi anni avventurosi ed entusiasmanti, e senza la quale il mio domani non apparirebbe così avvincente.

Contents

Chapter 1

Introduction

1.1 Towards a more efficient use of the spectrum

In the last ten years opportunistic unlicensed spectrum radio assess strategies have gained an increasing interest both in the academia and industries. This fact has been driven by two aspects: the so called *spectrum scarcity* problem and the attempt to reach a more *efficient utilization* of the spectrum resources.

Today we are experiencing an exponential proliferation of wireless devices and an increasing demand for wireless data capacity, and the traffic demand forecasts confirm this trend in the next few years [1, 2]. For example, in Fig. 1.1 we report the CISCO forecasts for the total and the mobile traffic demand till 2016 [3]. We can see that by 2016 the total traffic is expected to be three times larger than 2011, and this growth in proportion is more evident considering only the mobile traffic that is expected to be 14 times larger (which means an annual increment of 70%) growing from 520 PB per month to almost $7,5$ EB per month. Similar predictions can be found in [4,5]. These growth forecasts makes us wonder about the availability of sufficient spectrum to sustain such an enormous demand of wireless traffic. Indeed on the basis of the observation of the frequency allocation charts we can see that most of the useful radio spectrum has been already allocated [6, 7], thus the problem of spectrum scarcity is a realistic problem in modern wireless communications. The simplest and more traditional way to face this "capacity crunch" problem is the re-organization of the frequency allocation, providing more spectrum to the key services that lead the traffic demand growth. This is the case, for example, of the mobile broadband services for which the allocation of new spectrum is planned within the next five years in the USA [4]. Also in

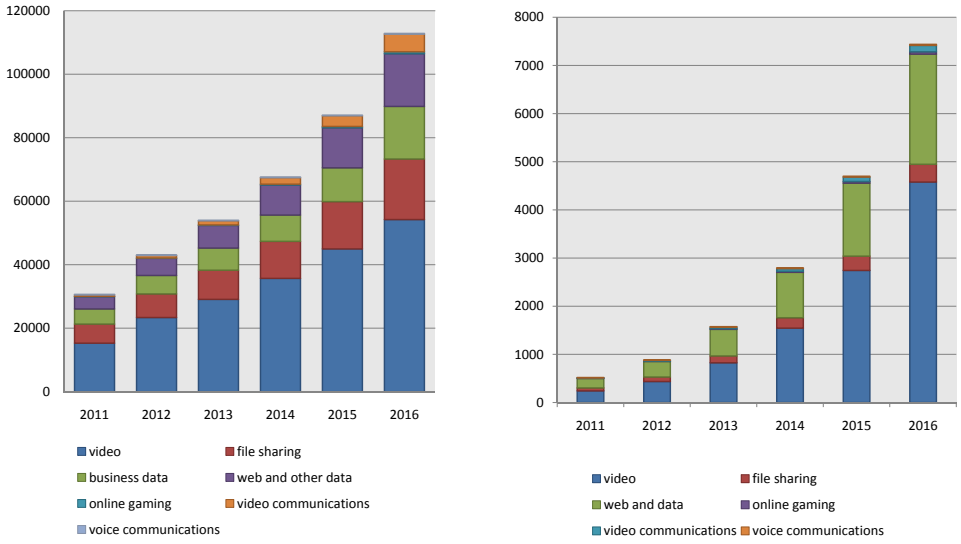

(a) Total

(b) Mobile

Figure 1.1: Traffic forecast in PB/month, CISCO VNI Feb. 2013 [3].

European Union (EU) since 2010 part of the digital divided in the 800 MHz band has been devoted to mobile systems in an harmonized manner [8], and UK will extend mobile broadband also to the 700 MHz band, reallocating the digital television (DTV) services [9].

However, in spite of the nominal absence of available spectrum, measurements of the radio frequency occupation indicate that large portions of the licensed bands are not used for significant periods of time [10]. This suggests that reallocation of spectrum bands to data services is only a part of the answer to the capacity crunch, since it reveals that behind the current spectrum scarcity problem the main issue is an inefficient use of the spectrum resources. Therefore one of the main objectives in the design of future wireless communication systems must be a more efficient use of the frequency spectrum.

1.2 Opportunistic spectrum access

A more efficient utilization of the spectrum can be reached through the adoption of flexible devices, able to analyze the surrounding radio environment, discover unused spectrum resources and use them without interfering higher priority users, called primary users (PUs). These actions describe the essential characteristics of the so called opportunistic spectrum access (OSA),

where users with a lower priority, named secondary users (SUs), "adopt dynamic spectrum access (DSA) techniques to exploit spectral opportunities"[1] [12]. The expression "spectral opportunities" can be generally used to indicate situations in which the SUs have some occasion to transmit. In this work, as in most of the cognitive radio (CR) literature, a spectral opportunity will indicate in particular the presence of a portion of spectrum that is temporarily or locally unused. These unoccupied bands are often referred as *spectrum holes* or *white spaces*[2]. This acceptation is related to the so called "interweave" approach to secondary access[3].

The OSA techniques have been studied in particular in the context of CR. The concept of CR has been defined for the first time by Mitola as a

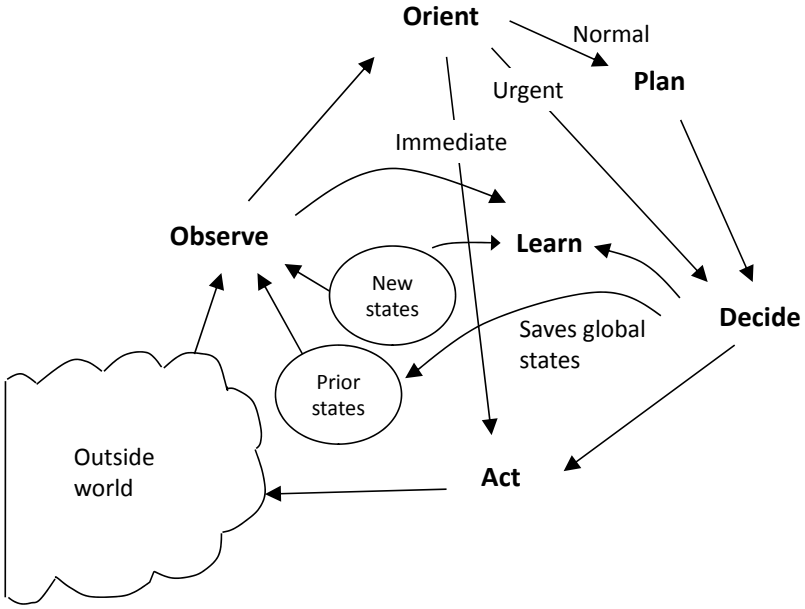

Figure 1.2: The cognitive cycle [13].

radio system whose behavior is described by the cognitive cycle depicted in

[1]The SUs are unlicensed or light-licensed users; in the former case the expression "opportunistic unlicensed access" is often used [11].

[2]The expression "white space" is mainly used with reference to DTV bands.

[3]Other possible strategies are the "underlay" approach, adopted by low spectral density transmissions such as ultrawide band (UWB) communications, and the "overlay" technique in which the SUs compensate the interference caused to the PUs supporting their transmissions adopting for example relaying strategies.

Fig. 1.2 [13]. Recently ITU provided a definition of the CR system as "a radio system employing technology that allows the system to obtain knowledge of its operational and geographical environment, established policies and its internal state; to dynamically and autonomously adjust its operational parameters and protocols according to its obtained knowledge in order to achieve predefined objectives; and to learn from the results obtained" [14]. Then we can identify three main key characteristics of CR systems [15]:

- capability to obtain knowledge;
- capability to dynamically and autonomously adjust its operational parameters and protocols;
- capability to learn.

Note that the feature that distinguish CR from DSA systems is essentially the *learn* step that provide great benefits for OSA systems, such as the ability to recognize PUs activity pattern and predict their behavior, to perceive channel state features and act on the basis of previous experience, to foresee interference levels, etc.. Therefore current OSA research is oriented to the study and implementation of cognitive systems. Mitola's cognitive cycle has been reformulated in terms of dynamic spectrum management (DSM) in [16] (see Fig. 1.3).

In order to implement CR devices for OSA the main technological requirements are given by flexible, fast and easily reprogrammable hardware, and proper signal processing algorithms that implement the cognitive functions, such as spectrum sensing and spectrum shaping algorithms, spectrum management strategies, decision and learning techniques, etc..

With regard to the hardware aspects, today we can benefit of so called software defined radios (SDRs) that is a radio equipment designed "trying to push the analog to digital converter (ADC) as close as possible to the antenna", in order to define most of the radio chain components via software. This approach is today possible thanks to modern developments in ADCs and fast electronic circuits. It offers a very high flexibility, allowing most of the parameters to be changed dynamically avoiding excessive time consumption and additional costs [17]. In contrast to traditional radio systems, generally designed to support a particular communication standard, SDRs can potentially allow to change dynamically the standard simply modifying the software that implements its transmit and receive chains.

With regard to the algorithms that implement CR/OSA functions we can say that today all the cognitive functions have been proposed by the research community and are subject to further investigations with an increasing interest [18–20].

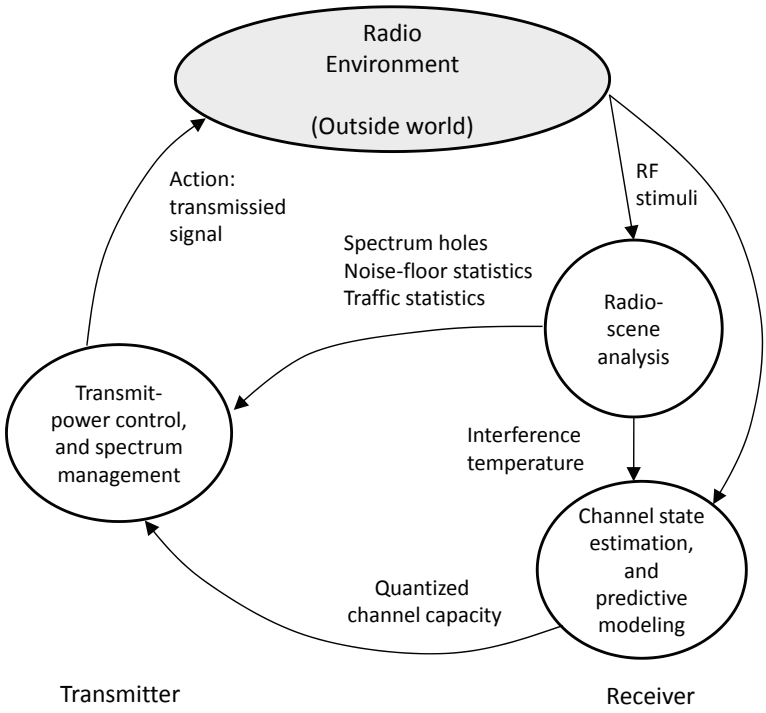

Figure 1.3: DSM reformulation of the cognitive cycle [16].

Also from a practical implementation point of view many CR testbeds have been developed [21, 22].

1.2.1 Current OSA Regulations and Standardizations

In addition to the technological implementation issues, the implementation of CR/OSA systems must be enabled by in second place communications regulatory bodies first and by standardization activities.

Some regulations related to CR systems have been formulated in the last few years, focusing mainly on opportunistic access to white spaces in the television VHF and UHF bands. This interest is related in particular to the great propagation characteristic of these bands, and the relatively predictable spatiotemporal usage of the main services that use them. Unlicensed access to the TV white space has been allowed in the USA first [23], followed by countries such as Canada [24] and, with some limitiations, Japan and Australia [25, 26]. Regulation studies are ongoing in Europe and other countries [6].

The standardization activities related to CR/OSA systems are currently under development on all levels of a CR systems. In Table 1.1 we report a summary of the main standardization activities in the last few years. In particular standards related to the TV white spaces attracted lots of attention. In this context the first standard developed is ECMA 392 [27, 28]. Among the IEEE activities the most popular are the IEEE 802.22 standard for TV white spaces wireless Regional Area Networks (RANs) operations [29] and the IEEE 802.11af (also called "White-Fi") that currently has not been released yet. Other standardization activities are under development by ITU and ETSI [15, 30, 31].

1.2.2 Implementing the "observe" step

In OSA systems, the SUs must implement strategies to acquire information from the radio environment in order to identify ongoing licensed transmissions and preserve them [32]. This corresponds to the "observe" CR step in OSA. The main task of this stage consists in identifying which channels are available for opportunistic transmissions, that is equivalent to a PU detection problem. Secondly, it can be useful to acquire some additional information, such as some characteristic of the identified signals, interference measurements, etc.. In literature mainly three solutions have been proposed [11]:

- Geolocation databases;
- Beacon signals.
- Spectrum sensing;

The geolocation database solution is based on the consultation by the SU network of a database that stores the information on the spectral occupancy in the nodes locations. The advantages of this approach are that it is virtually error free and is not affected by radio channel characteristics. However it is a quite expensive solution. Indeed the secondary nodes require to incorporate some location technique (such as GPS) Internet connection in order to access the database information. Moreover, additional costs that must be considered are the costs related to the design and implementation of the database, and the costs for gather the PU occupancy information.

The beacon based approach consists in the adoption of a beacon signal that is broadcasted to the secondary nodes providing the PU occupancy information. This solution has a very high infrastructural cost, requiring also some modifications of the current licensed systems. However, some CR networks implementations foresee the adoption of a cognitive pilot channel

IEEE 802.11af	Wireless LAN: TV white spaces operation	on going
IEEE 802.11y	Wireless LAN: 3650-3700 MHz operation in USA	Nov. 2008
IEEE 802.19.1	TV white space coexistence methods	on going
IEEE 802.22	Wireless RAN: Policies and procedure for operation in the TV bands	Jul. 2011
IEEE 802.22.1	Enhancing harmful interference protection	Nov. 2010
IEEE 1900.1	Definitions and concepts for dynamic spectrum access	Sep. 2008
IEEE 1900.1a	Amendment: addition of new terms and definitions	Feb. 2011
IEEE 1900.2	Practice for the analysis of in-Band and adjacent band interference	Jul. 2008
IEEE 1900.4	Architecture for optimized radio resource usage in heterogeneous wireless access networks	Feb. 2009
IEEE 1900.4.1	Interfaces and protocols for dynamic spectrum access networks in white space frequency bands	on going
IEEE 1900.4a	Architecture and interfaces for dynamic spectrum access networks in white space frequency bands	on going
IEEE 1900.5	Policy language requirements and architectures	on going
IEEE 1900.6	Spectrum sensing interfaces and data structures	Apr. 2011
IEEE 1900.6a	Amendment: procedures, protocols, and data archive enhanced interfaces	on going
IEEE 1900.7	Radio interface supporting fixed and mobile operation	on going
ECMA 392	MAC and PHY for operation in TV white space	Dec. 2009

Table 1.1: Current CR standardization.

(CPC) to support cognitive operations such as spectrum allocation [33]. This dedicated channel could be adopted also to convey sensing information among the SU nodes.

Spectrum sensing in defined by IEEE as the "The action of a radio measuring signal features" [12]. It consists therefore in the implementation of an autonomous process of the SUs, that on the basis of the received signals analyze the spectrum. It offers the advantage of no infrastructural costs nor modifications in the licensed systems. Moreover, it makes the SU network completely autonomous and capable of a reactive behaviour. The SU nodes implementation costs depend on the algorithms adopted. The main disadvantages of spectrum sensing (SS) is the fact that its behaviour is generally related to some tradeoffs between performance (e.g. detection rate) and observation time, and the fact that it can suffer adverse radio channel characteristic, leading to the hidden node problem [19, 34]. The choice of the proper technique to be adopted depends on the particular OSA problem we are studying. In particular the characteristics of the PUs (such as their dynamics, bandwidth and power) are the most important features to be considered for choosing the proper strategy. Indeed the adoption of geolocation database fits particularly with highly predictable PUs such as TV signals, that are continuous transmissions broadcasted from known locations. In this case, to evaluate the presence of a TV signal could be sufficient for example to enquire a database on a daily basis. Spectrum sensing instead is the most promising solution for unpredictable signals that transmit from unknown locations such as programme making and special events (PMSE) signals (like wireless microphones).

1.2.3 Sensing in the TV white spaces

In the context the TV white spaces, FCC recently decided to choose in favor of the geolocation database approach leaving the implementation of detection algorithms as an optional feature [35]. This decision comes from some studies on the minimum sensitivity required at the secondary nodes in order to ensure DTV and PMSE signal protection in the worst propagation conditions. This analysis demonstrated that common sensing approaches do not guarantee the detection performance required, leaving the implementation of sensing algorithms as an optional feature [35]. However this decision seems to be moved more by the willing to come up with a regulation on white space devices (WSDs) in a short time, enabling companies to access the white space market rather than a definitive mistrust in SS strategies. Indeed the Federal Communications Commission (FCC) states that [35]

Specifically, we are taking the following actions:

...

- TV Bands Devices (TVBDs)
  ◦ Eliminating the requirement that TV bands devices that incorporate geo-location and database access must also listen (sense) to detect the signals of TV stations and low power auxiliary service stations (wireless microphones).

...

While we are eliminating the sensing requirement for TVBDs, we are encouraging continued development of this capability because we believe it holds promise to further improvements in spectrum efficiency in the TV spectrum in the future and will be a vital tool for providing opportunistic access to other spectrum bands.

Then, while eliminating SS as a mandatory function, FCC strongly encourages research activities to make possible a sensing based WSDs second generation.
Also the Office of Communications (OFCOM) in the UK expressed a similar viewpoint [36]:

> As a result we propose to allow detection alone as well as geolocation. However, we note that implementation of detection-only devices is likely many years away and hence there is little advantage in rapidly making the necessary regulations to licence-exempt such devices.
>
> ...
>
> We conclude from the responses that the most important mechanism in the short to medium term will be geolocation.

In Europe, the European Communications Committee (ECC) came to the same conclusion in [37], on the basis of single user sensing algorithms. Studies on cooperative spectrum sensing are currently under investigation (see e.g. [38]). The ECC also suggests the potential benefit in using a combination of sensing and geolocation database to provide adequate protection to digital TV receivers [37].

In conclusion, in the next few years we expect the borne of the first generation of WSDs, that probably will be based on geolocation implementation

being the adoption of SS algorithms not mandatory. In spite of this fact, the research community is motivated anyway to continue the investigation in new sensing algorithms with the first aim to propose new algorithms with higher detection performances. The most promising approaches consist in advanced techniques based on cooperation among SUs or multiple antennas WSDs, that currently has not been deeply analyzed by regulatory bodies and that deserve more attention in the definition of future rules. Moreover a secondary system that is based on geolocation databases can adopt OSA strategies, but cannot be considered properly a cognitive system, due to the lack in autonomy and reactivity to the environment that characterize the original Mitola's proposal and that only SS can provide. Another important point is that beyond PU protection the sensing task has an important role in supporting higher level cognitive functionalities such as resource allocation and spectrum efficiency [39, 40].

1.3 Overview of spectrum sensing algorithms

In this section we present an overview the main algorithms proposed for SS. In general it is not simple to provide a unique classification of the sensing techniques, especially because there are lots of possible approaches and many algorithms can be included in more than one class. We choose in particular to adopt a classification based on the algorithms practical requirements, defining the following four groups:

- Fundamental algorithms
  We include in this group the basic algorithms, typically proposed for the observation of a single band, by a single antenna receiver.

- Diversity based algorithms
  These algorithms require some kind of diversity to be implemented, such as multiple antennas or oversampling. We include in this class in particular the eigenvalue based algorithms.

- Wideband algorithms
  We include in this group algorithms that are suited for the analysis of multiple bands observations.

- Cooperative algorithms
  These algorithms are based on the adoption of multiple CR nodes.

1.3.1 Fundamental algorithms

Since five years ago, many papers dealing with CR introduced the sensing topic asserting that "sensing algorithms can be classified in energy detector, matched filter and cyclostationarity detector". Indeed these techniques are the very basic strategies that can be adopted in simple sensing problems, by simple receivers with a single antenna and the observation of a single band.

- Energy based detection
  The energy detector (ED) is the most simple and popular algorithm for signal detection. Its implementation consists in an estimate of the received power (as sum of the squared received samples) followed by a comparison with a decision threshold. Theoretically the ED is derived as the generalized likelihood ratio test (GLRT) for the detection of a deterministic unknown signal in additive white Gaussian noise (AWGN) or as a sufficient likelihood ratio (LR) statistic when the signal to be detected is described as a zero mean Gaussian process. Its statistic has been widely studied in literature (see e.g. [19, 41]) and due to its simplicity of implementation and analysis, currently it is with no doubts the standard sensing algorithm adopted for example in studies on higher level CR functionalities and also by regulatory bodies [37,42]. Frequency domain EDs have been also proposed [43,44]. The main impairment of the ED is the fact that its statistic depends on the noise power level, therefore its knowledge is required for setting the decision threshold according to the Neyman-Pearson (NP) approach [41,45,46]. In practical applications errors on the noise power level experienced can cause performance losses due to an inaccurate threshold setting and in some cases the rise of the so called SNR wall phenomenon, which is a minimum SNR level under which it is impossible to rich the desired probability of detection (P_D) and probability of false alarm (P_{FA}) [47–49]. Recent literature has often emphasized the problem of the SNR wall, giving little attention to the strategies to counteract it, such as how to design noise power estimators that allows to avoid the SNR wall. We will discuss this topic in detail in Chapter 2.

- Feature based detection
  When some additional knowledge on the signal to be detected is available, we can adopt detectors that exploit this information. In particular, the most common algorithms in this class are:

  – Autocorrelation based detectors
    This algorithms can be adopted when the autocorrelation of the

signal to be detected present some peculiar peaks. The most popular autocorrelation based algorithm is the cyclic prefix (CP) based algorithm for the detection of orthogonal frequency-division multiplexing (OFDM) signals [50–52].

- Waveform based detector
  If some portion of the primary signal is known, we can build a detector that exploits this knowledge, usually correlating the known feature with the received signal sequence. This can be the case, for example, of signals with known preamble or with some known pilot pattern [53]. The extreme case is the matched filter (MF) detection, that requires the knowledge of the complete signal sequence. Even if the MF detector is often cited in SS algorithm surveys, the assumption of perfect knowledge of the PU (and thus the adoption of the MF detector) is unrealistic in practical CR implementations [50–52].

- Cyclostationarity based detectors
  When a signal presents some periodicity in the autocorrelation function, this corresponds to the presence of some correlation in the frequency domain, called cyclostationary feature [54]. As for the autocorrelation features in the time domain, this property can be adopted for detecting PU signals. Many cyclostationary detectors algorithms have been proposed in past literature, usually based on the estimation of the cyclic autocorrelation function or the cyclic spectrum [55–58].

Feature based algorithms are generally used for detecting the presence of specific PU signals. Being suited for particular communication standards, while they are unable to evaluate the presence of different transmissions. The main practical impairment of these algorithms is the susceptibility to synchronization errors and frequency offsets, that imply the adoption of a synchronization stage [59]. We can consider therefore the feature based detectors as simplification of the PU signal receiver chain, that aims at detecting the presence of this transmission without the need of extracting the information symbols. It is also possible to built general purpose feature detectors, capable for example of identifying any possible autocorrelation peak or cyclostationary feature, however these algorithms are very expensive from a computational point of view, are time consuming and suffer of synchronization errors [56, 59].

1.3.2 Diversity based detectors

In this section we present some algorithms that can be adopted in presence of some diversity reception mechanism. We refer in particular to multiple antennas system that have been widely studied in current communications literature [60–63]. The same techniques can be also adopted when we are considering the detection of an oversampled signal. In this situation from the original sample sequence we can extract a number of sub sequences which number corresponds to the oversampling factor and use them as they were collected at different antennas [64]. The same algorithms can be also adopted in cooperative sensing system (see also Section 1.3.4 and Chapter 3). In all these case studies it is possible to compute the sample covariance matrix (SCM) of the received samples, which is a square matrix with order that equals the degree of diversity of the system. In order to identify the presence of PUs we can adopt threshold based tests which metrics are functions of the SCM. These algorithms are generally called "eigenvalue based algorithms". Alternative approaches are based on the information theoretic criteria (ITC).

- Eigenvalue based detectors
  The eigenvalue based algorithms are binary tests in which the decision metrics are functions of the eigenvalues of the SCM. They have attracted a lot of attention providing good performance results without requiring the knowledge of the noise power nor any prior information on the PU signals [65–69]. Considering the most general scenario, with possible multiple PUs, the GLRT is the so called sphericity test, well known in statistics literature and recently re-proposed with the name arithmetic-geometric mean ratio test (AGM) [65, 70]. Alternatively, in situations in which we expect to have a single PU, the GLRT is the ratio of maximum eigenvalue to the trace (MET) [69]. Others metrics have been also proposed, such as the maximum to minimum eigenvalues ratio (MME) [66]. Recently also the case in which multiple antennas are uncalibrated have been considered [68, 71].

- ITC based detectors
  A different approach for the detection of PU signals is to estimate the dimension of the observed sample set. If it contains only the noise the eigenvalues of the SCM are all equal to the noise power σ^2; otherwise it will contain some eigenvalue greater than σ^2. This problem can be formulated as a model order selection problem, in which the order of the model is the number of eigenvalues of the SCM, and it can be solved by means of ITC [72]. If the estimated model order is greater than zero, it means that at least one PU has been detected [73, 74]. Mainly Akaike

information criterion (AIC) and minimum description length (MDL) has been adopted [73,74]. This approach allows to implement detectors that do not need to set a decision threshold. Note that this implies that we cannot control the tradeoff between false alarm and detection probabilities of the algorithm.

1.3.3 Wideband algorithms

Although most of the sensing algorithms has been conceived as single band detectors, wideband SS allows a better knowledge of the surrounding radio environment. Wideband SS consists in a joint observation of multiple frequency bands and joint decision on the occupancy of each subband. It allows therefore to acquire a more complete observation, avoiding time consuming sequential scan of the spectrum. Its applicability is therefore primarily related to hardware constraints. In CR many approaches have been proposed, starting form "multiband sensing" approaches, that consists simply in dividing the observed band in multiple subchannels. The most common solutions are based on spectral estimation techniques, in addition to some knew approaches such as compressive sensing. Here we include also ITC based wideband sensing, that will be described with more detail in Chapter 4.

- Detectors based on spectral estimation
  The scope of spectral analysis os to provide a reliable estimate of the energy distribution in the frequency domain, thus it has a big impact of the environment awareness of the SUs. In CR context non parametric techniques are the more suitable strategies because they do not require any assumptions on the received signal (except the stationarity assumption within the observation time) and thus do not require the estimation of any parameters. These approaches in general are constituted by a spectrum estimation stage followed by the adoption of some metric to evaluate the occupancy of each frequency component. The starting point of such techniques is the classical non parametric spectrum estimation theory, based on the periodogram and their derivatives, such as the Welch's periodogram. The most advanced spectrum estimation approach in this context is the multitaper method [75–77]. Also advanced filter design strategies can be adopted, such as filter banks approaches [78, 79]. If the SUs know the power spectral density to be detected, the optimum detector in signal-to-noise ratio (SNR) regimes assumes the structure of an estimator-correlator [80].

- Compressive sensing
  Compressive sampling is a special signal processing technique that can

be applied to signals with a sparse representation. In the context of CR it can be adopted in particular in situations in which the PU signal occupancy is sparse in the frequency domain, exploiting techniques known as compressive sensing. The main advantage of these techniques is that they allow to analyze a large portion of spectrum without the requirement of an high sampling rate. [81]

- Wideband ITC
  The wideband sensing problem can be formulated as a model order selection problem, in which the model of the order is the number of frequency bins considered. Then the joint detection of frequency components can be performed using ITC, that are commonly adopted for model order selection [82]. A general formulation of this approach is provided in detail in Chapter 4.

1.3.4 Cooperative algorithms

A very promising solution for improving the sensing performance of the SU networks is to exploit cooperation among the secondary nodes. In particular cooperative strategies, exploiting the SUs spatial diversity, can be adopted to counteract the channel effects such as multipath and shadowing, that cause the hidden node problem [19, 34]. Cooperative SS has reached an increasing attention in the last few years, and many different schemes have been proposed. A survey of cooperative sensing techniques can be found in [83]. There are many issues that must be addressed in the design of a cooperative SS strategy. We refer to [83] and the references therein for an extended overview. The main requirement is related to the availability of channels for sensing signaling among the SUs, that in most of the literature studies is a fixed control channel. In the following we provide a brief classification to highlight their main characteristics.

Cooperative algorithms can be classified on the basis of how SUs share their sensing data in the network and in which point of the network the final decision is taken. We have basically two approaches, the centralized and the distributed[4]. Also mixed strategies can be adopted.

- Centralized cooperative sensing
  In centralized cooperative strategies the sensing information from all the SUs are reported to a central identity, called *fusion center*, that combines them and takes the global decision. Then this information

[4]Note that in some works the term "distributed" is used as a synonym of cooperative, and expression such as "non-centralized" are adopted.

must be sent back to the SUs by means for example of broadcasting [19, 83].

- Distributed cooperative sensing
  Distributed schemes differs from centralized ones for the absence of a specific fusion center. In this case indeed the SUs communicate among themselves and converge to a unified decision. This process can be performed in an iterative way. In this scheme therefore the final decision is taken by each SU on the basis of a common decision policy [83].

- Mixed strategies
  Besides the centralized and distributed approaches, some mixed strategies can be adopted. For example, a relay assisted cooperative scheme can be adopted in cases in which some SUs experience a weak report channel and the remainders can be used for forwarding their sensing results to the fusion center [83]. Another solution is the clustered sensing scheme, in which clusterheads act as second level fusion centers, collecting the sensing results from the SUs within their cluster. Then this data can be shared among other clusterheads or can be forwarded to the fusion center. An example of cluster based cooperative sensing can be found in [42].

With respect to the data that are shared among the SUs, cooperative strategies can be divided in hard fusion and soft fusion schemes:

- Hard fusion schemes
  When the SUs share their local binary decisions on the presence of PUs, we talk about hard fusion schemes. Locally the SUs can adopt any of the single node sensing techniques described previously. These schemes are convenient for the minimum amount of data that must be exchanged among the secondary nodes. In this case the fusion strategies are typically linear fusion rules such as AND, OR and majority rules. Also Bayesian approaches can be adopted, such as the Chair-Varshney optimal fusion rule [19].

- Soft fusion schemes
  In place to the local binary decisions, the SUs can share a richer information, such as their likelihood ratios, in order to improve the sensing result. These schemes require therefore a larger secondary network capacity. Note that the amount of data to be shared depends of the metric chosen and its representation. For example, schemes very closed to hard combining, with only a two bit likelihood ratio representation, has

also been proposed [84]. Also in this case linear combining fusion are the most common strategies, such as the equal gain combining (EGC) and maximal ratio combiner (MRC) [84]. If the amount of data to be exchanged is not a problem, also algorithms that imply the transmission of all the SUs observations to the fusion center has been proposed. In this case eigenvalue based algorithms can be adopted also in the cooperative case [66, 85].

1.3.5 Spectrum sensing beyond signal detection

In CR literature the term sensing generally assumes the meaning of signal detection. The identification of the presence of PUs is with no doubts the most important functionality, required for detecting the presence of spectrum holes, and enabling PU protection. However generally speaking, the sensing functionality includes any kind of technique that allows the SUs to collect information from the radio environment that is useful to orient the CR network actions. In particular we emphasize three aspects: signal classification, estimation of the number of primary transmissions and PU localization.

Classification of PU signals can greatly improve CR functionalities. The first advantage is the identification of PUs, that is useful in particular in presence of other interferes[5]. In this case, when an occupied band is detected, general purpose detection algorithms, such as the ED, cannot distinguish between PUs and other transmissions, thus missing some spectrum opportunities. Note that considering PU identification, feature detectors (cyclostationarity based, autocorrelation based, etc.) can be considered classification algorithms. In the context of classification, another important aspect is PU features extraction, which can be adopted for example to support interference mitigation techniques. In particular, automatic modulation recognition algorithms has been developed both for civilian and military applications. An extended survey to these techniques can be found in [86].

In many CR scenarios SUs can experience the presence of multiple PUs signal sources. In this case, if the SUs are equipped with multiple antennas, spatial correlation can be exploited for detection purposes (as we mentioned with the diversity based algorithms) and for estimating the number of independent sources. In particular, non parametric methods that exploit the properties of the SCM can be adopted. A large sample based on ITC has been proposed in [72], while exact algorithms, based on the true distribution of the SCM have been proposed in [67].

Information about the PU position plays an important role allowing a

[5]These could be also malicious transmissions such as jammers in the military context.

better usage of the spectrum, avoiding and preventing harmful interference, making a better distribution of the radio resources in the spatial domain, aiding spectrum policy enforcement, etc. [19,87–89]. In chapter 5 we address some simple techniques to be adopted by cooperative SUs networks.

1.4 Thesis outline

Motivated by the fundamental role of spectrum sensing in enabling CR functionalities, in this dissertation we study sensing algorithms for spectrum holes detection. The analysis performed focuses both on the assessment of the detection performance and the statistical description of the algorithms, especially for threshold based algorithms. Far from the ambition of dealing with all the broad spectrum of SS algorithms, we aim at providing contributions to the main classes of sensing techniques, from basic energy detection, to cooperative eigenvalue based algorithms, to wideband approaches, touching also aspects of simple localization strategies for CR networks. In particular, the main contributions are:

- Chapter 2
  In Chapter 2 we analyze some fundamental aspects of energy detection, when noise power estimation techniques are adopted. Most of current literature has focused on the ED limitations in presence of noise uncertainty, emphasizing the phenomenon of the SNR wall as an unavoidable problem. Very little attention has been paid to the study of how this phenomenon can be counteracted in practical scenarios. We analyze the statistical properties of the ED, addressing the threshold design, describing its asymptotical behaviour and providing the conditions for the existence of the SNR wall. We prove that these conditions are related to the statistical properties of the noise power estimator, and in particular to the accuracy of the estimate. This analysis allows to foresee the appearance of the SNR wall or, in a design perspective, to orient the choice of the proper noise power estimator. We show how the analysis can be applied in CR systems where the ED is used for fast sensing.

- Chapter 3
  In the context of the eigenvalue based detection, in Chapter 3 we analyze two tests derived by the GLRT analysis. We apply this analysis in the cooperative SS scenario; note that the model adopted can be used for the multiple antennas scenario as well. The first test studied is the

sphericity test, derived assuming that all the nodes/antennas experience the same noise power level. Removing this assumption, that can be unrealistic in practical scenarios, the GLRT is the independence test. We address the statistical description of these tests, under the signal absent hypothesis, providing simple formulas for the derivation of the probability of false alarm and for setting the decision threshold under the NP framework. In particular, we approximate the tests as beta random variables (r.v.s) through a moment matching approach.

- Chapter 4
  Considering wideband sensing, in Chapter 4 we propose an ITC based approach for identifying which portions of such band contain only noise. We provide a general formulation of this technique valid for all spectral representations of the observed band. Then we specialize the study for the case in which a simple discrete Fourier transform (DFT) is adopted at the secondary node receiver. We adopt both the simple approach that considers only the power level in each frequency component and a new approach that jointly exploit spectral correlation and received energy to discern signals from noise in a blind way. The proposed algorithms do not require neither the knowledge of the noise power nor any a priori information about the number and the characteristics of the signals to be detected. Numerical results reveal that the algorithm proposed outperforms simple ED approaches to wideband sensing, especially in the presence of spectral correlation.

- Chapter 5
  Motivated by the fact that localizing the PU can be very helpful for many functional tasks of a CR system, in Chapter 5 we analyze the performance of weighted centroid localization (WCL) strategies, that are very promising thanks to their simplicity of implementation and computation and the fact that do not require any knowledge on the PU signal. In particular, we analyze the adoption of different weighting strategies, studying the dependence of the root mean square error (RMSE) on the PU position within the area considered, and identifying which strategies are more robust to situations in which the PU moves toward the side of the area. Two secondary user (SU) selection strategies are also proposed to alleviate the border and noisy measurements effects in harsh propagation environments.

1.5 Contribution

This thesis is the result of the work carried out within the telecommunications group of the Department of Electrical and Information Engineering "Guglielmo Marconi" of the University of Bologna, Cesena campus. The dissertation is based on original publications in international journals and conferences. The study of the effect of noise power estimation, that can be found in Chapter 2, has been presented in part in IEEE conferences [90, 91] and published in the IEEE Transactions on Communications journal [92]. The statistical analysis of the eigenvalue based detector in Chapter 3 has been presented in [93], and the wideband SS technique based on ITC, described in Chapter 4, has been presented in part in [94]. A review of spectrum sensing issues in CR context has been presented in [57]. The cooperative weighted centroid analysis in Chapter 5 has been presented in [95] and has been carried out in the context of a visit at the Royal Melbourne Institute of Technology (RMIT) in Melbourne, Australia, under the supervision of Prof. Sithamparanathan Kandeepan. This collaboration has also led to a study on spectrum sensing in presence of non continuous PU transmissions, currently under revision [96].

This thesis has been carried out also in the context of European projects including FP7 EUWB - "Coexisting short range radio by advanced Ultra-Wideband radio technology" [97–102], EDA-B CORASMA "COgnitive RAdio for dynamic Spectrum MAnagement" [103–106], FP7 SELECT "Smart and Efficient Localization, idEntification and Coopertation Techniques" [107, 108], and the COST Action IC0902 'Cognitive Radio and Networking for Cooperative Coexistence of Heterogeneous Wireless Networks".

1.6 Notation

Throughout this manuscript boldface letters denote vectors, $X \sim \mathcal{N}(\mu, \sigma^2)$ indicates a Gaussian r.v. with mean μ and variance σ^2 while $X \sim \mathcal{CN}(\mu, 2\sigma^2)$ indicates a complex Gaussian r.v. with mean μ and independent, identically distributed (i.i.d.) real and imaginary parts, each with variance σ^2. Also, $X \sim \chi^2_m(\lambda)$ indicates a chi-squared distributed r.v. with m degrees of freedom and non-centrality parameter λ, $X \sim \mathcal{F}_{\nu_1,\nu_2}(\lambda)$ indicates a F-distributed r.v., with degrees of freedom ν_1 and ν_2, and non-centrality parameter λ, and $Q(x) \triangleq \int_x^\infty 1/\sqrt{2\pi}\exp(-y^2/2)\,dy$ is the standard normal tail function [109,110]. $\mathbf{X} \sim \mathcal{CN}(\boldsymbol{\mu}, \boldsymbol{\Sigma})$ indicates a vector of complex Gaussian r.v.s with mean $\boldsymbol{\mu}$ and covariance matrix $\boldsymbol{\Sigma}$. Moreover, $\mathcal{M}_{m\times n}(\mathbb{C})$ represents the space of the $m \times n$ matrices with complex elements, $|\mathbf{A}|$ and $\mathrm{tr}\{\mathbf{A}\}$ stand respectively for the

determinant and the trace of the matrix $\mathbf{A}$, diag$\{\mathbf{A}\}$ stands for the principal diagonal of $\mathbf{A}$, $(\cdot)^{\mathrm{T}}$ and $(\cdot)^{\mathrm{H}}$ stand respectively for simple and Hermitian transposition. When possible, we use capital letters to denote r.v.s and lower case letters to denote the corresponding values.

Chapter 2

Effects of Noise Power Estimation on Energy Detection

2.1 Introduction

For single antenna receivers the simplest method to reveal the presence of a signal in AWGN consists in comparing the received energy, measured over a time interval T, with a suitable threshold. This energy detector (ED) can be adopted when the signal to be detected is completely unknown and no feature detection is therefore possible. Even when the SU has some knowledge about the signal to be detected, the ED may still be chosen for the simplicity of its implementation [18,20]. Moreover, for its generality, the ED is commonly used in measurements of the spectral occupation that involve wide frequency bands with different kind of signals [111].

The performance of the ED has been studied in many works including [41, 112–114], where a perfect knowledge of the noise power at the receiver was assumed, allowing thus a proper threshold design. In that case, the ED can work with arbitrarily small values of probability of false alarm and arbitrarily high probability of detection even in low SNR regimes, by using a sufficiently long observation interval. However, in real systems the detector does not have a perfect knowledge of the noise power level. Few works deal with the performance analysis of ED when the noise power is not perfectly known. In particular, in [47, 49, 115, 116], worst case design rules are provided for the ED, assuming that the detector knows that the noise power is within a limited range. Under this model, for a generic target performance, there exists a minimum value of SNR under which detection

is not possible even for infinitely long observation windows. This minimum is called *SNR wall* [49]. An idea that is growing into the spectrum sensing community is that the SNR wall phenomenon is an unavoidable problem in practical applications, since the estimated noise power always differs from the real noise power [49,116–118]. The aim of this paper is to establish the necessary and sufficient conditions for the existence of the SNR wall phenomenon in energy detection with estimated noise power (ENP-ED). We prove that the SNR wall phenomenon is not caused by the presence of an uncertainty in the noise power itself, but by an insufficient refinement of the estimation while the observation time increases. In particular, we provide two theorems regarding the conditions under which the SNR wall phenomenon occurs and the asymptotical behavior of the ENP-ED performance, as a function of the noise power estimator properties. The approach used in the paper is valid for all unbiased, asymptotically Gaussian noise power estimators. As a particular case of practical interest we consider noise power estimation performed by using the maximum likelihood (ML) criterion, assuming the availability of noise-only samples at the receiver.[1] These can be obtained in several ways including, e.g., the two-stage sensing methodology described in Section 2.2.1.

In signal detection problems, some works consider the signal to be detected as the realization of a random process ("Bayesian" model), others as an unknown deterministic signal ("classical" model) [46]. The former often assumes the signals to be Gaussian, that in many situations is a proper assumption [46]. Note that in this case the ENP-ED approach is equivalent to observe two Gaussian processes and determine whether they have the same power level. The classical model, where the signal is assumed unknown deterministic, is more general [46]. Hereafter we will consider both approaches, showing that for the considered problem the two models provide essentially the same results.

In this chapter we consider the detection of signals in AWGN, providing the following contributions.

- We derive the conditions for the existence of the SNR wall in ENP-ED relating the accuracy of the noise power estimator to the observation interval duration. In particular, we show that the wall arises only when the variance of the estimator does not decrease with the measurement time.

- We analyze the behavior of the ENP-ED for long observation intervals,

[1] Within the paper the noise is modeled as a stationary white Gaussian process. This AWGN is caused by thermal noise and may include other background noise sources, as for example interference, when these can be modeled by stationary white Gaussian processes.

providing the asymptotical relation between the minimum detectable SNR and the observation time (*design curves*).

- We derive the analytical expressions of the design curves for the ideal ED and for the ENP-ED with ML noise power estimator.
- We analyze the performance and the design curves of the ENP-ED for two-step sensing schemes in CR scenarios.

2.2 System Model

We address the detection of the presence of a signal in AWGN. After band-pass filtering over a bandwidth W, the received signal $r(t)$, observed for T seconds, is down converted and sampled at time $t_i = i/W$, obtaining the vector of complex samples $\mathbf{y} = (y_0, \ldots, y_{N-1})$, with $N = TW$.[2] The received energy to noise power spectral density ratio[3] can be approximated as (see also [41, Appendix])

$$\frac{2}{N_0}\int_0^T [r(t)]^2 dt \simeq \frac{1}{\sigma^2}\sum_{i=0}^{N-1} |y_i|^2 \tag{2.1}$$

where N_0 is the one-sided noise power spectral density and $\sigma^2 = N_0 W$. In this paper we assume $TW \gg 1$, so that the difference between the discrete time and the continuous time versions of the metric represented in (2.1) is negligible [41, 112]. Hence, in the following we will analyze the discrete time detection problem

$$\begin{array}{ll} \mathcal{H}_0: & y_i = n_i \\ \mathcal{H}_1: & y_i = x_i + n_i \end{array} \tag{2.2}$$

where x_i is the i-th signal sample, the noise samples $n_i \sim \mathcal{CN}(0, 2\sigma^2)$ are i.i.d., $\mathcal{H}_0$ and $\mathcal{H}_1$ are the "signal absent" and "signal present" hypotheses, respectively.

The ED test we will consider is

$$\Lambda(\mathbf{y}) \triangleq \frac{1}{2\sigma^2}\cdot\frac{1}{N}\sum_{i=0}^{N-1}|y_i|^2 \underset{\mathcal{H}_0}{\overset{\mathcal{H}_1}{\gtrless}} \xi. \tag{2.3}$$

The SNR is defined as $\mathsf{SNR} = S/\sigma^2$ with $S = \mathbb{E}\{|x_i|^2\}/2$ when the x_i are assumed i.i.d. Gaussian with $X_i \sim \mathcal{CN}(0, 2S)$ (Bayesian model), and

[2] We assume that TW is an integer number.

[3] The metric is therefore dimensionless.

as $\mathsf{SNR} = 1/(2\sigma^2 N) \cdot \sum_{i=0}^{N-1} |x_i|^2$ when the x_i are assumed unknown and deterministic (classical model).[4]

In the following, the ED performance will be expressed in terms of probability of false alarm $\mathrm{P_{FA}} = \mathrm{P}\{\Lambda(\mathbf{Y}) > \xi | \mathcal{H}_0\}$, and probability of detection $\mathrm{P_D} = \mathrm{P}\{\Lambda(\mathbf{Y}) > \xi | \mathcal{H}_1\}$.

According to the Neyman-Pearson criterion, the threshold ξ in (2.3) should be set for a given requirement in terms of $\mathrm{P_{FA}}$, and this is possible only if σ^2 is known [45]. However, in practical implementations we must generally assume that the ED has just an estimate, $\widehat{\sigma}^2$, of the true σ^2 [47,49,112]. Then, the ED test becomes in practice

$$\Lambda_{\mathrm{g}}(\mathbf{y}) = \frac{1}{2\widehat{\sigma}^2} \cdot \frac{1}{N} \sum_{i=0}^{N-1} |y_i|^2 \underset{\mathcal{H}_0}{\overset{\mathcal{H}_1}{\gtrless}} \xi. \tag{2.4}$$

The statistical distribution of $\Lambda_{\mathrm{g}}(\mathbf{y})$ depends on the particular estimation technique considered. We will refer to (2.4) as the ED with estimated noise power (ENP) (see also Fig. (2.2)).
Note that (2.3) is the log-likelihood ratio test for the detection problem (2.2), when the x_i i.i.d. r.v.s with zero mean Gaussian distribution. Moreover, (2.4) is the generalized likelihood ratio test when the receiver does not know anything about the signal to be detected (signal unknown and deterministic).

2.2.1 Two-step sensing

The simplest way to estimate the noise power is to perform ML estimation on noise-only samples. For impulse radar applications it is quite simple to locate some signal-free samples due to the sporadic occupation of the channel. In CR scenarios instead it is generally much more difficult to guarantee the availability of noise-only samples for environment measurements.
In this regards, in this section we describe the "two-step" sensing schemes, that can be adopted for the implementation of ML noise power estimation. Two-step schemes are motivated by the fact that, while the ED can be used with small sensing periods (even if with limited performance), other more sophisticated sensing methods, with better performance, generally require long observation intervals, with an impact on the efficiency of the SU communications [18]. An effective strategy consists in the combined adoption of sporadic long sensing periods (SPs) for fine sensing (called fine-SPs), and more frequent short SPs (called fast-SPs) in which simpler detectors, such as the ED, can be used (Fig. 2.1). This two-step sensing scheme is sup-

[4]Note that if the signal is ergodic, the two definitions of SNR are equivalent for $N \to \infty$.

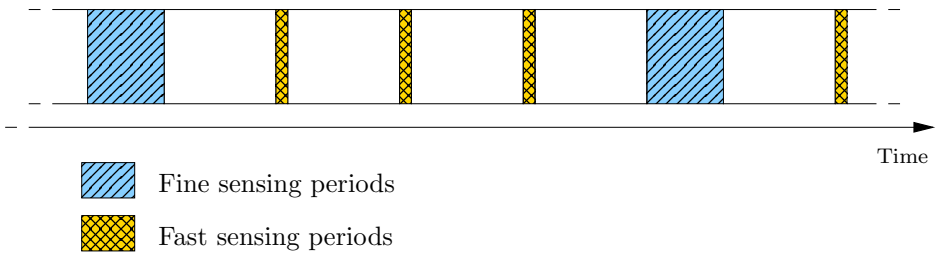

Figure 2.1: Two step sensing scenario in the IEEE 802.22 draft standard [119].

ported by recent CR standards; for example, the IEEE 802.22 draft includes the use of intra-frame periods (5-10 ms) and inter-frame periods (up to 158 ms) [119, 120], while the standard ECMA 392 uses regular SPs , of at least 5 ms, and optional on-demand SPs for further spectral measurements [27].
If, during a fine-SP, where a high accuracy detection algorithm is adopted[5], the decision is for $\mathcal{H}_0$, the samples collected can be considered signal-free; we propose to use them for noise power estimation for the subsequent fast-SPs. This detection strategy is depicted in Fig. 2.2.
More generally we can consider, for the fine-SP, the adoption of strategies that provide, beyond the detection decision, also an estimate of the noise power. Methods based on multiple antennas can be useful for this task [67].

2.2.2 Noise uncertainty

Noise power uncertainty is mainly caused by four factors [121]:

- temperature variation;
- change in low noise amplifier gain due to thermal fluctuations;
- initial calibration error;
- presence of interferers.

Noise power estimation with a sufficient rate can be used to overcome the first three factors because thermal changes are very slow phenomena. Indeed the noise power level is stationary typically for a few minutes [115]. The presence of interference caused by other SUs in the CR network instead introduces dynamics in the background RF energy that are too fast to be tackled with

[5]Then, failures in the fine-SP detection can be neglected.

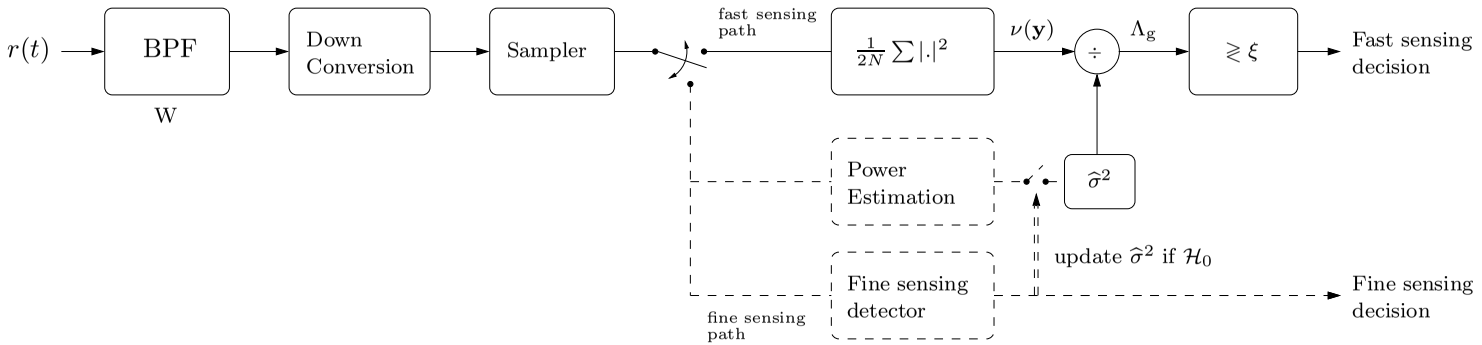

Figure 2.2: Two-step detection scheme supporting ED with noise power estimation for fast sensing.

periodical estimations. To overcome this problem, the SPs scheduled in the standards IEEE 802.22 [119,122] and ECMA 392 [27] are synchronized among the SUs to avoid mutual interference. These SPs are called quiet periods. Therefore to avoid the noise uncertainty problem the SU must periodically estimate the noise power during the quite periods.

2.2.3 Design curves

Let us indicate as $(\mathrm{P}_{\mathrm{FA}}^{\mathrm{DES}}, \mathrm{P}_{\mathrm{D}}^{\mathrm{DES}})$ the desired detector performance, with $\mathrm{P}_{\mathrm{FA}}^{\mathrm{DES}} < \mathrm{P}_{\mathrm{D}}^{\mathrm{DES}}$, so that the detector fulfills the requirement if its $\mathrm{P_{FA}}$, $\mathrm{P_D}$ satisfy both $\mathrm{P_{FA}} \leq \mathrm{P}_{\mathrm{FA}}^{\mathrm{DES}}$ and $\mathrm{P_D} \geq \mathrm{P}_{\mathrm{D}}^{\mathrm{DES}}$. The relation between the SNR and the number of samples N required to guarantee the desired performance will be referred as *design curve* [90, 91]. Note that, given the sampling frequency W, the number of samples is proportional to the time needed for the detection task. Then, the design curve can also be considered as the minimum signal-to-noise ratio, $\mathsf{SNR}_{\min}$, needed to fulfill the specification $(\mathrm{P}_{\mathrm{FA}}^{\mathrm{DES}}, \mathrm{P}_{\mathrm{D}}^{\mathrm{DES}})$, for a given sensing time duration.[6]
To derive the design curves we observe that, in general, the expressions of $\mathrm{P_D}$ and $\mathrm{P_{FA}}$ are functions of the threshold ξ, the number of samples N, the SNR, and possibly other parameters,

$$\mathrm{P_{FA}} = f_{\mathrm{FA}}\left(\xi; N, \dots\right) \tag{2.5}$$

$$\mathrm{P_D} = f_{\mathrm{D}}\left(\xi; N, \mathsf{SNR}, \dots\right) \tag{2.6}$$

where $f_{\mathrm{FA}}(\cdot)$ and $f_{\mathrm{D}}(\cdot)$ are specific functions depending on the particular detector statistic considered. The threshold ξ, corresponding to the target probabilities $\left(\mathrm{P}_{\mathrm{FA}}^{\mathrm{DES}}, \mathrm{P}_{\mathrm{D}}^{\mathrm{DES}}\right)$ can be expressed, using the inverse form of (2.5) and (2.6), as

$$\xi = f_{\mathrm{FA}}^{-1}\left(\mathrm{P}_{\mathrm{FA}}^{\mathrm{DES}}; N, \dots\right) \tag{2.7}$$

$$\xi = f_{\mathrm{D}}^{-1}\left(\mathrm{P}_{\mathrm{D}}^{\mathrm{DES}}; N, \mathsf{SNR}, \dots\right). \tag{2.8}$$

Then, the design curve can be obtained by solving explicitly for the variable $\mathsf{SNR}_{\min}$ the equation

$$f_{\mathrm{FA}}^{-1}\left(\mathrm{P}_{\mathrm{FA}}^{\mathrm{DES}}; N, \dots\right) = f_{\mathrm{D}}^{-1}\left(\mathrm{P}_{\mathrm{D}}^{\mathrm{DES}}; N, \mathsf{SNR}_{\min}, \dots\right). \tag{2.9}$$

If the $\mathrm{P_{FA}}$ and $\mathrm{P_D}$ formulas have not an analytical explicit inverse form, the problem can be solved numerically.

[6] Within the paper we plot the design curves as SNR vs. N like in [47]. The SNR on the y-axis emphasizes that the SNR wall (if present) is a minimum. Then we could also use the expression "SNR floor", but we choose to maintain the expression "SNR wall" in continuity with [49, 116].

If, even with an arbitrary long observation interval, $\mathsf{SNR}_{\min}$ does not go to zero, we have the SNR wall phenomenon [47, 49]. Formally, let us define

$$\mathsf{SNR}_{\min}^{(\infty)} = \lim_{N\to\infty} \mathsf{SNR}_{\min}. \tag{2.10}$$

Thus we have the SNR wall if $\mathsf{SNR}_{\min}^{(\infty)} > 0$. In this case, if the SNR at the receiver is below the asymptotical value $\mathsf{SNR}_{\min}^{(\infty)}$, detection with the desired performance is impossible.

2.3 SNR Wall Analysis

In this section we analyze the presence of the SNR wall and the asymptotical behavior of the design curves for the ENP-ED assuming that the noise power estimator $\widehat{\sigma}^2$ is unbiased and asymptotically Gaussian. For example, the ML-estimator, that we thoroughly analyze in the next section, is asymptotically Gaussian [45, par. 2.4.2]. We give two theorems on the existence of the SNR wall, and on the asymptotical behavior of the design curves, considering the ENP-ED test in (2.4). The theorems are valid for the detection of Gaussian signals as well as for unknown deterministic signals. Throughout this analysis we adopt the Landau notation: for the real functions f, g with $g(x) \neq 0$ in the neighborhood of a, $f(x) = \Theta(g(x))$ for $x \to a$ means that there exists two positive real number K_1 and K_2 such that $0 < K_1 \leq \lim_{x\to a} |f(x)/g(x)| \leq K_2$. Moreover $f(x) = o(g(x))$ for $x \to a$ means that $\lim_{x\to a} f(x)/g(x) = 0$.

Theorem 1 (Existence of the SNR wall)**.** *For the energy detection test defined in* (2.4)*, assuming that $\widehat{\sigma}^2$ is an unbiased asymptotically Gaussian estimator of the noise power σ^2, an arbitrary $(P_{FA}^{DES}, P_D^{DES})$ pair can be achieved by increasing the observation interval (i.e., increasing the number of collected samples N) for all values of SNR, if and only if the variance of the noise power estimator, $var(\widehat{\sigma}^2)$, is $o(1)$ for $N \to \infty$.*
*Moreover, if $var(\widehat{\sigma}^2)$ is $\Theta(1)$ for $N \to \infty$, there exists a minimum SNR (*SNR wall*), under which it is impossible to reach the desired $(P_{FA}^{DES}, P_D^{DES})$ pair; in this case, by defining $\alpha = Q^{-1}\big(P_{FA}^{DES}\big)$, $\delta = Q^{-1}\big(P_D^{DES}\big)$ and $\phi = var(\widehat{\sigma}^2/\sigma^2)$[7], the minimum SNR for $N \to \infty$ converges to*

$$\mathsf{SNR}_{min}^{(\infty)} = \frac{1 - \delta\sqrt{\phi}}{1 - \alpha\sqrt{\phi}} - 1. \tag{2.11}$$

Proof. see Appendix. □

[7]Note that in general ϕ depends on N, whose value will be clear from the context.

In other words Theorem 1 states that even in the presence of a non ideal estimation of the noise power, the SNR wall phenomenon does not arise if $\widehat{\sigma}^2$ is a consistent (with N) estimator of the noise power[8].

Theorem 2 (Asymptotical behavior of the design curves)**.** *For the energy detection test defined in* (2.4)*, assuming that* $\widehat{\sigma}^2$ *is an unbiased asymptotically Gaussian estimator of the noise power* σ^2*, let us consider the asymptotical behavior (for* $N \to \infty$*) of* SNR_{min}*, when there is no SNR wall.*
If $var(\widehat{\sigma}^2)$ *is* $\Theta(N^{-\gamma})$ *for* $N \to \infty$ *with* $0 < \gamma \leq 1$*, the design curve in log-log scale, i.e.* $\mathsf{SNR}_{min}(dB)$ *as a function of* $\log_{10} N$*, tends asymptotically to a straight line with a slope of* $-5\,\gamma$ *dB/decade. In particular, if, for large* N*,* $\phi \approx N^{-\gamma}/\lambda$ *with* $0 < \gamma < 1$ *and* $\lambda > 0$*, we get*

$$\mathsf{SNR}_{min}(dB) \approx -5\,\gamma \log_{10} N - 5 \log_{10} \lambda + 10 \log_{10}(\alpha - \delta) \tag{2.12}$$

while if $\phi \approx 1/(\lambda N)$*, we have*

$$\begin{aligned} \mathsf{SNR}_{min}(dB) \approx & -5 \log_{10} N + 5 \log_{10}\left(\frac{1+\lambda}{\lambda}\right) \\ & + 10 \log_{10}(\alpha - \delta). \end{aligned} \tag{2.13}$$

Moreover, if $var(\widehat{\sigma}^2)$ *is* $o\left(N^{-1}\right)$ *for* $N \to \infty$*, the design curve has a slope of* -5 *dB/decade and we have*

$$\mathsf{SNR}_{min}(dB) \approx -5 \log_{10} N + 10 \log_{10}(\alpha - \delta). \tag{2.14}$$

In addiction, since (2.14) *is also valid for the ideal ED, any practical implementation of the ED where the estimator of the noise power has* $var(\widehat{\sigma}^2)$ *decreasing faster than* $1/N$ *has asymptotically the same performance of the ideal ED.*

Proof. see Appendix. □

From Theorem 1 and Theorem 2 we see how $var(\widehat{\sigma}^2)$ determines not only the existence of the SNR wall, but also the asymptotical behavior of the design curve. Theorem 2 also confirms, for the particular case of the ideal ED, the behavior $N = \Theta\left(1/\mathsf{SNR}_{\text{min}}^2\right)$ observed in [49, 116]. Some examples of design curves for $var(\widehat{\sigma}^2)$ decreasing with different rates are provided in Section 2.6.

[8]We define $\widehat{\sigma}^2$ as *consistent* with N if, for any $\epsilon > 0$, satisfies [46]

$$\lim_{N \to \infty} Pr\left\{|\widehat{\sigma}^2 - \sigma^2| < \epsilon\right\} = 0.$$

2.4 Performance of ED with ENP

In this section we specialize the analysis to ENP-ED with ML noise power estimation, providing the explicit $\mathrm{P_{FA}}$ and $\mathrm{P_D}$ formulas. Besides the well known ideal ED [41, 112], we first review some known results for the ENP-ED [123, 124], and give new explicit expressions for large N. For simplicity of notation we assume that the samples y_i for $i < 0$, i.e. before the detection window $t_0, \ldots, t_{N-1}$, do not contain the signal, so that in the following we denote $n_{-1}, \ldots, n_{-M}$ the M noise-only samples used for noise power estimation. Then, the receiver can evaluate the ML noise power estimate

$$\widehat{\sigma}^2_{\mathrm{ML}} = \frac{1}{2M} \sum_{i=1}^{M} |n_{-i}|^2. \tag{2.15}$$

Note that $\widehat{\sigma}^2_{\mathrm{ML}}$ is an efficient[9] estimator of the noise power.

2.4.1 Detection of a Gaussian signal

Assuming that the signal samples X_i are i.i.d. with $X_i \sim \mathcal{CN}(0, 2S)$, the $\mathrm{P_{FA}}$ and $\mathrm{P_D}$ of the ideal ED (2.3) are given by [90]

$$P_{\mathrm{FA,\,ED}} = \widetilde{\Gamma}\left(N, N\xi\right) \tag{2.16}$$

$$P_{\mathrm{D,\,ED}} = \widetilde{\Gamma}\left(N, \frac{N\,\xi}{1+\mathsf{SNR}}\right) \tag{2.17}$$

where $\widetilde{\Gamma}\left(a, z\right) \triangleq \frac{1}{\Gamma(a)} \int_z^\infty x^{a-1} \exp\left(-x\right) dx$ the regularized gamma function and $\Gamma\left(\cdot\right)$ is the gamma function [109, ch. 6]. Usually, these expressions are simplified by means of their Gaussian approximations that are valid for large number of samples N [109, eq. 26.4.11]

$$P_{\mathrm{FA,\,ED}} \simeq Q\left(\frac{\xi - 1}{1/\sqrt{N}}\right) \tag{2.18}$$

$$P_{\mathrm{D,\,ED}} \simeq Q\left(\frac{\xi - (1+\mathsf{SNR})}{(1+\mathsf{SNR})/\sqrt{N}}\right). \tag{2.19}$$

Considering the ENP-ED (2.4) with $\widehat{\sigma}^2_{\mathrm{ML}}$, let us note that the numerator and the denominator are independent since they refer to different time windows. Then, in the hypothesis that the y_i and the n_i are i.i.d. and complex Gaussian, the metric[10] Λ_{g}, with the proper scaling, is the ratio of two

[9] In the sense that it reaches the Cramer-Rao bound.

[10] To simplify the notation, in the following we will write Λ_{g} instead of $\Lambda_{\mathrm{g}}(\mathbf{y})$.

chi-squared distributions, and its distribution can be written as [123, 124]

$$\begin{array}{ll} \mathcal{H}_0: & \Lambda_{\mathrm{g}} \quad\quad \sim \mathcal{F}_{2N,2M}(0) \\ \mathcal{H}_1: & \Lambda_{\mathrm{g}} \cdot \frac{\sigma_{\mathrm{t}}^2}{\sigma^2} \sim \mathcal{F}_{2N,2M}(0) \end{array} \tag{2.20}$$

where $\sigma_{\mathrm{t}}^2 = \sigma^2 + S = \sigma^2(1+\mathsf{SNR})$.
The probability distribution function (p.d.f.) of the metric Λ_{g} is therefore

$$f_{\Lambda_{\mathrm{g}}|\mathcal{H}_0}(x) = \frac{N^N\, M^M\, x^{N-1}}{B(N,M)\,(Nx+M)^{N+M}}\, u(x) \tag{2.21}$$

$$f_{\Lambda_{\mathrm{g}}|\mathcal{H}_1}(x) = \frac{N^N\, [M(1+\mathsf{SNR})]^M\, x^{N-1}}{B(N,M)\,[Nx+M(1+\mathsf{SNR})]^{N+M}}\, u(x) \tag{2.22}$$

where $u(\cdot)$ is the unity step function and $B(a,b) = \Gamma(a)\Gamma(b)/\Gamma(a+b)$ is the beta function [109, ch. 6]. Then $\mathrm{P_{FA}}$ and $\mathrm{P_D}$ are given by

$$P_{\mathrm{FA,\,ENP\text{-}ED}} = \widetilde{B}\left(M, N, \frac{M}{M+N\xi}\right) \tag{2.23}$$

$$P_{\mathrm{D,\,ENP\text{-}ED}} = \widetilde{B}\left(M, N, \frac{M(1+\mathsf{SNR})}{M(1+\mathsf{SNR})+N\xi}\right) \tag{2.24}$$

where the incomplete beta function can be expressed with its integral representation $\widetilde{B}(a,b,z) = \frac{1}{B(a,b)}\int_0^z x^{a-1}(1-x)^{b-1}dx$, (with $\mathrm{Re}\{a\}>0$, $\mathrm{Re}\{b\}>0$ and $|z|<1$) [109, eq. 6.6.2] or its series form $\widetilde{B}(a,b,z) = z^{a+b-1}\sum_{i=0}^{b-1}\binom{a+b-1}{i}\left(\frac{1-z}{z}\right)^i$ (with integer b and $|z|<1$) [109, eq. 26.5.7]. Alternative series representations for (2.23) and (2.24) are provided in [123], where the radar cell-averaging constant false alarm rate (CA-CFAR) technique is studied. More precisely, our system model corresponds to the CA-CFAR scheme, where N is the number of samples of the cell to be tested and M is the number of reference samples. The adoption of the compact forms (2.23) and (2.24) based on the incomplete beta function leads to an easier subsequent analysis.

For large N and M, the probabilities (2.23) and (2.24) can be expressed through their Gaussian approximations [109, eq. 26.6.13]

$$P_{\mathrm{FA,\,ENP\text{-}ED}} \simeq Q\left(\frac{\xi-1}{\sqrt{\frac{N+M}{N\,M}}}\right) \tag{2.25}$$

$$P_{\mathrm{D,\,ENP\text{-}ED}} \simeq Q\left(\frac{\frac{\xi}{1+\mathsf{SNR}}-1}{\sqrt{\frac{N+M}{N\,M}}}\right). \tag{2.26}$$

2.4.2 Detection of an unknown deterministic signal

Assuming that the signal to be detected is unknown deterministic, under $\mathcal{H}_1$ we have $Y_i \sim \mathcal{CN}(x_i, 2\sigma^2)$. Obviously this assumption does not modify the detector performance in the hypothesis $\mathcal{H}_0$, where $\mathrm{P_{FA}}$ is always given by (2.16) and (2.23). Under this assumption the ideal ED statistic Λ_{g}, in hypothesis $\mathcal{H}_1$, has a non-central chi-squared distribution with non-centrality parameter equal to $2N \cdot \mathsf{SNR}$, with the SNR defined in Section 2.2. Then $P_{\mathrm{D,\,ED}}$ is given by [41, 112, 125]

$$P_{\mathrm{D,\,ED}} = Q_N\left(\sqrt{\mathsf{SNR}}, \sqrt{2N\xi}\right) \tag{2.27}$$

where $Q_k(\alpha, \beta) = \int_\beta^\infty x \left(\frac{x}{\alpha}\right)^{k-1} \exp\left(-\frac{x^2+\alpha^2}{2}\right) I_{k-1}(\alpha x)\, dx$ is the generalized Marcum's Q function of order k [126] and $I_n(\cdot)$ is the modified Bessel function of the first kind with order n.

Considering the ENP case, in hypothesis $\mathcal{H}_1$ the metric Λ_{g} has a singly non-central F-distribution with non-centrality parameter $2N \cdot \mathsf{SNR}$, hence

$$\Lambda_{\mathrm{g}} \sim \mathcal{F}_{2N,2M}\left(2N \cdot \mathsf{SNR}\right). \tag{2.28}$$

Therefore, Λ_{g} has p.d.f.

$$\begin{aligned} f_{\Lambda_{\mathrm{g}}|\mathcal{H}_1}(x) =& f_{\Lambda_{\mathrm{g}}|\mathcal{H}_0}(x) \exp\left(-N \cdot \mathsf{SNR}\right) \\ & \cdot {}_1F_1\left(N+M; N; \frac{\mathsf{SNR}\, N^2 x}{(M+Nx)}\right) \end{aligned} \tag{2.29}$$

where ${}_1F_1(\cdot;\cdot;\cdot)$ is the confluent hypergeometric function [109, eq. 13.1.2]. Then, $\mathrm{P_D}$ is given by

$$\begin{aligned} P_{\mathrm{D,\,ENP\text{-}ED}} =& \exp\left(-N\,\mathsf{SNR}\right) \\ & \cdot \sum_{k=0}^{\infty} \frac{\left(N\,\mathsf{SNR}\right)^k}{k!} \widetilde{B}\left(M, N+k, \frac{M}{M+N\xi}\right). \end{aligned} \tag{2.30}$$

The exact expression (2.30) has been obtained by using the series version of the confluent hypergeometric function. Note that (2.30) is a particular case of [124, eq. 3]. An alternative series representation is provided in [123]. Although (2.30) is quite complicated for detector design, it can be simplified using the central F-distribution approximation for the tail distribution of the non-central F-distribution [109, eq. 26.6.26], resulting in

$$\begin{aligned} P_{\mathrm{D,\,ENP\text{-}ED}} \simeq & \\ & \widetilde{B}\left(M, N+\frac{N \cdot \mathsf{SNR}^2}{1+2\mathsf{SNR}}, \frac{M\left(1+\frac{\mathsf{SNR}}{1+\mathsf{SNR}}\right)}{M\left(1+\frac{\mathsf{SNR}}{1+\mathsf{SNR}}\right)+N\xi}\right). \end{aligned} \tag{2.31}$$

Note that (2.31) is equivalent to (2.24) for low SNR. In this regime, that is the most interesting in CR, the Bayesian and classical model approaches are equivalent. By virtue of this equivalence, in the reminder of the paper we will just consider the Bayesian model.

2.5 ENP-ED Design Curves

In this section we provide the analytical expressions of the design curves both for the ideal ED and the ENP-ED, considering the Bayesian model. We also discuss the worst-case approach that has been proposed in the previous literature.

2.5.1 Design through ENP analysis

For the ideal ED, from (2.16) and (2.17), we get the design curve

$$\mathsf{SNR}_{\text{min, ED}} = \frac{\text{Inv}\widetilde{\Gamma}\left(N, \text{P}_{\text{FA}}^{\text{DES}}\right)}{\text{Inv}\widetilde{\Gamma}\left(N, \text{P}_{\text{D}}^{\text{DES}}\right)} - 1 \tag{2.32}$$

where $\text{Inv}\widetilde{\Gamma}(\cdot,\cdot)$ is the inverse gamma regularized function (if $w = \Gamma(a,z)$, then $z = \text{Inv}\widetilde{\Gamma}(a,w)$).

Instead, for the ENP-ED, the inversion of (2.23) and (2.24) leads to

$$\mathsf{SNR}_{\text{min, ENP-ED}} = \frac{1/\text{Inv}\widetilde{B}\left(M, N, \text{P}_{\text{FA}}^{\text{DES}}\right) - 1}{1/\text{Inv}\widetilde{B}\left(M, N, \text{P}_{\text{D}}^{\text{DES}}\right) - 1} - 1 \tag{2.33}$$

where $\text{Inv}\widetilde{B}(\cdot,\cdot,\cdot)$ is the inverse beta regularized function (if $w = \widetilde{B}(a,b,z)$, then $z = \text{Inv}\widetilde{B}(a,b,w)$). Note that all expressions given are easily computed by using standard mathematical software. Alternatively, (2.33) can be approximated for large N and M through (2.25) and (2.26) as

$$\mathsf{SNR}_{\text{min, ENP-ED}} \simeq \frac{1 + \alpha\sqrt{\frac{N+M}{N\,M}}}{1 + \delta\sqrt{\frac{N+M}{N\,M}}} - 1. \tag{2.34}$$

2.5.2 Design for ED with a worst-case approach

In literature the SNR wall analysis is usually performed assuming that the uncertain noise power is constrained in a limited range [47]

$$\widehat{\sigma}^2 \in \left[\sigma_{\min}^2, \sigma_{\max}^2\right] \tag{2.35}$$

where the interval includes the true σ^2. This bounded worse beaviour (BWB) model has been introduced to face situations in which the noise power statistic is unknown or when the noise power is estimated very rarely, causing the estimated value to be no longer reliable. Then, with the aim to get a bound on the performance, the $\mathrm{P_{FA}}$ is evaluated when the estimated noise power assumes the lowest value σ^2_{min}, while for the $\mathrm{P_D}$ it assumes the highest value, σ^2_{max}, giving the BWB probabilities

$$P_{\mathrm{FA,\,BWB}} = \widetilde{\Gamma}\left(N, \frac{\sigma^2_{\mathrm{min}}}{\sigma^2} N\xi\right) \tag{2.36}$$

$$P_{\mathrm{D,\,BWB}} = \widetilde{\Gamma}\left(N, \frac{\sigma^2_{\mathrm{max}}}{\sigma^2_{\mathrm{t}}} N\xi\right). \tag{2.37}$$

Although easy to compute, these bounds cannot be jointly achieved by any limited-support distribution for $\widehat{\sigma}^2$. In this case we obtain the design curve

$$\mathsf{SNR}_{\mathrm{min,\,BWB}} = \frac{\sigma^2_{\mathrm{max}}}{\sigma^2_{\mathrm{min}}} \cdot \frac{\mathrm{Inv}\widetilde{\Gamma}\left(N, \mathrm{P}^{\mathrm{DES}}_{\mathrm{FA}}\right)}{\mathrm{Inv}\widetilde{\Gamma}\left(N, \mathrm{P}^{\mathrm{DES}}_{\mathrm{D}}\right)} - 1. \tag{2.38}$$

The BWB model always leads to an SNR wall, as for increasing N the design curve tends to the positive finite value[11] [47]

$$\mathsf{SNR}^{(\infty)}_{\mathrm{min,\,BWB}} \triangleq \lim_{N\to\infty} \mathsf{SNR}_{\mathrm{min,\,BWB}} = \frac{\sigma^2_{\mathrm{max}}}{\sigma^2_{\mathrm{min}}} - 1 \tag{2.39}$$

which is related to the noise uncertainty throughout $\sigma^2_{\mathrm{max}}/\sigma^2_{\mathrm{min}}$. We remark that the adoption of an incorrect model for the noise estimate could lead to an improper design. Similar problems have been observed also in different contexts [127]. In the numerical results section we show that applying the BWB model to the ENP-ED is overly pessimistic, since it not only always implies an SNR wall, while there is no SNR wall under the conditions stated in Theorem 1, but also, when it does occur, the wall predicted by (2.39) is often considerably higher than the true wall given by (2.11).

2.6 Numerical Results

In this section we analyze the performance of the ENP-ED based on the ML noise power estimator defined in section 2.4, assuming $\mathrm{P}^{\mathrm{DES}}_{\mathrm{FA}} = 1 - \mathrm{P}^{\mathrm{DES}}_{\mathrm{D}} = 0.1$, as required from the IEEE 802.22 draft standard [119].

[11] The difference with respect to [49, eq. (6)] by a factor $\sqrt{\sigma^2_{\mathrm{max}}/\sigma^2_{\mathrm{min}}}$ is due to the different definitions of signal-to-noise ratio.

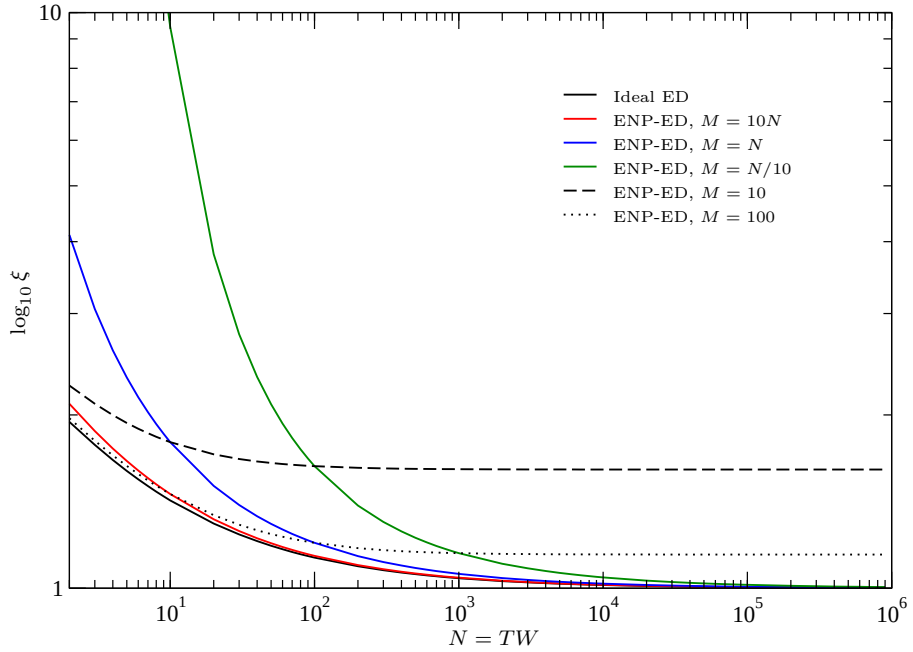

Figure 2.3: Thresholds as a function of the number of received samples N for $\mathrm{P}_{\mathrm{FA}}^{\mathrm{DES}} = 0.1$. Thresholds refer to the ideal ED, and to the ENP-ED for $M = 10N$, N, $N/10$, 100, 10.

2.6.1 Threshold mismatch, CFAR and CDR

Here we show some examples of ED design and performance losses due to noise power estimation and threshold mismatch. For threshold mismatch we intend that the threshold is set assuming that the noise power is perfectly known (from (2.16) or (2.17) for ideal ED) when the effectively adopted metric is (2.4). In Fig. 2.3 we compare the thresholds required for $\mathrm{P}_{\mathrm{FA}}^{\mathrm{DES}} = 0.1$ for the ideal ED and for the ENP-ED. As we can see, the ideal ED model requires threshold values that differ from those of the ENP-ED; the adoption of the proper statistic is therefore fundamental in real applications. Note that the mismatch effect is reduced for high N and M. In Fig. 2.4 we compare the P_{FA} and P_{D} for the ideal ED, and for the ENP-ED with mismatched threshold (ENPMT), with $M = N = 10^5$, when the constant false alarm rate (CFAR) strategy is adopted. Note that the ENP-ED has a reduced performance compared to the ideal-ED even with the correct threshold. This effect is called "CFAR loss" in radar literature and can be mitigated by increasing M. The figure also shows that using the wrong threshold for the ENP-ED produces $\mathrm{P}_{\mathrm{FA}} = 0.18$ instead of the target $\mathrm{P}_{\mathrm{FA}}^{\mathrm{DES}} = 0.1$, with a resulting excess

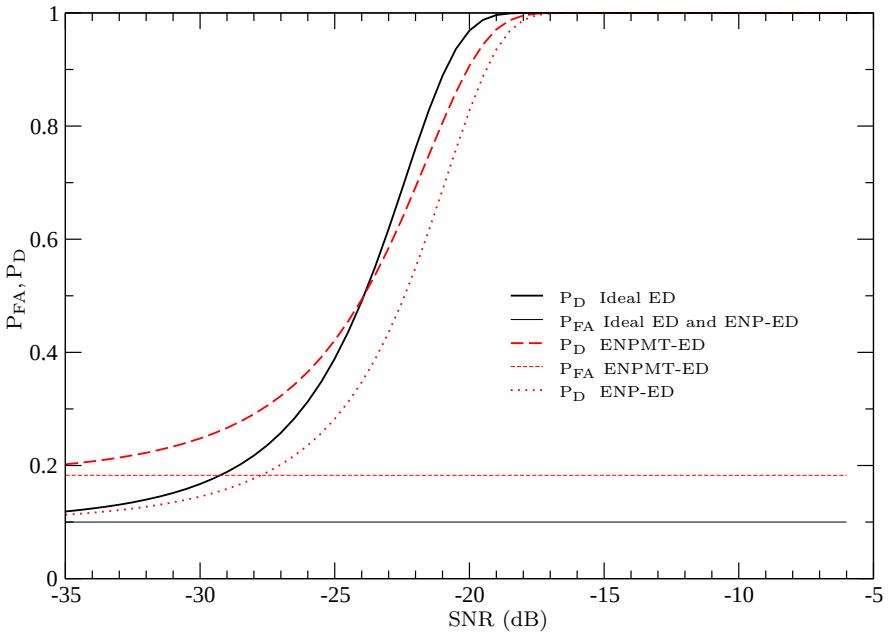

Figure 2.4: $\mathrm{P_{FA}}$ and $\mathrm{P_D}$ as functions of the SNR for different choices of the threshold and $N = 10^5$, using the CFAR design approach. Ideal ED (eq.s (2.16), (2.17)): corresponding threshold set for $\mathrm{P_{FA}^{DES}} = 0.1$. ENPMT-ED: ED with ENP (eq.s (2.23), (2.24)) and with the same threshold of the ideal ED (mismatched threshold). ENP-ED: ED with ENP and corresponding threshold set for $\mathrm{P_{FA}^{DES}} = 0.1$. For the ENP case $M = N$.

in the silent time for the SU.

In CR systems, fixing the $\mathrm{P_D}$ can be more appropriate than fixing the $\mathrm{P_{FA}}$, because of the need of avoid interfering the PUs. We refer to this approach as constant detection rate (CDR) design strategy, where the threshold must be chosen to guarantee $\mathrm{P_D} \geq \mathrm{P_D^{DES}}$ for all SNRs above a given value. Even for CDR, the ED design requires taking into account the effect of imperfect noise power estimation. In Fig. 2.5 the performance of an ideal ED, an ENPMT-ED and an ENP-ED with the proper threshold, are reported. The target performance is $\mathrm{P_D} \geq 0.9$ for all SNR ≥ -21 dB, that is a realistic requirement for the IEEE 802.22 standard [128]. In the figure we consider ENP-ED with $M = N$ and with $M = N/10$. Clearly, with larger M the curve is closer to the ideal ED performance. In any case, the threshold mismatch decreases the effective detection probability, making the detector failing to fulfill the requirements.

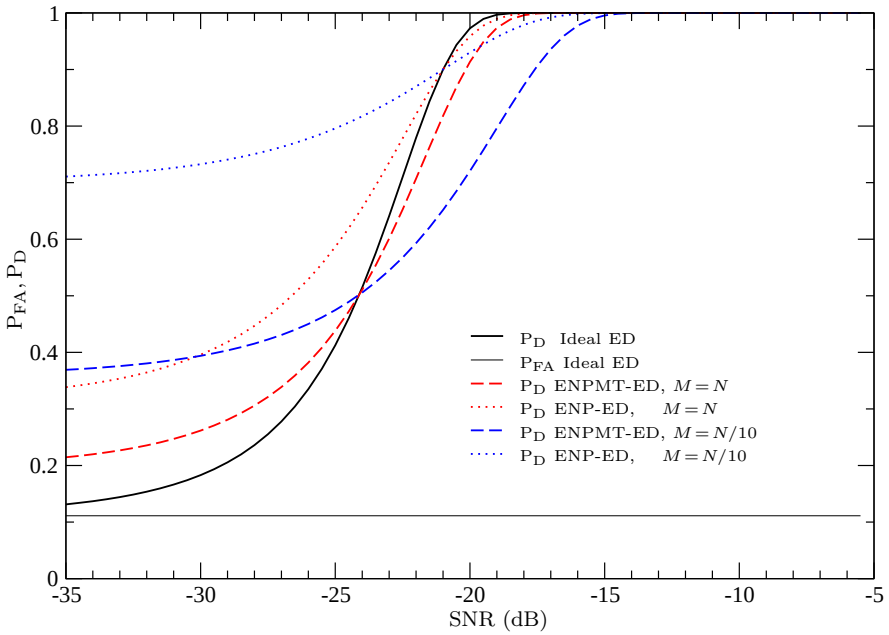

Figure 2.5: P_{FA} and P_D as functions of the SNR for different choices of the threshold and $N = 10^5$ in CDR design. Ideal ED (eq.s (2.16), (2.17)): corresponding threshold set for $P_D^{DES} = 0.9$ at SNR $= -21$ dB. ENPMT-ED: ED with ENP (eq.s (2.23), (2.24)) and with the same threshold of the ideal ED (mismatched threshold). ENP-ED: ED with ENP and corresponding threshold set for $P_D^{DES} = 0.9$ at SNR $= -21$ dB.

2.6.2 Design curves

In order to use the theorems in Section 2.3, we observe that, considering the notation used in Section 2.3, for the $\widehat{\sigma}^2_{ML}$ in (2.15) we have $\phi = 1/M$.
In Fig. 2.6 we plot some examples of the design curve (2.34), considering different relations between M and N. We observe in this figure the behaviors predicted by the theorems. In particular, if we use a fixed (independent on N) number of samples for noise power estimation (e.g., $M = 100$), we have $\phi = \Theta(1)$ for $N \to \infty$ and the SNR converges quickly to a positive value, the SNR wall, given by (2.11). When M increases as a logarithmic function of N, the curve decreases very slowly. When $M = N^\gamma$ (i.e. $\phi = N^{-\gamma}$) with $0 < \gamma \leq 1$, we have an asymptotically linear trend, as predicted by Theorem 2, with $-5\,\gamma$ dB/decade slope. This is the case for the design curves with $M = \sqrt{N}$ and $M = N$, that approach slopes of -2.5 and -5 dB/decade, respectively. Moreover, if $M = N$ we have $\phi = 1/N$ and, from (2.13), we see that the

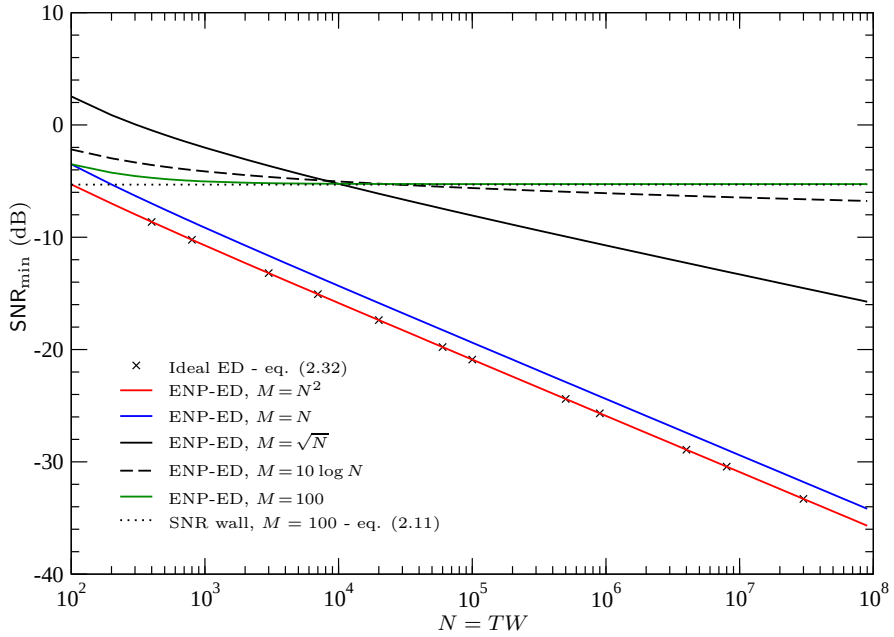

Figure 2.6: Design curves for ENP-ED (2.34) with different M. Ideal ED curve (2.32) is also shown. $\mathrm{P}_{\mathrm{FA}}^{\mathrm{DES}} = 1 - \mathrm{P}_{\mathrm{D}}^{\mathrm{DES}} = 0.1$.

difference with respect to the ideal ED is $5 \log \left(\frac{1+\lambda}{\lambda}\right) = 5 \log (2) \simeq 1.5\,\mathrm{dB}$ in terms of $\mathsf{SNR}_{\mathrm{min}}$. In Fig. 2.6 we also plot the $M = N^2$ curve, as an example of the case $\phi = o\,(1/N)$ for which Theorem 2 applies. This curve approaches the maximum slope obtainable ($-5\,\mathrm{dB/decade}$) and the design curve is indistinguishable from that with σ^2 perfectly known. Even if M grows faster than N, the design curve slope is limited by the growth of N.

To further assess the analysis, in Fig. 2.7 the design curves (2.33) are compared with numerical simulations and with the asymptotic behaviors of Theorem 2. Note that, as predicted from Theorem 2, the ENP-ED curve with $M = N^{1.5}$ (M grows faster than N producing $\phi = o\,(1/N)$) closely approaches the ideal ED curve for large N (e.g $N \gtrsim 100$).

2.6.3 Two-step sensing schemes

In two-step sensing schemes if the SU decides for $\mathcal{H}_0$ in the fine-SP, we propose to use those samples for noise power estimation to set the threshold in the subsequent fast-SP energy detection. In the following we show some numerical performance when the decision is based on a single fast-SP. Note that if the same fine sensing noise level estimate is used for several fast-SPs, the resulting decision variables are correlated due to the same noise level

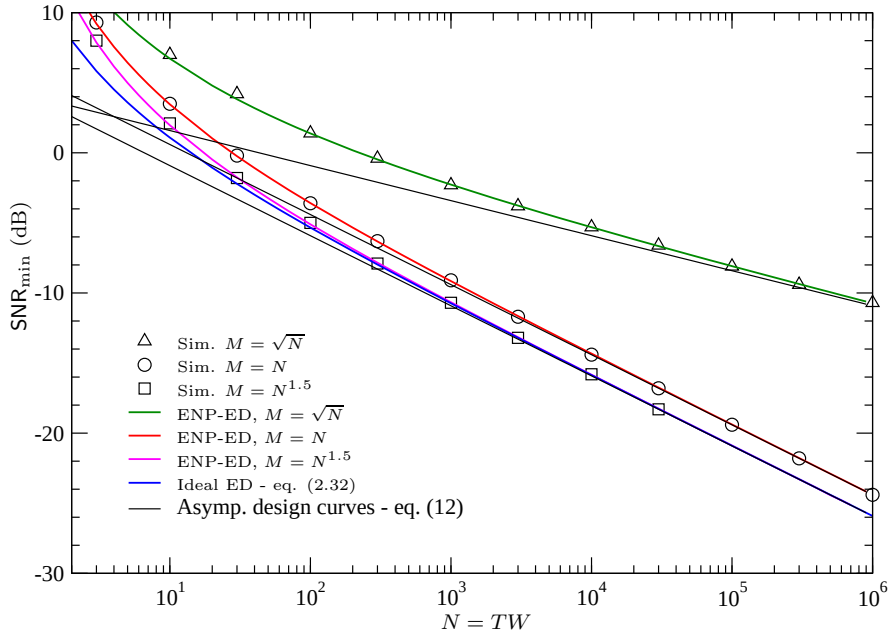

Figure 2.7: Comparison between the theoretical (2.33) and numerically simulated design curves. Simulations performed for $M = \sqrt{N}$, N, $N^{1.5}$ and $\mathrm{P}_{\mathrm{FA}}^{\mathrm{DES}} = 1 - \mathrm{P}_{\mathrm{D}}^{\mathrm{DES}} = 0.1$. The corresponding asymptotical curves (2.12) and the ideal ED curve (2.32) are also plotted.

estimate being used.

To analyze the ENP-ED with $\widehat{\sigma}^2_{\mathrm{ML}}$ in two-step sensing schemes we report in Fig. 2.8 the curves for $M = \lambda \cdot N$ where λ is thus the ratio between the durations of the fine and fast sensing windows. As predicted by (2.13), in this case the difference between the ENP-ED curve and the ideal ED is $10 \log_{10} \left(\frac{1+\lambda}{\lambda}\right)$ dB. This is confirmed in the figure, where for $M = N$ and $M = N/10$ the distance in SNR from the ideal ED curve is about 1.5 dB and 5.2 dB, respectively. The most interesting case for practical situations is when $M > N$. For instance, if the fine-SP is ten times longer than the fast-SP ($M = 10\,N$), the design curve will differ from the ideal one of about 0.2 dB. Then, such schemes allow to exploit the potentiality of ENP-ED providing an asymptotical design curve that can be very tight to the ideal case (2.32).

2.6.4 SNR wall examples

In Fig. 2.8 we also show some examples of the design curve for M assuming constant values, causing the rise of the SNR wall. From (2.11) with $\phi = 1/M$,

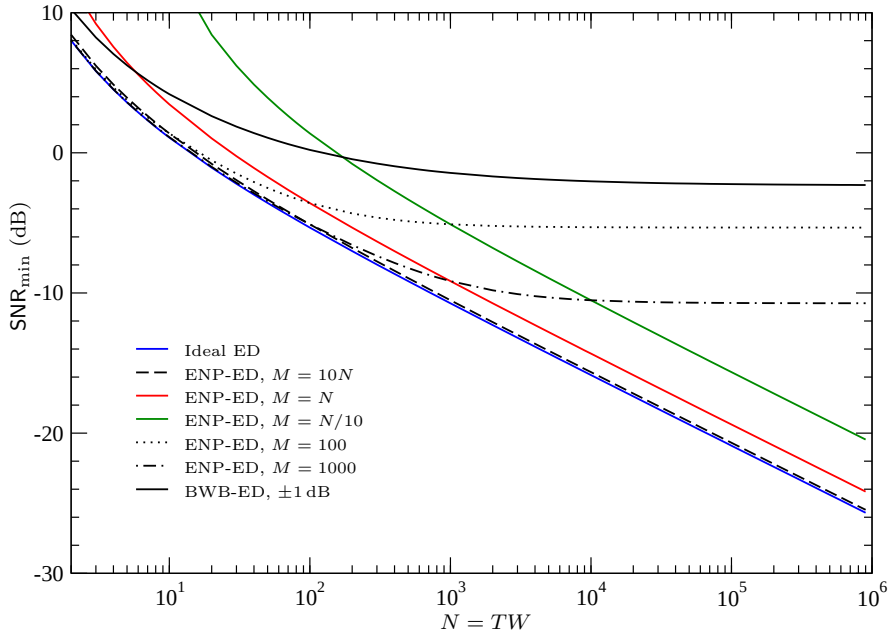

Figure 2.8: Ideal ED (2.32) and ENP-ED design curves (2.33) for $\mathrm{P}_{\mathrm{FA}}^{\mathrm{DES}} = 1 - \mathrm{P}_{\mathrm{D}}^{\mathrm{DES}} = 0.1$. Noise estimation is performed with $M = 10N$, N, $N/10$, 100 and 1000 samples. BWB design curve corresponding to 1 dB noise uncertainty is also shown.

we obtain[12]

$$\mathsf{SNR}_{\mathrm{min,\,ENP\text{-}ED}}^{(\infty)} = \frac{1 - \delta\sqrt{\frac{1}{M}}}{1 - \alpha\sqrt{\frac{1}{M}}} - 1. \tag{2.40}$$

As can be seen in the figure, when $M = 100$, 1000, the $\mathsf{SNR}_{\mathrm{min}}$ approaches -5.3 dB and -10.7 dB, respectively. These values are exactly those predicted by (2.40). It is interesting to investigate if a BWB model could predict similar values for the design curves. Unfortunately, the choice of the range $[\sigma^2_{\mathrm{min}}, \sigma^2_{\mathrm{max}}]$ for the BWB is crucial, and can cause high overestimation of $\mathsf{SNR}_{\mathrm{min}}$. For example, in Fig. 2.8 we report the design curve obtained with the BWB approach, with $\sigma^2_{\mathrm{max}}/\sigma^2 = 1$ dB and $\sigma^2_{\mathrm{min}}/\sigma^2 = -1$ dB as considered in the IEEE 802.22 draft standard [121]. In this case, according to (2.39), we obtain $\mathsf{SNR}_{\mathrm{min}}^{(\infty)} \simeq -2.3$ dB, that is a very high SNR wall value. A further comparison between the two models is shown in Fig. 2.9, where we report the design curves for the ENP-ED with $\widehat{\sigma}^2_{\mathrm{ML}}$ and fixed M, and those for the

[12]Note that (2.34) for $N \to \infty$ and high M is equivalent to (2.40).

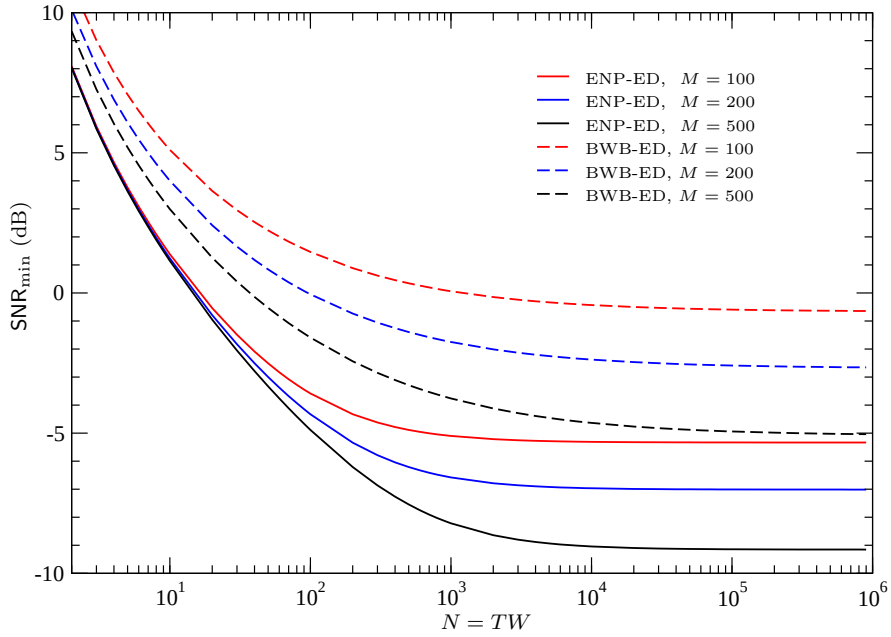

Figure 2.9: Design curve comparison between the ENP-ED with $M = 100, 200, 500$ (eq. (2.33)) and the corresponding BWB case (2.38), with $\sigma^2_{\mathrm{min}} = \sigma^2 - 3\sqrt{var(\widehat{\sigma}^2_{\mathrm{ML}})}$ and $\sigma^2_{\mathrm{max}} = \sigma^2 + 3\sqrt{var(\widehat{\sigma}^2_{\mathrm{ML}})}$. $\mathrm{P}_{\mathrm{FA}}^{\mathrm{DES}} = 1 - \mathrm{P}_{\mathrm{D}}^{\mathrm{DES}} = 0.1$.

BWB assuming $[\sigma^2_{\mathrm{min}}, \sigma^2_{\mathrm{max}}] = \left[\sigma^2 - 3\sqrt{var(\widehat{\sigma}^2_{\mathrm{ML}})}, \sigma^2 + 3\sqrt{var(\widehat{\sigma}^2_{\mathrm{ML}})}\right]$, which corresponds to 99.7% of the cases when $\widehat{\sigma}^2_{\mathrm{ML}}$ is Gaussian. In this case, as can be noted, the SNR wall given by the BWB approach overestimates the exact one by more than 4 dB.

2.7 Conclusion

We analyzed the effect of ENP on the performance of the ED. We proved that noise estimation can avoid the SNR wall if the estimate is consistent with the observation interval. So, the SNR wall phenomenon is not caused by the presence of an uncertainty itself, but is rather due to the impossibility to refine the noise power estimation process while the observation time increases. We proved that the asymptotical behavior of the design curve for the ENP-ED in a log-log scale is linear, and we found its relationship with the variance of the noise power estimator, showing that the maximum slope is -5 dB/decade.

Our analytical expressions are useful for the design of practical ED with direct application to two-step sensing schemes currently considered in CR

standards.

2.8 Appendix

In this section we prove the theorems enunciated in Section 2.3, considering both the Bayesian and the classical models for the signal. The noise variance estimator $\widehat{\sigma}^2$ is assumed unbiased and asymptotically Gaussian, so that, for high N, $\widehat{\sigma}^2 \sim \mathcal{N}(\sigma^2, var(\widehat{\sigma}^2))$. We define the measured received power over the observation window as

$$\nu(\mathbf{y}) \triangleq \frac{1}{2N} \sum_{i=0}^{N-1} |y_i|^2 \tag{2.41}$$

which allows to rewrite (2.4) as $\Lambda_{\mathrm{g}} = \nu(\mathbf{y}) / \widehat{\sigma}^2$.

2.8.1 Gaussian signal

For the Bayesian detection model, $\nu(\mathbf{y})$ in (2.41) has a central chi-squared distribution with $2N$ degrees of freedom, and can therefore be considered Gaussian for large N [109, eq. 26.4.11]. Then we have

$$\begin{array}{ll} \mathcal{H}_0: & \nu(\mathbf{Y}) \sim \mathcal{N}\left(\sigma^2, \sigma^4/N\right) \\ \mathcal{H}_1: & \nu(\mathbf{Y}) \sim \mathcal{N}\left(\sigma_{\mathrm{t}}^2, {\sigma_{\mathrm{t}}}^4/N\right). \end{array} \tag{2.42}$$

Proof of Theorem 1, under Gaussian signal assumption. The $\mathrm{P_{FA}}$ and $\mathrm{P_D}$ computed as the tail probabilities of Gaussian r.v.s are

$$\begin{aligned} \mathrm{P_{FA}} &= \mathrm{P}\left\{\nu(\mathbf{y}) - \xi\,\widehat{\sigma}^2 > 0 | \mathcal{H}_0\right\} \\ &= Q\left(\left(\xi - 1\right) / \sqrt{\frac{1}{N} + \xi^2\,\phi}\right) \end{aligned} \tag{2.43}$$

$$\begin{aligned} \mathrm{P_D} &= \mathrm{P}\left\{\nu(\mathbf{y}) - \xi\,\widehat{\sigma}^2 > 0 | \mathcal{H}_1\right\} \\ &= Q\left(\left(\xi - (1+\mathsf{SNR})\right) / \sqrt{\frac{(1+\mathsf{SNR})^2}{N} + \xi^2\,\phi}\right). \end{aligned} \tag{2.44}$$

From these equations we can compute the minimum value of SNR required to reach the $\mathrm{P_{FA}^{DES}}$ and $\mathrm{P_D^{DES}}$ by solving, in the variables $(\xi_{\mathrm{asymp}}, \mathsf{SNR}_{\mathrm{min}})$, the second order system of equations

$$\begin{cases} \alpha\sqrt{\frac{1}{N} + \xi_{\mathrm{asymp}}^2\,\phi} = \xi_{\mathrm{asymp}} - 1 \\ \delta\sqrt{\frac{(1+\mathsf{SNR}_{\mathrm{min}})^2}{N} + \xi_{\mathrm{asymp}}^2\,\phi} = \xi_{\mathrm{asymp}} - (1+\mathsf{SNR}_{\mathrm{min}}). \end{cases} \tag{2.45}$$

The system above leads to

$$\begin{cases} \xi_{\text{asymp}} = \frac{1+\alpha\sqrt{\phi+1/N-\alpha^2\,\phi/N}}{1-\alpha^2\,\phi} \\ \mathsf{SNR}_{\min} = \frac{1+\alpha\sqrt{\phi+1/N-\alpha^2\,\phi/N}}{1-\alpha^2\,\phi} \cdot \frac{1-\delta\sqrt{\phi+1/N-\delta^2\,\phi/N}}{1-\delta^2/N} - 1. \end{cases} \tag{2.46}$$

From (2.43) and (2.44) we can see that as the SNR decreases, the only way to maintain the same $\mathrm{P_D}$, given a fixed $\mathrm{P_{FA}}$, is to increase N. For this reason it is important to discuss the limit condition $N \to \infty$.

Sufficiency: if $\phi = o\,(1)$ for $N \to \infty$ the system in (2.45) has the solution

$$\begin{cases} \xi_{\text{asymp}}^{(\infty)} = 1 \\ \mathsf{SNR}_{\min}^{(\infty)} = 0. \end{cases} \tag{2.47}$$

Then the SNR wall does not occur.

Necessity: from the system of equations (2.45), we can also see that imposing $\mathsf{SNR}_{\min} = 0$ implies that the left members of the two equations must be equal. Since $\alpha \neq \delta$, the two left members are equal only if they are both equal to zero, i.e. $\phi = o\,(1)$ for $N \to \infty$. Then the condition $\phi = o\,(1)$ is sufficient and necessary for the absence of the SNR wall.

For the second part of the theorem we see that, if $\phi = \Theta\,(1)$ for $N \to \infty$, i.e. if it converges to a finite constant value, ϕ,the solution of (2.45) is

$$\begin{cases} \xi_{\text{asymp}}^{(\infty)} = \frac{1}{1-\alpha\,\sqrt{\phi}} \\ \mathsf{SNR}_{\min}^{(\infty)} = \frac{1-\delta\,\sqrt{\phi}}{1-\alpha\,\sqrt{\phi}} - 1. \end{cases} \tag{2.48}$$

Then, we get a minimum value of SNR under which detection with the target probabilities $(\mathrm{P_{FA}^{DES}}, \mathrm{P_D^{DES}})$ is impossible (SNR wall). Note that, since $var(\widehat{\sigma}^2)$ is proportional to ϕ, then it has exactly the same asymptotical behavior defined by the Landau symbols in the discussion above. □

Proof of Theorem 2, under Gaussian signal assumption. We can prove the asymptotical behaviors of the design curve from equation (2.46).
Assume first that $\phi = \Theta(N^{-\gamma})$ for $N \to \infty$ with $0 < \gamma \leq 1$. Hence we have:

$$\mathsf{SNR}_{\min} \approx (\alpha - \delta)\ \Theta\left(\sqrt{1/N^{\gamma}}\right) + o\left(\sqrt{1/N^{\gamma}}\right) \tag{2.49}$$

that is, in dB:

$$\mathsf{SNR}_{\min}(\mathrm{dB}) \approx -5\,\gamma \log_{10} N + \text{constant} \tag{2.50}$$

which means that the design curve is asymptotically a straight line in the log-log scale.

In particular, if $\phi \approx N^{-\gamma}/\lambda$ for $N \to \infty$, with $0 < \gamma < 1$ and $\lambda > 0$, we get

$$\mathsf{SNR}_{\min} \approx (\alpha - \delta) \sqrt{\frac{1}{\lambda \cdot N^{\gamma}}} + o\left(\sqrt{\frac{1}{N^{\gamma}}}\right) \tag{2.51}$$

that, in dB, is equivalent to (2.12). If $\gamma = 1$, i.e. $\phi = 1/(\lambda N)$, we have

$$\mathsf{SNR}_{\min} \approx (\alpha - \delta) \sqrt{\frac{1+\lambda}{\lambda}\frac{1}{N}} + o\left(\sqrt{1/N}\right) \tag{2.52}$$

that is the same as (2.13).

If $\phi = o(1/N)$ we get

$$\mathsf{SNR}_{\min} \approx (\alpha - \delta) \sqrt{1/N} + o\Big(\sqrt{1/N}\Big) \tag{2.53}$$

that is equivalent to (2.14). Therefore, as N increases, $\mathsf{SNR}_{\min}$ tends to 0 with a slope of $-5\,\mathrm{dB}$/decade as in the $\phi = O(1/N)$ case.
The design curve for the ideal ED can be derived considering $\phi = 0$ in (2.46), that gives exactly (2.53) and (2.14). □

2.8.2 Unknown deterministic signal

In this section we assume the classical model, where the received signal is deterministic. We prove that under this assumption the theorems enunciated in Section 2.3 are still true.
For this model, (2.41) assumes a chi-squared distribution with $2N$ degrees of freedom and non-centrality parameter $2N \cdot \mathsf{SNR}$. For large N, we can use the Gaussian approximation of the non-central chi-squared distribution, and then $\nu(\mathbf{Y}) \sim \mathcal{N}\left(\sigma^2\left(1+\mathsf{SNR}\right), \sigma^4\left(1+2\,\mathsf{SNR}\right)/N\right)$.

Proof of Theorem 1, under unknown deterministic signal assumption. In this case the $\mathrm{P_D}$ for the detection metric (2.4) is

$$\mathrm{P_D} = Q\left(\frac{\xi - (1+\mathsf{SNR})}{\sqrt{\frac{1+2\,\mathsf{SNR}}{N} + \xi^2\,\phi}}\right) \tag{2.54}$$

while the $\mathrm{P_{FA}}$ is still given by (2.43). Imposing the target performance $\left(\mathrm{P_{FA}^{DES}}, \mathrm{P_D^{DES}}\right)$, we get the system of equations

$$\begin{cases} \alpha\sqrt{\frac{1}{N} + \xi_{\text{asymp}}^2\,\phi} = \xi_{\text{asymp}} - 1 \\ \delta\sqrt{\frac{(1+2\,\mathsf{SNR}_{\min})}{N} + \xi_{\text{asymp}}^2\,\phi} = \xi_{\text{asymp}} - (1+\mathsf{SNR}_{\min}) \end{cases} \tag{2.55}$$

that leads to

$$\begin{cases} \xi_{\text{asymp}} = \frac{1+\alpha\sqrt{\phi+1/N-\alpha^2\phi/N}}{1-\alpha^2\phi} \\ \mathsf{SNR}_{\min} = \frac{\delta^2}{N} + \xi_{\text{asymp}} - 1 - \delta\sqrt{\frac{2}{N}(\xi_{\text{asymp}}-1) + \frac{1}{N} + \phi\,\xi_{\text{asymp}}^2 + \frac{\delta^2}{N^2}} \end{cases} \tag{2.56}$$

If $\phi = o(1)$ for $N \to \infty$ we get the same result as in (2.47). Moreover, if we force the solution $\mathsf{SNR}_{\min} = 0$, we see that the only way to satisfy the system (2.56) is that $\phi = o(1)$ for $N \to \infty$, as in the Gaussian signal case.
Similarly, if $\phi = \Theta(1)$, in the limit condition $N \to \infty$ the system (2.56) leads to (2.48). □

Proof of Theorem 2, under unknown deterministic signal assumption. Considering the system of equations (2.56), if $\phi = \Theta\left(N^{-\gamma}\right)$ for $N \to \infty$, we get again (2.49). So all other cases are coincident with the Bayesian model. □

Chapter 3

Test of Independence for Cooperative Spectrum Sensing with Uncorrelated Receivers

3.1 Introduction

Many spectrum sensing techniques have been proposed in literature, starting from the traditional algorithms such as the ED and feature-based detectors. These algorithms can be implemented by a single node or by multiple SUs that cooperates sharing their sensing information. However it has been shown that these techniques present some limitations. Indeed, the adoption of the ED in practical scenarios requires the implementation of a proper noise power estimation strategy [92], and feature detectors can suffer synchronization errors and frequency offsets in realistic environments [59]. Recently, algorithms that exploit the properties of the covariance matrix of the observed signals, often called eigenvalue-based algorithms, have attracted a lot of attention providing good performance results without requiring the knowledge of the noise power nor any prior information on the PU signals [65–69]. Considering a cooperative SUs network, when there are no PUs, the different nodes receive uncorrelated noise observations, that means that the covariance matrix is diagonal. Otherwise, when primary communications are active, the received signals present a certain degree of correlation and we have a non-diagonal covariance matrix. Therefore a proper detection strategy can be based on the observation of the SCM in order to discriminate between correlated received signal and white noise, i.e. to distinguish if PUs are present or not. Most popular detection metrics are based on functions of the SCM, such as the the MME [66], the AGM [65] and the MET [69]. Beyond detection, algorithms

that aim at estimating the number of PUs have been proposed [67].

The GLRT approach, when the noise power level is the same for all SUs, leads to the so called sphericity test, derived by [70]. This algorithm has been recently proposed for sensing in CR systems[1] [65]. However, in a cooperative scenario, different nodes could experience different temperatures or could even have a different RF front-end. Therefore we must consider different levels of noise experienced by the SUs. The generalized likelihood ratio (GLR) in this case has been derived by [129]. We refer to it as independence test. Recently this test has been proposed for signal detection purposes [68, 71]. An alternative approach for exploiting spatial diversity is the adoption of multiple antennas [67–69]. Note that even in this case, if the different antennas are not properly designed and calibrated, the independence test must be adopted in place of the sphericity test [71].

In this chapter we address the analysis of the independence and sphericity tests, studying the threshold setting problem under the Neyman-Pearson framework. In order to reduce the complexity of the analysis we approximate the tests to beta distributed r.v.s using a moment-matching approach. We provide simple and analytically tractable expressions easy to use for the computation of the probability of false alarm and for setting the decision threshold. Numerical simulations show that these approximated forms match very well the empirical cumulative distribution function (CDF), even with a small number of samples collected, outperforming the asymptotical chi squared approximation for the GLR.

3.2 System model

Given n_{R} cooperative SUs, we assume that, after bandpass filtering and down-conversion, the output of the receiving antennas at the i-th time instant is

$$\mathbf{y}_i = \mathbf{H}\,\mathbf{x}_i + \mathbf{n}_i \tag{3.1}$$

where $\mathbf{x}_i$ is the vector of the symbols transmitted by the n_{T} PUs present, $\mathbf{H} \in \mathcal{M}_{n_{\mathrm{R}} \times n_{\mathrm{T}}}(\mathbb{C})$ is the matrix describing the gain of the radio channel between the n_{T} signal sources and the n_{R} users, and $\mathbf{n}_i \in \mathbb{C}^{n_{\mathrm{R}}}$ represents the thermal noise. We assume that the elements of $\mathbf{n}_i$ are independent zero mean complex Gaussian r.v.s and that $\mathbf{x}_i \sim \mathcal{CN}(\mathbf{0}, \mathbf{R}_x)$. Collecting n_{S} instances of

[1] Note that the sphericity test, adopted throughout the paper, is the reciprocal of the AGM.

$\mathbf{y}_i$ we form the matrix

$$\mathbf{Y} = (\mathbf{y}_1 | \cdots | \mathbf{y}_{n_\mathrm{S}}) . \tag{3.2}$$

Based on the observation of $\mathbf{Y}$ we would like to decide whether PUs signals are absent or present, i.e. whether $n_\mathrm{T} = 0$ or $n_\mathrm{T} > 0$. We indicate these two hypotheses with $\mathcal{H}_0$ and $\mathcal{H}_1$, respectively. Under $\mathcal{H}_0$ we have $\mathbf{y}_i = \mathbf{n}_i$, then the columns of $\mathbf{Y}$ are independent vectors and the covariance matrix of $\mathbf{Y}$, $\mathbf{\Sigma}_0$, is diagonal. Under $\mathcal{H}_1$ the columns of $\mathbf{Y}$ are correlated. In order to consider the most general case we do not assume any particular structure of the covariance matrix $\mathbf{\Sigma}_1$. Within the paper we always assume $n_\mathrm{S} > n_\mathrm{R}$.

3.2.1 GLRT derivation

Under the $\mathcal{H}_j$ hypothesis, with $j = 0, 1$, the likelihood function of $\mathbf{Y}$ is given by

$$\mathcal{L}(\mathbf{Y}|\mathbf{\Sigma}_j) = \frac{1}{\pi^{n_\mathrm{R} n_\mathrm{S}} \left|\mathbf{\Sigma}_j\right|^{n_\mathrm{S}}} \exp\left(-n_\mathrm{S} \operatorname{tr}\left\{\mathbf{\Sigma}_j^{-1}\mathbf{S}\right\}\right) \tag{3.3}$$

where the SCM is defined as

$$\mathbf{S} = \frac{1}{n_\mathrm{S}} \mathbf{Y}\mathbf{Y}^\mathrm{H}. \tag{3.4}$$

The GLR to detect the hypothesis $\mathcal{H}_0$ is

$$\frac{\mathcal{L}\left(\mathbf{Y}|\widehat{\mathbf{\Sigma}}_0\right)}{\mathcal{L}\left(\mathbf{Y}|\widehat{\mathbf{\Sigma}}_1\right)}. \tag{3.5}$$

Given the assumptions on the covariance matrix, inserting (3.3) in (3.5) and using the ML estimates $\widehat{\mathbf{\Sigma}}_0$ and $\widehat{\mathbf{\Sigma}}_1$, it is easy to see that the sufficient statistic is the ratio of the determinants of $\widehat{\mathbf{\Sigma}}_1$ and $\widehat{\mathbf{\Sigma}}_0$. Therefore the GLRT reduces to the test

$$\mathrm{T} = \frac{\left|\widehat{\mathbf{\Sigma}}_1\right|}{\left|\widehat{\mathbf{\Sigma}}_0\right|} \underset{\mathcal{H}_1}{\overset{\mathcal{H}_0}{\gtrless}} \xi. \tag{3.6}$$

where $0 \leq \xi \leq 1$.

3.3 Approximated GLR distributions

3.3.1 Moment matching based Beta approximation

In order to derive an approximated distribution of the GLR we propose a moment-matching approach. Although the exact distribution of the GLR can assume complex forms, often its moments can be derived in simple expressions. Then we can approximate the distribution of T adopting a simpler distribution model chosen among the most common ones (Gaussian, chi-squared, ...), and setting its k parameters in order to match the first k true moments of T. This moment-matching approach has been proposed in recent studies on statistical signal processing, such as [130]. Considering that the GLR lies between 0 and 1, it is natural to choose a beta distribution to approximate its p.d.f..

The p-th moment of a beta distributed r.v. with parameters a and b is given by

$$\mathsf{m}_p^{(\beta)} = \frac{\Gamma(\mathsf{a}+\mathsf{b})\,\Gamma(\mathsf{a}+p)}{\Gamma(\mathsf{a})\,\Gamma(\mathsf{a}+\mathsf{b}+p)}. \tag{3.7}$$

Denoting with m_1 and m_2 the first and the second moments of T respectively, we can match them to $\mathsf{m}_1^{(\beta)}$ and $\mathsf{m}_2^{(\beta)}$ obtaining

$$\mathsf{a} = \frac{\mathsf{m}_1\,(\mathsf{m}_2-\mathsf{m}_1)}{\mathsf{m}_1^2-\mathsf{m}_2}, \tag{3.8}$$

$$\mathsf{b} = \frac{(1-\mathsf{m}_1)\,(\mathsf{m}_2-\mathsf{m}_1)}{\mathsf{m}_1^2-\mathsf{m}_2}. \tag{3.9}$$

Thus, the approximated p.d.f. of T is given by

$$f(\mathrm{T};t) \simeq \begin{cases} \frac{1}{B(\mathsf{a},\mathsf{b})}\,t^{\mathsf{a}-1}\,(1-t)^{\mathsf{b}-1}, & 0\le t\le 1 \\ 0, & \text{otherwise} \end{cases} \tag{3.10}$$

where $B(\mathsf{a},\mathsf{b}) = \int_0^1 x^{\mathsf{a}-1}\,(1-x)^{\mathsf{b}-1}\,dx$ is the beta function [131].

Defining the probability of false alarm for T as $\mathrm{P_{FA}} \triangleq \Pr\{\mathrm{T} < \xi|\mathcal{H}_0\}$, from (3.10) we obtain

$$\mathrm{P_{FA}} \simeq \int_0^{\xi} \frac{1}{B(\mathsf{a},\mathsf{b})}\,t^{\mathsf{a}-1}\,(1-t)^{\mathsf{b}-1}\,dt = \widetilde{B}(\mathsf{a},\mathsf{b},\xi) \tag{3.11}$$

where $\widetilde{B}(\mathsf{a},\mathsf{b},\xi) = \frac{1}{B(\mathsf{a},\mathsf{b})}\int_0^{\xi} x^{\mathsf{a}-1}\,(1-x)^{\mathsf{b}-1}\,dx$ is the regularized beta function [131].

In the Neyman-Pearson framework the decision threshold is set in order to provide a target probability of false alarm, $\mathrm{P}_{\mathrm{FA}}^{\mathrm{DES}}$. In our case the threshold can be obtained inverting (3.11) as

$$\xi = \widetilde{B}^{-1}\big(\mathsf{a}, \mathsf{b}, \mathrm{P}_{\mathrm{FA}}^{\mathrm{DES}}\big)\,. \tag{3.12}$$

Note that $\widetilde{B}^{-1}(\cdot,\cdot,\cdot)$ can be easily computed by using standard mathematical software.

3.3.2 Chi-squared approximation

Alternative approximated distributions have been studied for the GLR in (3.6). In particular, [132] shows that asymptotically the CDF of the GLR can be expressed as a linear combination of gamma functions. However these expressions are not practical for threshold setting because they do not have an analytical inverse form.

A more common approximation is the asymptotical chi-squared distribution [46]

$$-2\,n_{\mathrm{S}} \log \mathrm{T} \sim \chi^2_{\Delta_{\mathsf{dof}}}(0) \tag{3.13}$$

where Δ_{dof} is the difference between the degrees of freedom (d.o.f.) of T in the hypothesis $\mathcal{H}_1$ and in the hypothesis $\mathcal{H}_0$. From (3.13) we obtain the approximated P_{FA}

$$\mathrm{P}_{\mathrm{FA}} \approx \widetilde{\Gamma}(\Delta_{\mathsf{dof}}/2, -n_{\mathrm{S}}\, \log \xi) \tag{3.14}$$

where $\widetilde{\Gamma}(n,x) = \frac{1}{\Gamma(n)} \int_x^\infty x^{n-1} \exp(-x) dx$ is the regularized gamma function. Given the target probability of false alarm $\mathrm{P}_{\mathrm{FA}}^{\mathrm{DES}}$, the threshold level can be set as

$$\xi = \exp\left(-\frac{1}{n_{\mathrm{S}}} \widetilde{\Gamma}^{-1}\big(\Delta_{\mathsf{dof}}/2, \mathrm{P}_{\mathrm{FA}}^{\mathrm{DES}}\big)\right). \tag{3.15}$$

3.4 Independence test

In this section we characterize the previous analysis for the independence test, that is the GLR when each node experiences a different noise power level. In this case, under $\mathcal{H}_0$, $\boldsymbol{\Sigma}_0$ is diagonal and its ML estimate is $\widehat{\boldsymbol{\Sigma}}_0 = \mathrm{diag}\{\mathbf{S}\}$. Under $\mathcal{H}_1$ we have $\widehat{\boldsymbol{\Sigma}}_1 = \mathbf{S}$. Then we can express the GLRT as

$$\mathrm{T}^{(\mathrm{ind})} = \frac{|\mathbf{S}|}{\prod_{k=1}^{n_{\mathrm{R}}} s_{k,k}} \underset{\mathcal{H}_1}{\overset{\mathcal{H}_0}{\gtrless}} \xi \tag{3.16}$$

where $s_{i,j}$ is the (i,j) element of $\mathbf{S}$. Note that $\mathrm{T}^{(\mathrm{ind})}$ equals the determinant of the sample correlation matrix given by $\mathbf{C} = \mathbf{WSW}$, where the matrix $\mathbf{W}$ is diagonal with $\mathrm{diag}\{\mathbf{W}\} = \left(1/\sqrt{s_{1,1}}, \ldots, 1/\sqrt{s_{n_\mathrm{R},n_\mathrm{R}}}\right)$ [71, 132].

In order to study the distribution of the independence test it is useful to decompose $\mathrm{T}^{(\mathrm{ind})}$ using a proper factorization. Assuming that $\mathbf{S}_{(k)}k$ is the k-th order upper left principal minor of $\mathbf{S}$, we define

$$\mathrm{T}_k \triangleq \frac{\left|\mathbf{S}_{(k)}k\right|}{\left|\mathbf{S}_{(k)}k-1\right| \cdot s_{k,k}}. \tag{3.17}$$

Then from (3.16) we can write

$$\mathrm{T}^{(\mathrm{ind})} = \mathrm{T}_{n_\mathrm{R}}\mathrm{T}_{n_\mathrm{R}-1}\cdots\mathrm{T}_2 = \prod_{k=2}^{n_\mathrm{R}} \mathrm{T}_k. \tag{3.18}$$

Using the following theorem it is possible to demonstrate that under $\mathcal{H}_0$ the factors T_k are independent beta distributed r.v.s.

Theorem 3 (On the distribution of the independence test)**.** *Consider the test statistic defined in* (3.16)*, where* $\mathbf{S}$ *is the SCM of a* n_R*-variate complex Gaussian population with zero mean and diagonal covariance matrix. Then* $T^{(ind)}$ *equals the product of* n_R-1 *independent beta distributed r.v.s* T_k*, with* $k = 2, \ldots, n_R$*, with p.d.f.*

$$\begin{cases} \frac{1}{B(n_S-k+1,k-1)}\, t^{n_S-k}\,(1-t)^{k-2}, & 0 \le t \le 1 \\ 0, & \textit{otherwise.} \end{cases} \tag{3.19}$$

The proof of this theorem has been presented for real r.v.s in [132], recalling some results on multivariate linear regression hypothesis testing. In the appendix we provide a proof valid for complex r.v.s (see also [133]).

The exact distribution of the product of independent beta distributed r.v.s has been expressed in closed form as the Meijer G-function multiplied by a normalizing constant in [134]. However, setting the decision threshold requires the inversion of this expression, that is analytically intractable. Using the expressions of the moments of $\mathrm{T}^{(\mathrm{ind})}$ we can adopt the beta distribution described in the previous section. Thanks to the independence of the factors T_k in (3.18), we can derive the p-th moment of $\mathrm{T}^{(\mathrm{ind})}$, $\mathsf{m}_p^{(\mathrm{ind})}$, as the product of the p-th moments of the $(k-1)$ r.v.s T_k. Therefore using (3.7) we get

$$\mathsf{m}_p^{(\mathrm{ind})} = \left(\frac{\Gamma(n_\mathrm{S})}{\Gamma(n_\mathrm{S}+p)}\right)^{n_\mathrm{R}-1} \prod_{k=1}^{n_\mathrm{R}-1} \frac{\Gamma(n_\mathrm{S}-k+p)}{\Gamma(n_\mathrm{S}-k)}. \tag{3.20}$$

Substituting $\mathsf{m}_1^{(\mathrm{ind})}$ and $\mathsf{m}_2^{(\mathrm{ind})}$ in (3.8) and (3.9) we obtain the parameters, named $\mathsf{a}^{(\mathrm{ind})}$ and $\mathsf{b}^{(\mathrm{ind})}$, of the beta r.v. that approximate $\mathrm{T}^{(\mathrm{ind})}$. Replacing $\mathsf{a}^{(\mathrm{ind})}$ and $\mathsf{b}^{(\mathrm{ind})}$ in (3.11) and (3.12) we get the corresponding approximated $\mathrm{P_{FA}}$ and threshold level.

Note that, when $n_{\mathrm{R}}=2$, $\mathrm{T}^{(\mathrm{ind})}=\mathrm{T}_2$. Therefore from Theorem 3 we obtain the exact distribution of $\mathrm{T}^{(\mathrm{ind})}$ as

$$\begin{cases}(n_{\mathrm{S}}-1)\,t^{n_{\mathrm{S}}-2}, & 0\le t\le 1\\ 0, & \text{otherwise}\end{cases} \tag{3.21}$$

and $\mathrm{P_{FA}}=\xi^{n_{\mathrm{S}}-1}$, with $0\le\xi\le 1$.

3.5 Sphericity test

In this section we characterize the analysis in Section 3.2 for the sphericity test. If the SUs experience the same noise level, σ^2, under $\mathcal{H}_0$ we have a covariance matrix that is proportional to the identity matrix, i.e. $\mathbf{\Sigma}_0 = \sigma^2\,\mathbf{I}_{n_{\mathrm{R}}}$. In this case we have the ML estimate $\widehat{\mathbf{\Sigma}}_0 = \widehat{\sigma}^2\,\mathbf{I}_{n_{\mathrm{R}}}$, where $\widehat{\sigma}^2 = \mathrm{tr}\{\mathbf{S}\}/n_{\mathrm{R}}$, while under $\mathcal{H}_1$ we still have $\widehat{\mathbf{\Sigma}}_1=\mathbf{S}$. Then from (3.6) we get

$$\mathrm{T}^{(\mathrm{sph})}=\frac{|\mathbf{S}|}{\left(\mathrm{tr}\{\mathbf{S}\}/n_{\mathrm{R}}\right)^{n_{\mathrm{R}}}}\underset{\mathcal{H}_1}{\overset{\mathcal{H}_0}{\gtrless}}\xi. \tag{3.22}$$

The exact distribution of $\mathrm{T}^{(\mathrm{sph})}$ is given by [135] as infinite sums expressions that are not easily tractable for threshold setting. Using the moments of $\mathrm{T}^{(\mathrm{sph})}$, provided by [135] as

$$\mathsf{m}_p^{(\mathrm{sph})}=\frac{n_{\mathrm{R}}^{n_{\mathrm{R}}p}\Gamma(n_{\mathrm{S}}n_{\mathrm{R}})}{\Gamma(n_{\mathrm{S}}n_{\mathrm{R}}+n_{\mathrm{R}}p)}\prod_{i=1}^{n_{\mathrm{R}}}\frac{\Gamma(n_{\mathrm{S}}-i+1+p)}{\Gamma(n_{\mathrm{S}}-i+1)} \tag{3.23}$$

we can adopt the moment-matching beta distribution. The corresponding beta parameters $\mathsf{a}^{(\mathrm{sph})}$ and $\mathsf{b}^{(\mathrm{sph})}$ can be obtained inserting $\mathsf{m}_1^{(\mathrm{sph})}$ and $\mathsf{m}_2^{(\mathrm{sph})}$ in (3.8) and (3.9). Replacing $\mathsf{a}^{(\mathrm{sph})}$ and $\mathsf{b}^{(\mathrm{sph})}$ in (3.11) and (3.12) we get the corresponding approximated $\mathrm{P_{FA}}$ and threshold level.

In [135] a simple exact distribution of $\mathrm{T}^{(\mathrm{sph})}$ for the case $n_{\mathrm{R}}=2$ has been provided as[2]

$$\begin{cases}\frac{1}{B\left(n_{\mathrm{S}}-1,\frac{3}{2}\right)}\,t^{n_{\mathrm{S}}-2}\,(1-t)^{1/2}, & 0\le t\le 1\\ 0, & \text{otherwise.}\end{cases} \tag{3.24}$$

Therefore the corresponding probability of false alarm is given by $\mathrm{P_{FA}}=\widetilde{B}\left(n_{\mathrm{S}}-1,\frac{3}{2},\xi\right)$, with $0\le\xi\le 1$.

[2]Note that in [135, eq. (3.8)] $\Gamma(N-1/2)$ should be replaced with $\Gamma(N+1/2)$.

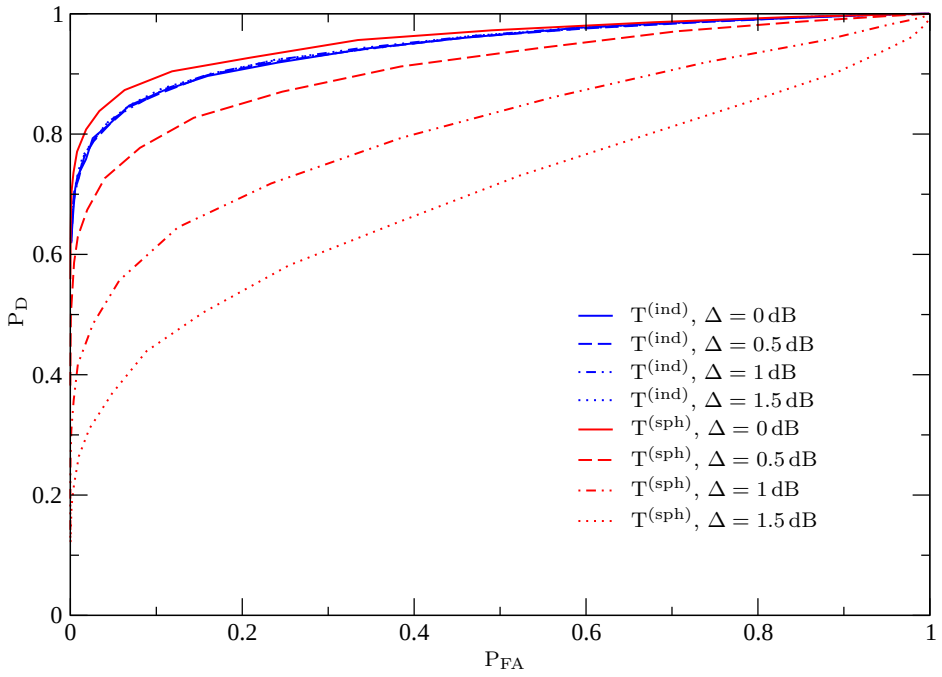

Figure 3.1: ROC comparison between $T^{(ind)}$ and $T^{(sph)}$ in presence of 4 SUs and a single PU. We assume that the noise power levels in dB at the SUs' receivers equal $(\sigma^2_{ref}, \sigma^2_{ref} + \Delta, \sigma^2_{ref} - \Delta, \sigma^2_{ref})$. The reference level σ^2_{ref} correspond to $\mathsf{SNR} = -10\,dB$. $n_S = 500$.

3.6 Numerical results

3.6.1 Detection in presence of uncalibrated receivers

Many studies in literature present cooperative CR systems in which the SUs are supposed to have the same noise power. However the different nodes could experience a different temperature level, have receiver chains with different characteristics or even with a completely different architecture. Therefore it is unlikely that they experience exactly the same noise power. Considering the GLRT analysis this implies that the independence test is preferable to the sphericity test in cooperative scenarios. In Fig. 3.1 we show a comparison between the receiver operating characteristic (ROC) curves of the $T^{(ind)}$ and $T^{(sph)}$, with $n_R = 4$ and $n_S = 500$. We consider the presence of a single PU, therefore the vector $\mathbf{x}_i$ in (3.1) reduces to a single complex number $x_i \sim \mathcal{CN}(0, \sigma_x^2)$. We assume that the elements of the channel matrix are i.i.d. zero mean complex Gaussian elements (Rayleigh fading) and that $\mathbf{H}$ is constant during the n_S observations. The reference noise power level is σ^2_{ref}

$(n_{\mathrm{R}}, n_{\mathrm{S}})$	(8,10)	(8,20)	(8,50)	(8,100)	(8,500)
β approx.	0.0598	0.0965	0.0999	0.1012	0.1010
χ^2 approx.	0.8366	0.3737	0.1765	0.1361	0.1074
$(n_{\mathrm{R}}, n_{\mathrm{S}})$	(20,100)	(20,200)	(20,500)	(20,1000)	(20,2000)
β approx.	0.0986	0.0969	0.1006	0.1005	0.0998
χ^2 approx.	0.4082	0.2197	0.1407	0.1189	0.1093

Table 3.1: Estimated $\mathrm{P_{FA}}$ for $\mathrm{T}^{(\mathrm{ind})}$ for selected values of n_{R} and n_{S} and $\mathrm{P}_{\mathrm{FA}}^{\mathrm{DES}} = 0.1$.

and the SNR is defined as $\mathsf{SNR} = \sigma_x^2/\sigma_{\mathrm{ref}}^2$. We can see that $\mathrm{T}^{(\mathrm{sph})}$ performs better than $\mathrm{T}^{(\mathrm{ind})}$ when all the SUs have the same noise power σ_{ref}^2. However, in a cooperative scenario it is very likely that the noise power level is not the same at different SUs. In Fig. 3.1 we consider the case in which the noise power in dB experienced by the four nodes equal $(\sigma_{\mathrm{ref}}^2, \sigma_{\mathrm{ref}}^2 + \Delta, \sigma_{\mathrm{ref}}^2 - \Delta, \sigma_{\mathrm{ref}}^2)$, where Δ represents a deviation from σ_{ref}^2. We can see that the ROC of $\mathrm{T}^{(\mathrm{sph})}$ rapidly lowers down with an increasing Δ, while the performance $\mathrm{T}^{(\mathrm{ind})}$ does not depend on its value. Therefore, in presence of uncalibrated receivers it is better to adopt the independence test, which is robust to imbalances of the noise power level.

3.6.2 Approximated distributions

In this section we present some comparisons between the moment-matching beta approximation and the estimated CDF for the $\mathrm{T}^{(\mathrm{ind})}$ and $\mathrm{T}^{(\mathrm{sph})}$ under $\mathcal{H}_0$.[3] The beta approximation is evaluated using the exact moments, derived in sections 3.4 and 3.5, into the general expressions (3.8), (3.9) and (3.11).

Fig 3.2 shows the CDF of $\mathrm{T}^{(\mathrm{ind})}$ with $n_{\mathrm{S}} = 20$ and $n_{\mathrm{R}} = 4, 6, 8$. We can see that the beta approximation matches very well the empirical curves, also when n_{S} is relatively small. In Fig. 3.4 a similar comparison is reported, showing that the beta distribution provide a good approximation even for higher values of n_{S}. In Fig. 3.3 and 3.5 we show analogous comparisons for $\mathrm{T}^{(\mathrm{sph})}$. We can see that also for this test the beta distribution provides a very good approximation to the empirical curve.

Alternatively, $\mathrm{T}^{(\mathrm{ind})}$ and $\mathrm{T}^{(\mathrm{sph})}$ can be approximated using the asymptotical chi-squared approximations described is section 3.3.2, where the number of d.o.f. is $n_{\mathrm{R}}\,(n_{\mathrm{R}} - 1)$ for $\mathrm{T}^{(\mathrm{ind})}$ and $n_{\mathrm{R}}^2 - 1$ for $\mathrm{T}^{(\mathrm{sph})}$. In Fig. 3.4 and 3.5 we can see that the chi-squared approximation matches the empirical CDF only

[3]Note the CDF under $\mathcal{H}_0$ correspond to the $\mathrm{P_{FA}}$.

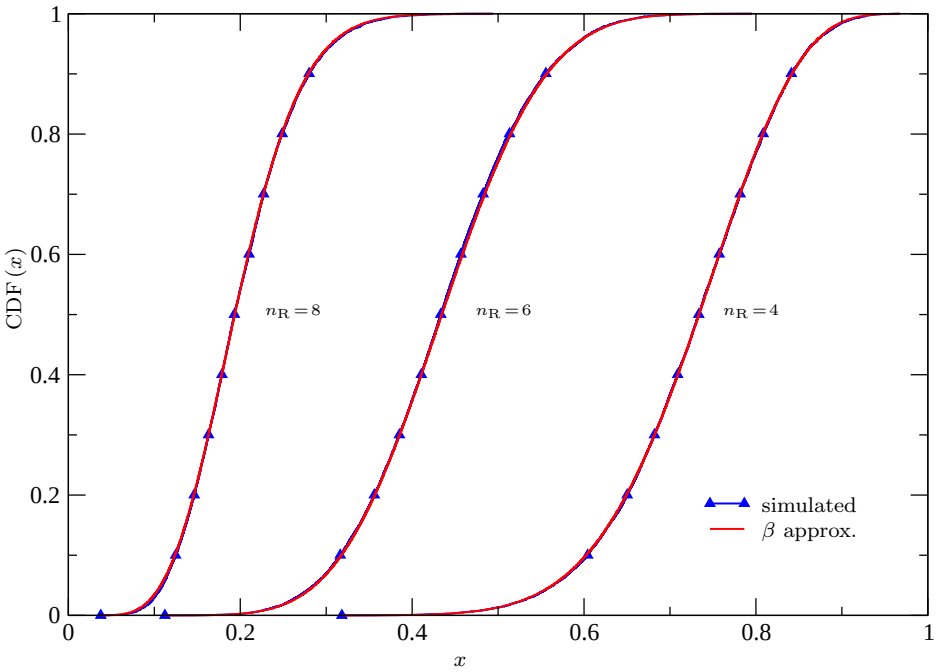

Figure 3.2: Comparison between the CDF based on the moment matching strategy and numerically simulated curve for $T^{(ind)}$ under $\mathcal{H}_0$ with $n_S = 20$.

for large n_S.

In table 3.1 we report some numerical values of the estimated P_{FA} for the test $T^{(ind)}$ for selected values of (n_R, n_S) with $P_{FA}^{DES} = 0.1$. Monte-Carlo simulations have been performed with 50000 trials. To evaluate the performance of the beta approximation we set the decision threshold according (3.12) using $\mathsf{a}^{(ind)}$ and $\mathsf{b}^{(ind)}$. For the chi-squared approximation the threshold is set using (3.12) with $\Delta_{\mathsf{dof}} = n_R (n_R - 1)$. We can see that the beta approximation provides in every case an estimated P_{FA} that is closer to the desired value P_{FA}^{DES}, even for low values of n_S. On the contrary, the chi-squared based threshold setting provides an acceptable P_{FA} only when $n_S \gg n_R$.

3.7 Conclusions

We studied the problem of cooperative spectrum sensing in CR networks. When the noise level is the same for all the SUs, the GLRT approach leads to the sphericity test. However, in cooperative scenarios the most proper assumption is that every node experiences a different noise power level. The GLRT in this case is the independence test. We showed that both tests can be approximated as beta distributed r.v.s and provided easy to use expressions

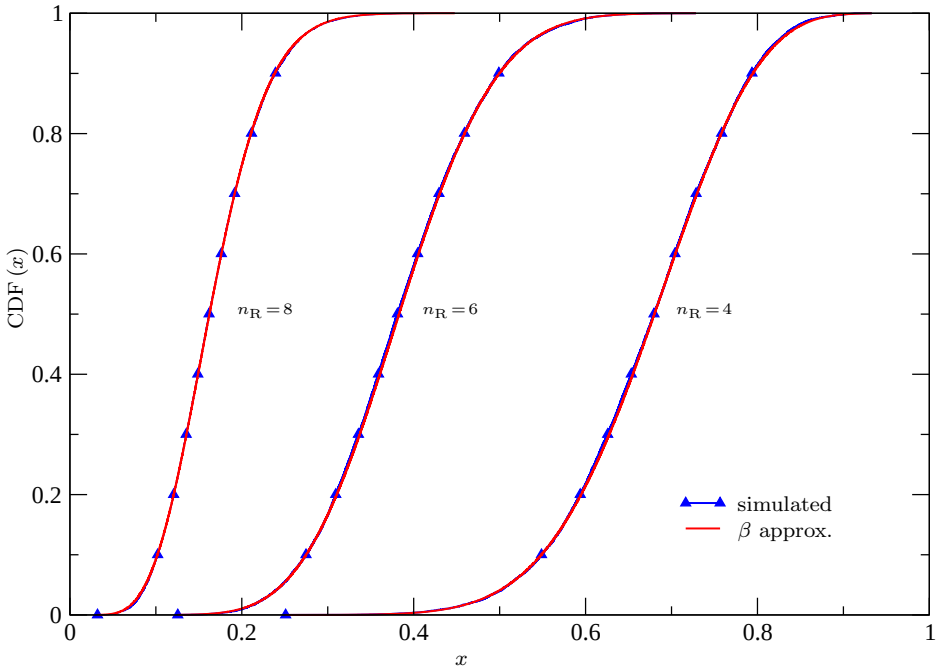

Figure 3.3: Comparison between the CDF based on the moment matching strategy and numerically simulated curve for $\mathrm{T}^{(\mathrm{sph})}$ under $\mathcal{H}_0$ with $n_{\mathrm{S}} = 20$.

for evaluation of the probability of false alarm and for setting the decision threshold. Numerical simulations confirm the accuracy of the approximations. It is concluded that, due to its robustness to unbalanced SU receivers, the independence test is a good candidate for cooperative spectrum sensing.

3.8 Appendix

Proof of Theorem 3. We define $\widetilde{\mathbf{y}}_k \in \mathbb{C}^{n_{\mathrm{S}}}$ as the k-th row of the observation matrix $\mathbf{Y}$ and $\mathbf{Y}_k \in \mathcal{M}_{k\times n_{\mathrm{S}}}(\mathbb{C})$ as $\left(\widetilde{\mathbf{y}}_1^{\mathrm{T}}|\cdots|\widetilde{\mathbf{y}}_k^{\mathrm{T}}\right)^{\mathrm{T}}$. Then the T_k in (3.17) can be expressed as

$$\begin{aligned}\mathrm{T}_k &= \frac{\left|\mathbf{Y}_k\,\mathbf{Y}_k^{\mathrm{H}}\right|}{\left|\mathbf{Y}_{k-1}\,\mathbf{Y}_{k-1}^{\mathrm{H}}\right|\cdot\widetilde{\mathbf{y}}_k\,\widetilde{\mathbf{y}}_k^{\mathrm{H}}} \\ &= \frac{\widetilde{\mathbf{y}}_k\widetilde{\mathbf{y}}_k^{\mathrm{H}} - \widetilde{\mathbf{y}}_k\mathbf{Y}_{k-1}^{\mathrm{H}}\left(\mathbf{Y}_{k-1}\mathbf{Y}_{k-1}^{\mathrm{H}}\right)^{-1}\mathbf{Y}_{k-1}\widetilde{\mathbf{y}}_k^{\mathrm{H}}}{\widetilde{\mathbf{y}}_k\,\widetilde{\mathbf{y}}_k^{\mathrm{H}}}\end{aligned} \tag{3.25}$$

where the second equality can be applied because $\mathbf{Y}_{k-1}\mathbf{Y}_{k-1}^{\mathrm{H}}$ is a non singular matrix [46]. Under $\mathcal{H}_0$, $\mathbf{Y}_k = \mathbf{W}_k\,\mathbf{Z}_k$, where $\mathbf{W}_k$ is a diagonal matrix with

$\mathrm{diag}\{\mathbf{W}_k\} = \left(\sqrt{\sigma_1^2}, \ldots, \sqrt{\sigma_k^2}\right)$ and $\mathbf{Z}_k \in \mathcal{M}_{k\times n_\mathrm{S}}(\mathbb{C})$ is a matrix with complex Gaussian distributed elements with zero mean and unitary variance. Thus we can write $\widetilde{\mathbf{y}}_k = \sigma_k\, \widetilde{\mathbf{z}}_k$, where $\widetilde{\mathbf{z}}_k$ is the k-th row of $\mathbf{Z}_k$. From (3.25) we can express T_k as

$$\mathrm{T}_k = \frac{\widetilde{\mathbf{z}}_k\widetilde{\mathbf{z}}_k^\mathrm{H} - \widetilde{\mathbf{z}}_k\mathbf{Z}_{k-1}^\mathrm{H}\left(\mathbf{Z}_{k-1}\mathbf{Z}_{k-1}^\mathrm{H}\right)^{-1}\mathbf{Z}_{k-1}\widetilde{\mathbf{z}}_k^\mathrm{H}}{\widetilde{\mathbf{z}}_k\,\widetilde{\mathbf{z}}_k^\mathrm{H}} \tag{3.26}$$

due to the properties of the inverse of a product of matrices. The rows of the matrix $\mathbf{Z}_{k-1}$ are $(k-1)$ independent vectors, therefore they can be considered as the generators of a $(k-1)$-dimensional subspace, $\mathcal{W}$, in a n_S-dimensional space. Denoting the orthogonal projection of $\widetilde{\mathbf{z}}_k$ on $\mathcal{W}$ and on $\mathcal{W}^\perp$ as $\mathrm{P}_\mathcal{W}(\widetilde{\mathbf{z}}_k)$ and $\mathrm{P}_{\mathcal{W}^\perp}(\widetilde{\mathbf{z}}_k)$, respectively, we can compute $\mathrm{P}_\mathcal{W}(\widetilde{\mathbf{z}}_k)$ as $\mathbf{A}\,\mathbf{Z}_{k-1}$, where the projection matrix is

$$\mathbf{A} = \widetilde{\mathbf{z}}_k\mathbf{Z}_{k-1}^\mathrm{H}\left(\mathbf{Z}_{k-1}\mathbf{Z}_{k-1}^\mathrm{H}\right)^{-1}.$$

Note that the numerator of (3.26) equals

$$||\mathrm{P}_{\mathcal{W}^\perp}(\widetilde{\mathbf{z}}_k)\,||^2 = \left(\widetilde{\mathbf{z}}_k - \mathbf{A}\mathbf{Z}_{k-1}\right)\left(\widetilde{\mathbf{z}}_k - \mathbf{A}\mathbf{Z}_{k-1}\right)^\mathrm{H}. \tag{3.27}$$

This measure is the squared length of a complex vector laying in a $(n_\mathrm{S}-k+1)$-dimensional space and thus is a chi-squared distributed r.v. with $2\,(n_\mathrm{S}-k+1)$ d.o.f.. Similarly, it is easy to show that $||\mathrm{P}_\mathcal{W}(\widetilde{\mathbf{z}}_k)\,||^2$ is chi-squared distributed with $2\,(k-1)$ d.o.f.. Rewriting T_k as

$$\mathrm{T}_k = \frac{||\mathrm{P}_{\mathcal{W}^\perp}(\widetilde{\mathbf{z}}_k)\,||^2}{||\mathrm{P}_{\mathcal{W}^\perp}(\widetilde{\mathbf{z}}_k)\,||^2 + ||\mathrm{P}_\mathcal{W}(\widetilde{\mathbf{z}}_k)\,||^2} \tag{3.28}$$

it follows that it is a beta distributed r.v., with p.d.f. given by (3.19) [131, sec. 26.5].

Since this distribution does not depend on $\mathbf{Z}_{k-1}$, we see that T_k is independent of $\mathbf{Z}_{k-1}$, and hence independent of $\mathrm{T}_2, \ldots, \mathrm{T}_{k-1}$. Then $\mathrm{T}_2, \ldots, \mathrm{T}_k$ are independent [132]. □

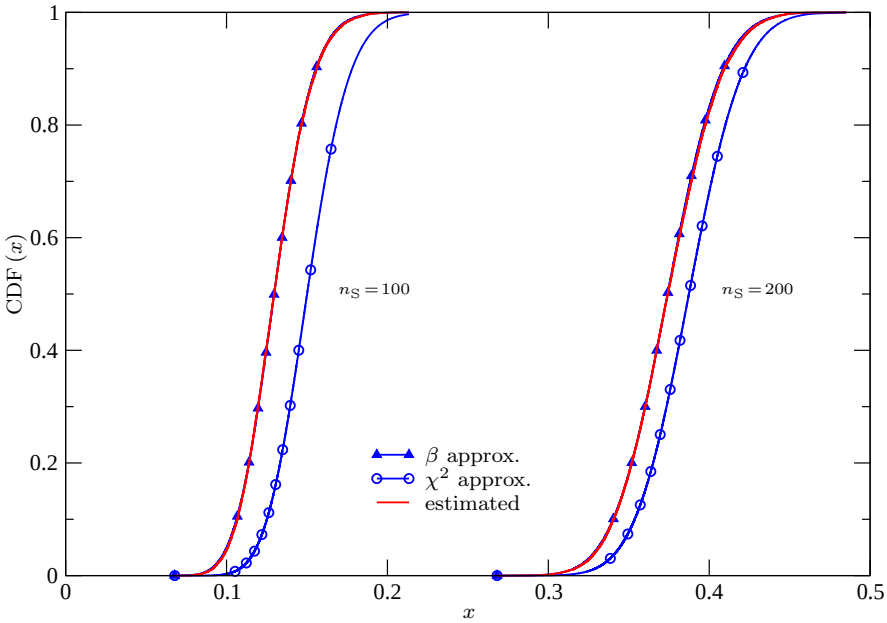

(a)

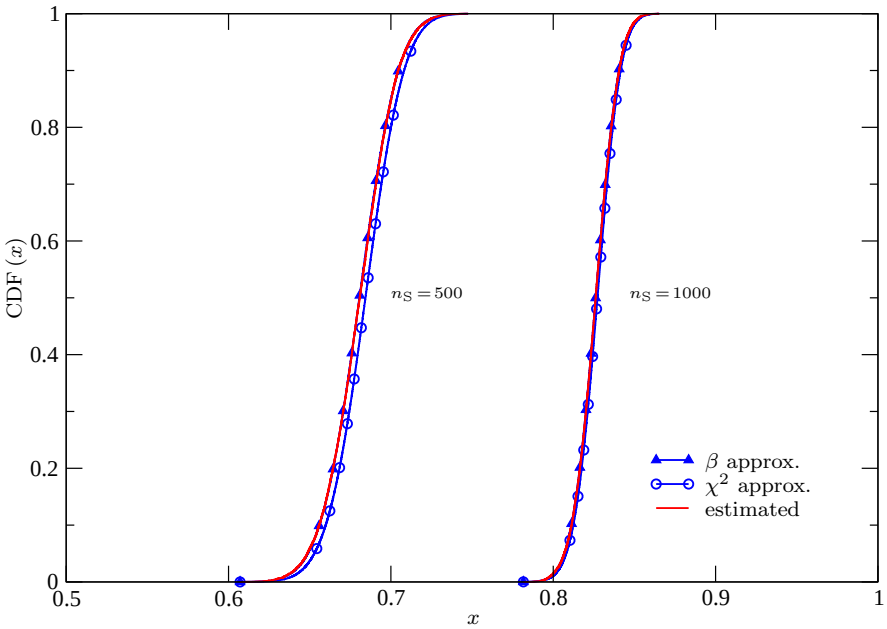

(b)

Figure 3.4: Comparison among the CDF obtained using (3.11), (3.14) and the empirically estimated curve for $\mathrm{T}^{(\mathrm{ind})}$ under $\mathcal{H}_0$. $n_{\mathrm{R}} = 20$.

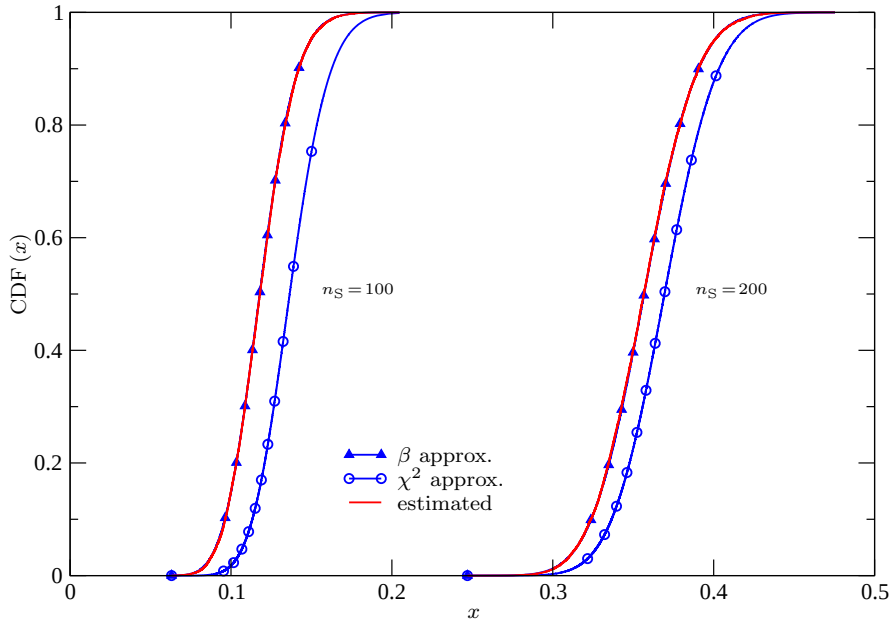

(a)

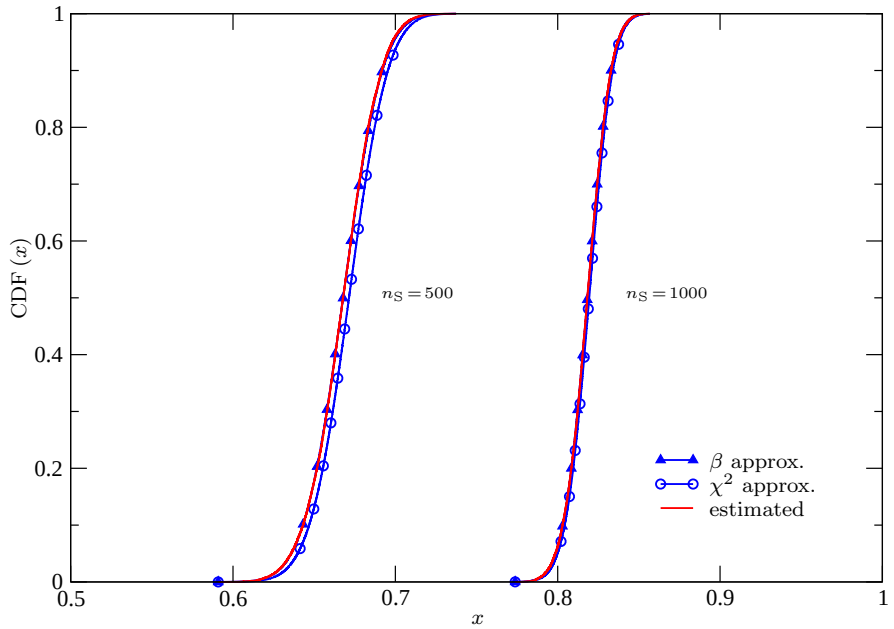

(b)

Figure 3.5: Comparison among the CDF obtained using (3.11), (3.14) and the empirically estimated curve for $T^{(sph)}$ under $\mathcal{H}_0$. $n_R = 20$.

Chapter 4

Wideband Spectrum Sensing by Information Theoretic Criteria

4.1 Introduction

Most of the SS techniques proposed in literature have been conceived to assess the presence of transmissions (such as PU signals) within a single frequency band [20]. This is the case, for instance, of energy detection and eigenvalue based approaches described in the previous chapters. A better knowledge of the surrounding radio environment can be reached exploiting wideband spectrum sensing, that consists in a joint observation of multiple frequency bands and joint decision on the occupancy of each sub-band.

Wideband SS has attracted much attention in current CR systems research. Its application is primarily related to hardware front-end requirements such as the linearity of analog components and ADCs characteristics [136, 137]. To get around such constraints some techniques proposed are based on sequential sensing on multiple bands, frequency sweeping or filter-banks approaches [78, 138, 139], and strategies to reduce hardware complexity have been studied in the context of compressed sensing [81, 140]. Wideband sensing has been also studied in the framework of the so called multiband joint detection, that is based on the maximisation of a the aggregate opportunistic throughput, a metric that takes into account the trade-off between sensing time and transmission time in CR systems [141]. In [142] wideband SS has been formalized as a GLR detector, assuming the presence of a given amount of unoccupied spectrum. Similar approaches can be found also in [143–145]. Alternative wideband approaches are based on ITC, e.g. in [146], where such tools are proposed in a channelized sub-Nyquist framework. In [147] standard ITC have been adopted to detect the presence of

occupied subbands using an ED in each subband and a similar approach has been applied to multiband (MB)-OFDM in [148].

In this chapter we formulate wideband SS as a model order selection problem, to detect which frequency components contain PUs signals and which contain only noise. The model order selection problem is solved using ITC. Most of the sensing algorithms proposed in literature are based on the comparison to a decision threshold, which setting is a difficult task in practice due to the dependence on unknown parameters. In particular, considering energy based techniques, including frequency domain analysis, the threshold setting depends on the noise power level that must be properly estimated in real implementations [92]. The wideband approach proposed is blind instead, since it does not require noise power knowledge nor any a priori information about the number and the characteristics of the signals present in the observed frequency band. The proposed technique is based on the computation of a frequency representation of the observed signal and the adoption of ITC to identify the occupied bands. Recently many spectral analysis techniques have been proposed to implement sensing functionalities, such as multitaper algorithms, filter banks and sub-Nyquist approaches [149] [77] [140]. We propose a general formulation of the wideband sensing strategy that can in principle be applied to any spectral representation of the observed signal and then specialize the analysis when simple DFT is adopted. This choice is motivated by the simplicity and low complexity of the approach and by the fact that DFT blocks are often already implemented in common systems such as OFDM receivers. In particular, we analyze both the cases with uncorrelated and correlated frequency bins. The first case exploits only the energy content, while the latter jointly exploits the energy level and spectral correlation to discern PUs signals from noise. The analysis is supported by extensive numerical simulations to identify which algorithm provides the best wideband sensing performance. Moreover we show that the simple DFT based algorithm derived can be also adopted as an approximated approach for the case in which more accurate spectral representation, such as multi taper method (MTM) based spectrum and Welch periodogram, are used. This analysis shows the potential of ITC that can be applied even in situations in which the distribution of the data is not known exactly.

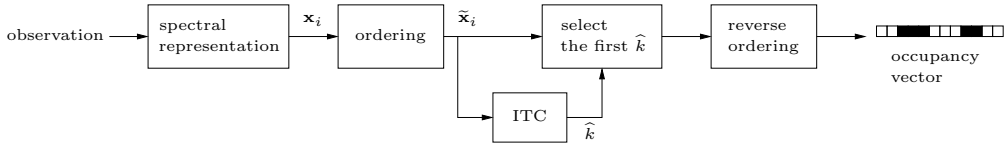

Figure 4.1: Block diagram of the proposed wideband SS strategy.

4.2 Wideband sensing by model order selection

The wideband sensing technique proposed is based on N observations of a frequency domain vector $\mathbf{x}_i = (x_{i,1} \dots x_{i,q} \dots x_{i,N_\mathrm{b}})^\mathrm{T}$ where $i = 1, \dots, N$ and N_b is the number of frequency components considered. We will refer to the elements of $\mathbf{x}_i$ as frequency bins.[1] The problem can be formulated considering a very general approach, in which the vector $\mathbf{x}_i$ can be any kind of frequency-domain representation. For instance, it can be a power spectral density estimate, the output of a filter bank, a compressed sampling reconstruction of the spectrum or, simply, the result of an N_b points DFT.

If PU signals are present in the observed frequency band, we assume that they occupy k^* frequency bins while the remaining $N_\mathrm{b} - k^*$ contains only noise. Our objective is to identify which are the k^* bins that contain PU signals. In order to accomplish this goal, we formulate wideband SS as a model order selection problem in which k^* is the order of the model. The algorithm proposed estimates k^* and also identifies the occupied bins.

Assuming the radio environment is stationary during the overall sensing period, we collect the N vectors $\mathbf{x}_i$ in the observation matrix

$$\mathbf{Y} = (\mathbf{x}_1 | \dots | \mathbf{x}_i | \dots | \mathbf{x}_N) \,. \tag{4.1}$$

Let us sort all vectors $\mathbf{x}_i$ such that the power in each frequency bin are now arranged in decreasing order. We denote with $\widetilde{\mathbf{x}}_i$ and $\widetilde{\mathbf{Y}}$ the ordered vectors and the corresponding ordered matrix, respectively. Thanks to ordering, once the model order is estimated, the frequency bins containing PUs signals are the first k^* bins of the vectors $\widetilde{\mathbf{x}}_i$. Thus after recovering the order of the model we identify the bins that contain signal components and thanks to a reverse ordering operation we obtain the occupancy vector, which is a N_b length binary vector in which the q-th element is one if the q-th bin is occupied. This wideband sensing process can be represented by the block diagram in Fig. 4.1; the first three steps are depicted in detail in Fig. 4.2.

[1] This is in accordance to the DFT-based scenario studied in the following.

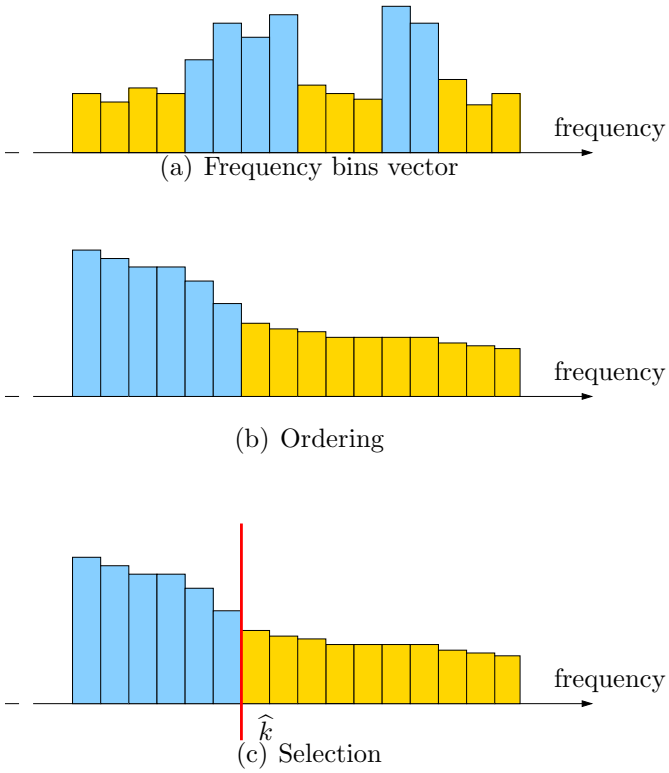

Figure 4.2: ITC based wideband sensing process. First a frequency representation vector $\mathbf{x}_i$ is collected (a) and it is ordered (b). Using ITC we obtain $\widehat{k}$ that estimates k^*. Thus the bins that contains signal components are identified as the first $\widehat{k}$ bins of the ordered vector (c).

Note that in practical implementations the ordering operation is based on the estimate received power in each frequency bin.

For solving the model order selection problem (i.e. estimating k^*) we adopt ITC, a typical approach in statistics for choosing the model that better fits data among a family of possible models [82]. In our problem we have N_b possible models, where the k-th corresponds to the case in which we assume that only k bins are occupied.[2] To adopt ITC, we start from the analysis of the log-likelihood of the received observation matrix, $\ln f\left(\widetilde{\mathbf{Y}}|\boldsymbol{\Theta}^*\right)$. where $\boldsymbol{\Theta}^*$ is the vector that contains the unknown parameters of the model, which number depends on k^*.[3] According to ITC, the best choice for estimating of k^* is given by

$$\widehat{k} = \arg\min_k \left\{ -2\ln f\left(\widetilde{\mathbf{Y}}|\widehat{\boldsymbol{\Theta}}^{(k)}\right) + \mathcal{P}\{k\} \right\} \tag{4.2}$$

where $\widehat{\boldsymbol{\Theta}}^{(k)}$ is the vector of the estimated parameters in the k-th hypothesis and $\mathcal{P}\{k\}$ is the ITC penalty term.[4] Different choices of the penalty term lead to different criteria, each one characterized by different performance and complexity. In the next section we review the most common and simple techniques, adopted throughout the paper.

The advantage of using model order selection is that it leads to a blind algorithm which does not require any a priori knowledge of unknown parameters, e.g. the noise power or PUs characteristics. In addition, it does not require the setting of threshold, avoiding common problems of threshold based algorithms such as deriving the exact threshold selection rule. The unique assumption of the proposed strategy is that at least one frequency bin contains only noise. This "minimum sparsity requirement" make this method appealing for scenarios in which wideband algorithms that require an high level of sparsity (such as compressive sensing algorithms [81,140]) of the received signal are not satisfied.

4.3 Information Theoretic Criteria

In [150] Akaike first proposed an information theoretic criterion for statistical model identification. The observation consists in N i.i.d. samples of the

[2] We will refer to the k-th model also as the k-th hypothesis.

[3] Varying the number of occupied frequency bins we will have a different set of parameters that describe the model.

[4] Using the notation $\mathcal{P}\{k\}$ we emphasize that the penalty depends on k through the vector $\widehat{\boldsymbol{\Theta}}^{(k)}$. Note that in general $\mathcal{P}\{k\}$ could also depend on other parameters, e.g. N_b, N and other statistical functions of the observation.

N_b dimensional r.v. $\mathbf{X}$, generated by the "true" distribution $f(\mathbf{X}|\boldsymbol{\Theta}^*)$. The model selection problem consists in identifying the model that better fits data among a set of possible models $\left\{f\left(\mathbf{X}|\boldsymbol{\Theta}^{(k)}\right)\right\}$, characterized by the model order k. Akaike proposed to select the model that minimize the Kullback-Leibler (K-L) distance from $f(\mathbf{X}|\boldsymbol{\Theta}^*)$, i.e.

$$\widehat{k} = \min_k \mathbb{E}\left\{\ln \frac{f\left(\mathbf{X}|\boldsymbol{\Theta}^{(k)}\right)}{f(\mathbf{X}|\boldsymbol{\Theta}^*)}\right\}. \tag{4.3}$$

This criterion is equivalent to minimize the cross entropy

$$-\int f(\mathbf{X}|\boldsymbol{\Theta}^*) \ln f\left(\mathbf{X}|\boldsymbol{\Theta}^{(k)}\right) d\mathbf{X} \tag{4.4}$$

which natural estimate, under the k-th hypothesis, is given by the average log likelihood

$$\frac{1}{N}\sum_{i=1}^{N} \ln f\left(\mathbf{x}_i|\widehat{\boldsymbol{\Theta}}^{(k)}\right). \tag{4.5}$$

Akaike noted that the average log likelihood is a biased estimate of the cross entropy, and added a penalty term which can be considered as a term that asymptotically, for large N, compensates the estimation error. Exploiting the asymptotical chi squared distribution of the log likelihood, Akaike derived the AIC, in which the penalty term is

$$\mathcal{P}_{\mathrm{AIC}}\{k\} = 2\,\phi(k) \tag{4.6}$$

where $\phi(k)$ is the number of degrees of freedom in the k-th hypothesis. Alternative ITC can be derived adopting the Bayesian approaches, which chooses the model that maximize the posterior probability $\mathrm{P}\left\{\boldsymbol{\Theta}^{(k)}|\mathbf{X}\right\}$ [151, 152]. In this context the most popular and simple criterion is the Bayesian information criterion (BIC) which set the penalty term [151]

$$\mathcal{P}_{\mathrm{BIC}}\{k\} = \phi(k)\,\log N. \tag{4.7}$$

For large enough samples BIC coincides with the MDL criterion, which attempts to construct a model which permits the shortest description of the data [153]. The AIC and BIC approaches are the most popular ITC adopted in many statistical and engineering problems [67, 72, 147]. Although the AIC metric provides an unbiased estimate of the K-L divergence, in many situations it tends to overestimate the true order of the model, even asymptotically [154]. In some case studies consistency can be reached by properly

modelling the penalty term [72, 155]. In particular, when the penalty is in the form $\mathcal{P}\{k\} = \phi(k) \cdot c$, it can be demonstrated that it is required, for N that goes to infinity, that $c/N \to 0$ to avoid underestimation and $c/\log\log N \to +\infty$ to avoid overestimation [156]. Further conditions can be derived in order to solve specific selection problems [157]. Here we consider three consistent criteria, defined by the penalty terms

$$\mathcal{P}_{\text{CAIC1}}\{k\} = \phi(k)\ (\log N + 1) \tag{4.8}$$

$$\mathcal{P}_{\text{CAIC2}}\{k\} = 2\,\phi(k)\ \log N \tag{4.9}$$

$$\mathcal{P}_{\text{CAIC3}}\{k\} = 3\,\phi(k)\ \log N. \tag{4.10}$$

Note that CAIC1 has been proposed by [154] and CAIC2 has been adopted in [158].

An alternative criterion based on the large sample distribution of ML estimators is the consistent AIC with Fisher information (CAICF), with the penalty term [154]

$$\mathcal{P}_{\text{CAICF}}\{k\} = \phi(k)\ (\log N + 2) + \log\left|\mathbf{J}\left(\widehat{\boldsymbol{\Theta}}^{(k)}\right)\right| \tag{4.11}$$

where $\mathbf{J}\left(\widehat{\boldsymbol{\Theta}}^{(k)}\right)$ is the estimate of the Fisher information matrix (FIM) of the observation.

Note that the formulation of the ITC as in (4.2) supports the interpretation of these techniques as extensions of the ML principle in the form of penalized likelihood, where the penalty term is introduced as a cost for the increased complexity of the model, related to the presence of unknown parameters that must be estimated [150, 159]. Thus ITC can be interpreted as an extension of the ML approach that takes into account both the estimation (of the unknown parameters) and the decision (among the possible models) processes. Indeed it has been noted that the ML approach performs poorly in model selection problems, always leading to the choice of the maximum number of parameters considered [151].

4.4 DFT based wideband algorithms

In this section we apply the ITC based wideband sensing strategy described in section 4.2 to the case in which simple DFT is used as spectral representation of the received signal. We adopt DFT motivated by its simplicity and by the fact that the its implementation can be already available in many systems, such as OFDM receivers.

At the i-th time instant, the output of the DFT can be expressed as

$$\mathbf{x}_i = \mathbf{s}_i + \mathbf{n}_i \tag{4.12}$$

where $\mathbf{n}_i$ represents the AWGN and $\mathbf{s}_i$ is the aggregation of the PUs signals.[5] We assume that the time domain received samples are modeled as zero mean complex Gaussian vector, that is a common assumption in communications literature.[6] Thanks to the linearity of the DFT operation, $\mathbf{x}_i$ is a vector of zero mean complex Gaussian r.v.s. with covariance matrix $\mathbf{\Sigma}_{\mathbf{x}} = \mathbb{E}\left\{\mathbf{x}_i {\mathbf{x}_i}^{\mathrm{H}}\right\}$. After the collection of N DFT outputs we perform ordering of the vector $\mathbf{x}_i$ according to the received power in each bin, i.e., according to the vector $(\nu_1, \ldots, \nu_q, \ldots, \nu_{N_\mathrm{b}})$, where $\nu_q = (1/N)\sum_{i=1}^{N} |x_{i,q}|^2$. Thus we obtain a new vector $\widetilde{\mathbf{x}}_i$ with power in each frequency bin in descending order. If the number of frequency bins containing signals are k, we have $\widetilde{\mathbf{x}}_i \sim \mathcal{CN}(\mathbf{0}, \mathbf{\Sigma}_{\widetilde{\mathbf{x}}})$, where the covariance matrix $\mathbf{\Sigma}_{\widetilde{\mathbf{x}}} = \mathbb{E}\left\{\widetilde{\mathbf{x}}_i \widetilde{\mathbf{x}}_i^{\mathrm{H}}\right\}$ can be expressed as

$$\mathbf{\Sigma}_{\widetilde{\mathbf{x}}} = \mathbf{\Sigma}_{(k)} \bigoplus \sigma^2 \mathbf{I}_{N_\mathrm{b}-k} \tag{4.13}$$

where $\mathbf{\Sigma}_{(k)}$ is a $k \times k$ submatrix, $\mathbf{I}_p$ is a $p \times p$ identity submatrix, σ^2 is the unknown noise power at each frequency bin, and $\bigoplus$ represents the direct sum operator [160]. Note in particular that $\mathbf{\Sigma}_{(k)} = \mathbb{E}\left\{\widetilde{\mathbf{x}}_{(k)} \widetilde{\mathbf{x}}_{(k)}^{\mathrm{H}}\right\}$, with $\widetilde{\mathbf{x}}_i^{\mathrm{T}} = \left[\widetilde{\mathbf{x}}_{(k),i}^{\mathrm{T}}\ \widetilde{\mathbf{n}}_{(k),i}^{\mathrm{T}}\right]$. Then the likelihood function of observed data can be written as

$$\begin{aligned} f\left(\widetilde{\mathbf{Y}}; \mathbf{\Theta}^{(k)}\right) &= \prod_{i=1}^{N} \frac{1}{\pi^{N_\mathrm{b}} |\mathbf{\Sigma}_{\widetilde{\mathbf{x}}}|} \exp\left(-\widetilde{\mathbf{x}}_i^{\mathrm{H}} \mathbf{\Sigma}_{\widetilde{\mathbf{x}}}^{-1} \widetilde{\mathbf{x}}_i\right) \\ &= \prod_{i=1}^{N} \frac{1}{\pi^{N_\mathrm{b}} |\mathbf{\Sigma}_{(k)}| \left(\sigma^2\right)^{N_\mathrm{b}-k}} \\ &\qquad \cdot \exp\left(-\widetilde{\mathbf{x}}_{(k),i}^{\mathrm{H}} {\mathbf{\Sigma}_{(k)}}^{-1} \widetilde{\mathbf{x}}_{(k),i}\right) \exp\left(-\frac{1}{\sigma^2} \widetilde{\mathbf{n}}_{(k),i}^{\mathrm{H}} \widetilde{\mathbf{n}}_{(k),i}\right). \end{aligned}$$

Then the log-likelihood function can be expressed as

$$\begin{aligned} \ln f\left(\widetilde{\mathbf{Y}}; \mathbf{\Theta}^{(k)}\right) = &- N_\mathrm{b} N \ln \pi - N \ln |\mathbf{\Sigma}_{(k)}| - N\left(N_\mathrm{b} - k\right) \ln \sigma^2 \\ &- N \mathrm{tr}\left\{{\mathbf{\Sigma}_{(k)}}^{-1} \mathbf{S}_{(k)}\right\} - \frac{N}{\sigma^2} \mathrm{tr}\left\{\mathbf{N}_{(k)}\right\}. \end{aligned} \tag{4.14}$$

where $\mathbf{S}_{(k)} = (1/N)\sum_{i=1}^{N} \widetilde{\mathbf{x}}_{(k),i} \widetilde{\mathbf{x}}_{(k),i}^{\mathrm{H}}$ and $\mathbf{N}_{(k)} = (1/N)\sum_{i=1}^{N} \widetilde{\mathbf{n}}_{(k),i} \widetilde{\mathbf{n}}_{(k),i}^{\mathrm{H}}$.

[5] Including the channel effects.

[6] This is a proper assumption for many practical problems, such as the case of OFDM signals that are widely adopted in recent communication systems.

4.4.1 Independent frequency bins

In the case in which the frequency bins are independent, $\mathbf{\Sigma}_{(k)}$ is diagonal, and the log-likelihood reduces to

$$\ln f\left(\widetilde{\mathbf{Y}};\mathbf{\Theta}^{(k)}\right) = -N_{\mathrm{b}}N\ln\pi - N\sum_{q=1}^{k}\ln\sigma_q^2 - N\left(N_{\mathrm{b}}-k\right)\ln\sigma^2 - N\sum_{q=1}^{k}\frac{\widehat{\sigma}_q^2}{\sigma_q^2} - \frac{N}{\sigma^2}\mathrm{tr}\left\{\mathbf{N}_{(k)}\right\}.$$

where $(\sigma_1^2,\ldots,\sigma_k^2) = \mathrm{diag}\left\{\mathbf{\Sigma}_{(k)}\right\}$ and $(\widehat{\sigma}_1^2,\ldots,\widehat{\sigma}_k^2) = \mathrm{diag}\left\{\mathbf{S}_{(k)}\right\}$. In this case the parameter vector is given by $\mathbf{\Theta}^{(k)} = (\sigma_1^2,\ldots,\sigma_k^2,\sigma^2)$, that can be estimated as $\widehat{\mathbf{\Theta}}^{(k)} = (\widehat{\sigma}_1^2,\ldots,\widehat{\sigma}_k^2,\widehat{\sigma}^2)$ where

$$\widehat{\sigma}^2 = \frac{\mathrm{tr}\left\{\mathbf{N}_{(k)}\right\}}{\left(N_{\mathrm{b}}-k\right)}. \tag{4.15}$$

Then, removing the terms that do not depend on k, the log-likelihood can be expressed as

$$\ln f\left(\widetilde{\mathbf{Y}};\widehat{\mathbf{\Theta}}^{(k)}\right) = -N\sum_{q=1}^{k}\ln\widehat{\sigma}_q^2 - N\left(N_{\mathrm{b}}-k\right)\ln\widehat{\sigma}^2. \tag{4.16}$$

Note that (4.16) corresponds to the result derived in [147]. For independent frequency components the number of degrees of freedom corresponds to the length of $\mathbf{\Theta}^{(k)}$, i.e. $\phi(k) = k+1$.

4.4.2 Correlated frequency bins

In this section we consider a more general scenario in which we remove the assumption that the frequency bins are uncorrelated. Considering different spectral correlation conditions, different models can be assumed for the matrix $\mathbf{\Sigma}_{(k)}$. Here we study the most general case, assuming no particular structures for the correlation matrix. In this case the number of degrees of freedom of the model is given by $\phi(k) = k^2+1$, that accounts for the $k\times k$ Hermitian matrix $\mathbf{\Sigma}_{(k)}$ and the noise power. Then in this case the log-likelihood (4.14) can not be further simplified. Adopting the ML estimates $\widehat{\sigma}^2$ and $\widehat{\mathbf{\Sigma}}_{(k)} = (1/N)\sum_{i=1}^{N}\widetilde{\mathbf{x}}_{(k),i}\,\widetilde{\mathbf{x}}_{(k),i}^{\mathrm{H}}$, removing the terms that do not depend on k, we obtain

$$\ln f\left(\widetilde{\mathbf{Y}};\widehat{\mathbf{\Theta}}^{(k)}\right) = -N\sum_{q=1}^{k}\ln\widehat{\alpha}_q - N\left(N_{\mathrm{b}}-k\right)\ln\widehat{\sigma}^2. \tag{4.17}$$

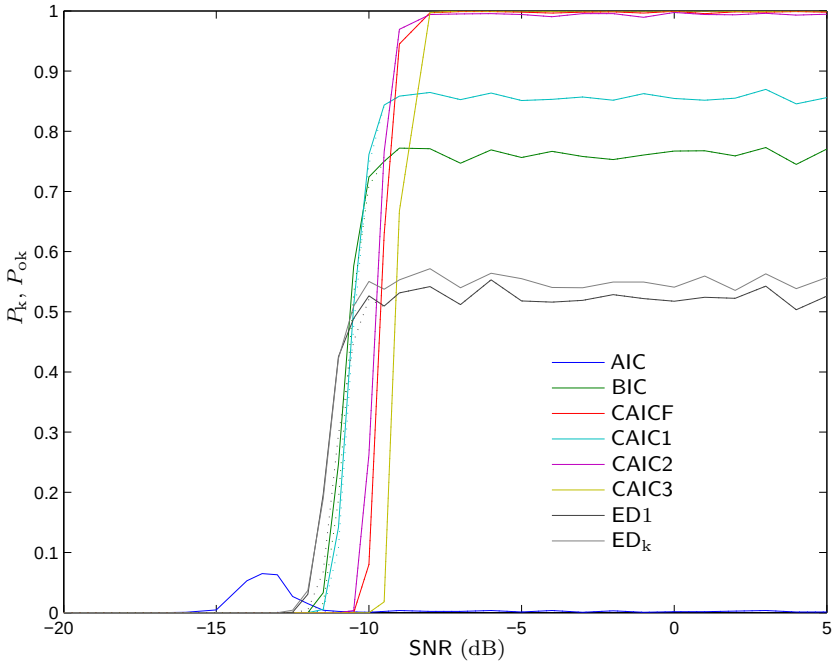

Figure 4.3: Probability to estimate the correct number of occupied bins (continuous line), and probability to detect the occupied frequency bins (dotted lines), as function of the SNR. The number of occupied bins is 16, $N_{\rm b} = 128$ and $N = 1000$.

where $\widehat{\alpha}_q$ is the q-th eigenvalue of the sample covariance matrix $\mathbf{S}_{(k)}$. In this case the vector of the unknown parameters is given by $\widehat{\boldsymbol{\Theta}}^{(k)} = (\widehat{\alpha}_1, \ldots, \widehat{\alpha}_k, \widehat{\sigma}^2)$.

4.5 Numerical results and discussion

In this section, we show some numerical examples to assess the performance of the proposed wideband sensing technique. We compare the ITC algorithms to simple energy based approaches in which the estimated received power of each frequency bin is compared to the decision threshold. We indicate with ED the ideal ED, which assumes that the noise power is known exactly, and with $\mathsf{ED}_{\rm k}$ the ENP-ED described in Chapter 2 in which the $N_{\rm b} - k^*$ bins with lower estimated received power are used for estimating the received noise

power [7]. The threshold is set according to the Neyman-Pearson criterion considering a probability of false alarm $P_{\mathrm{FA}} = 0.01$.

The performance of the wideband approach will be evaluated in terms of probability to correctly detect k^*, $P_{\mathrm{k}} \triangleq \mathrm{P}\left\{\widehat{k} = k^*\right\}$, and the number of correctly identify the set of occupied frequency bins, P_{ok}. The probability of incorrect detection will be evaluated in terms of probability of overestimation, $P_{\mathrm{over}} \triangleq \mathrm{P}\left\{\widehat{k} > k^*\right\}$, and the probability of underestimation, $P_{\mathrm{under}} \triangleq \mathrm{P}\left\{\widehat{k} < k^*\right\}$. In both the cases we will also consider the probability of declare occupied some free bins, P_{false}, and the probability of declare free some occupied bins P_{mis}. Note that these performance metrics are very severe metrics, that allows us to understand which among ITC is more accurate. For example the cases in which $\widehat{k} = k^* + 1$ and $\widehat{k} = k^* + 10$ are both considered overestimation events, irrespective of the actual distance from k^*. As will be discussed later, in some practical applications the adoption of algorithms that tend to overestimate k^* can be useful by means of including a protection margin to preserve low SNR PU transmissions. For some practical case study we will also analyze the probability of detection related to the q-th bin, P_{D}^q.

4.5.1 Independent frequency bins

In this section we consider the case of independent frequency bins, that is the most interesting case in practice due to the fact that most of communications signals are generated by white data sequences, which give spectral uncorrelated transmissions [161]. In particular, to compare the performance of the algorithms we adopt "artificial" numerically generated signals which bandwidth is exactly known. Note that, using real signals, establishing the exact number of occupied bins occupied can be a non trivial task, due to sideband leakage.

In Fig. 4.3 we consider the adoption of the wideband SS strategy proposed using DFT with $N_{\mathrm{b}} = 128$, in presence of a single white Gaussian signal, that occupy exactly 64 bins, and AWGN. The number of DFT outputs considered is $N = 1000$ and the probabilities P_{k} and P_{ok} are presented. We can see that, increasing the SNR, all the consistent ITC studied present a step wise behaviour, assessing the correct detection probability to a fixed value for high SNR. The AIC instead confirms its non consistency behaviour.

[7] For simplicity, here do not use the exact distribution of the ordered vector. Thus the ENP-ED approach adopted can be considered an approximated strategy valid for large samples use cases.

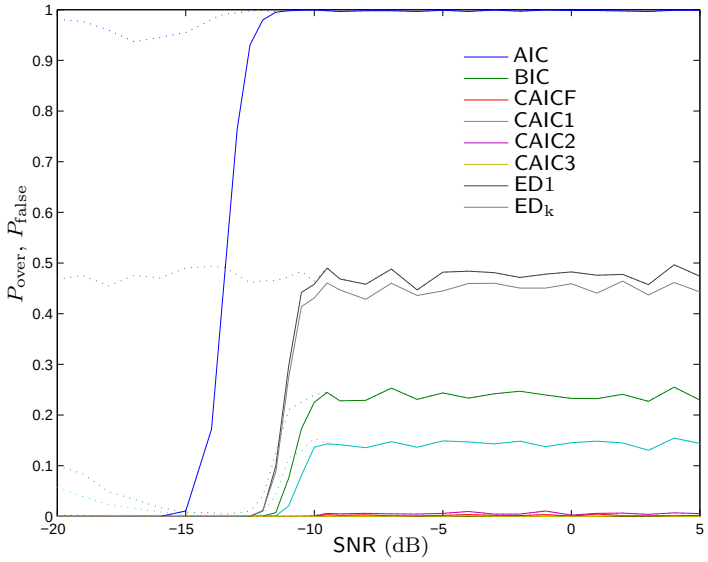

(a) Probability of overestimation

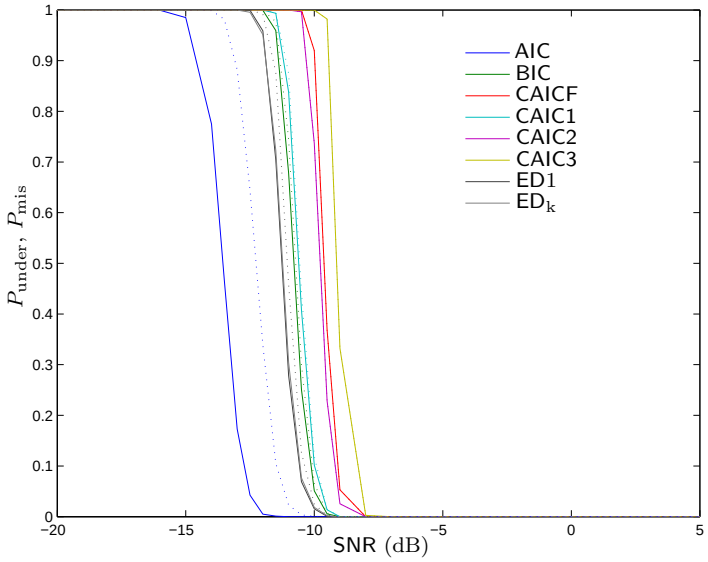

(b) Probability of underestimation

Figure 4.4: Probabilities to overestimate and underestimate the correct number of occupied bins (continuous line), and probability to detect incorrectly the occupied frequency bins (dotted lines) as function of the SNR. The number of occupied bins is 64, $N_b = 128$ and $N = 1000$.

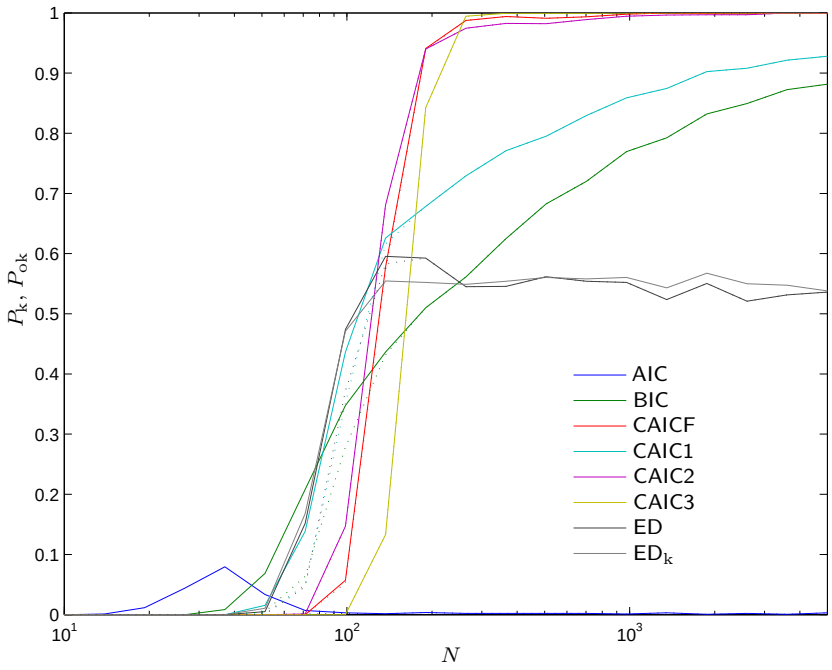

Figure 4.5: Probability to estimate the correct number of occupied bins (continuous line), and probability to detect the occupied frequency bins (dotted lines) as function of N. The number of occupied bins is 64, $N = 1000$ and $\mathsf{SNR} = -5\,\mathrm{dB}$.

Note in particular that for all ITC P_{ok} always is overlapped with P_{k}. Make exception some points in the transition phase, in which the difference among the probabilities is quite small. This means that when the algorithms correctly estimate k^* they generally correctly estimate also the set of occupied frequency bins. The corresponding probabilities of incorrect estimation are shown in Fig. 4.4. We can see that at high SNR P_{under} and P_{mis} go to zero and an incorrect detection always consists in a false alarm event. Note that this property is very important in CR scenarios, because it imply that ITC never misdetect the presence of PUs if the SNR is sufficient. Considering the ED based approaches we can see that they perform quite poorly providing almost 50% of overestimations for high SNR levels. In Fig. 4.5 we show P_{ok} and P_{k} as function of the number of collected DFT outputs N, with $k^* = 64$, $N_{\mathrm{b}} = 128$ and $\mathsf{SNR} = -5\,\mathrm{dB}$. The graph confirms that the performance is better for higher N, and we can see that CAICF, $\mathsf{CAIC2}$ and $\mathsf{CAIC3}$ reach a

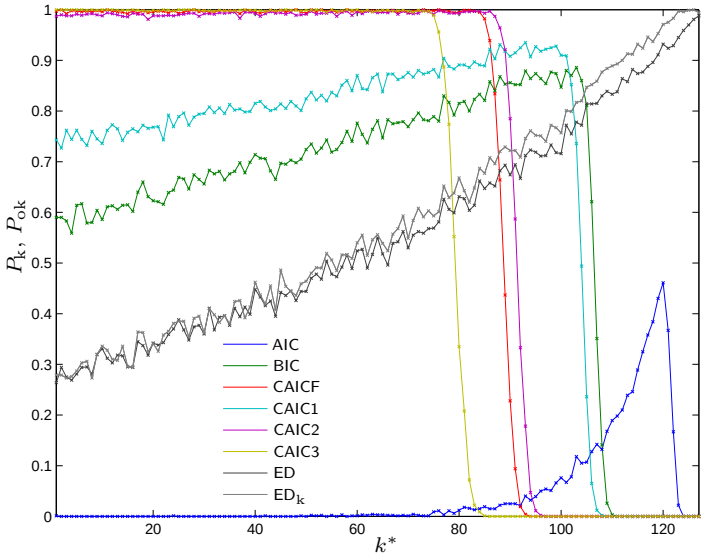

(a) SNR $= -5\,\mathrm{dB}$

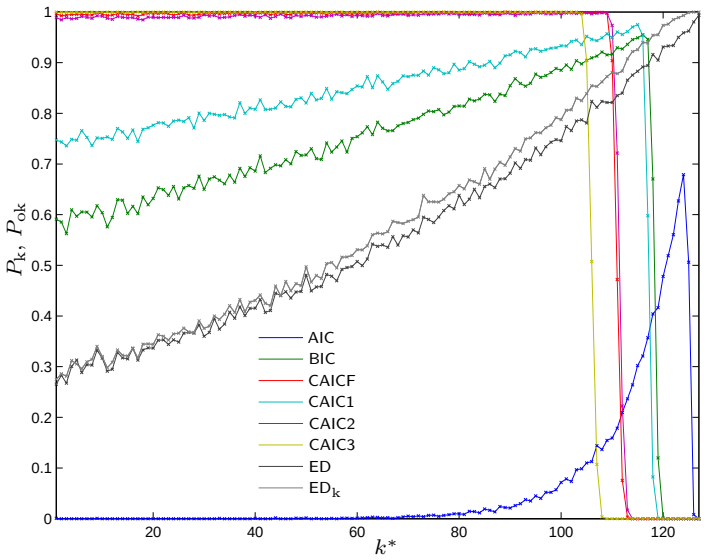

(b) SNR $= 0\,\mathrm{dB}$

Figure 4.6: Probability to estimate the correct number of occupied bins (continuous line), and probability to detect the occupied frequency bins (marked with crosses) as function of the number of occupied bins k^*. The simulation has been performed considering $N_\mathrm{b} = 128$ and $N = 1000$.

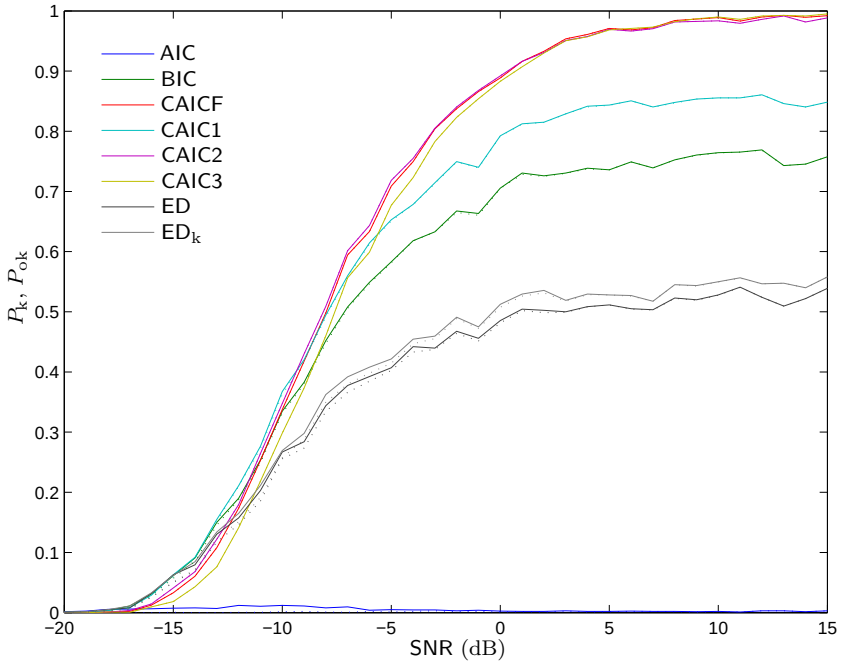

Figure 4.7: Probability to estimate the correct number of occupied bins (continuous line), and probability to detect the occupied frequency bins (dotted lines) as function of the SNR in Rayleigh fading. The number of occupied bins is 64, $N_b = 128$ and $N = 1000$.

very high P_{ok} values. It is interesting to note that BIC and CAIC1 present a slower increase with respect to N.
The probabilities of correct detection as function of the number of occupied bins is k^* are plotted in Fig. 4.6. For this case the SNR considered is the signal to noise power ratio for single bin (it is not the ratio of the overall power collected in the whole bandwidth, adopted for the previous simulations), and it assumes the values -5 and 0 dB. Also in this case we can see that the best performances are provided by CAICF, CAIC2 and CAIC3. It is interesting to note that the probabilities of correct detection drop off at some high value of k^*, for all the ITC. We can consider this phenomenon as a "sparsity constraint" that appears in numerical performance evaluation. Note however that increasing the SNR this effect is less evident, with a drop that moves to higher k^* values.
In Fig. 4.7 we perform the same analysis of Fig. 4.3 in Rayleigh fading sce-

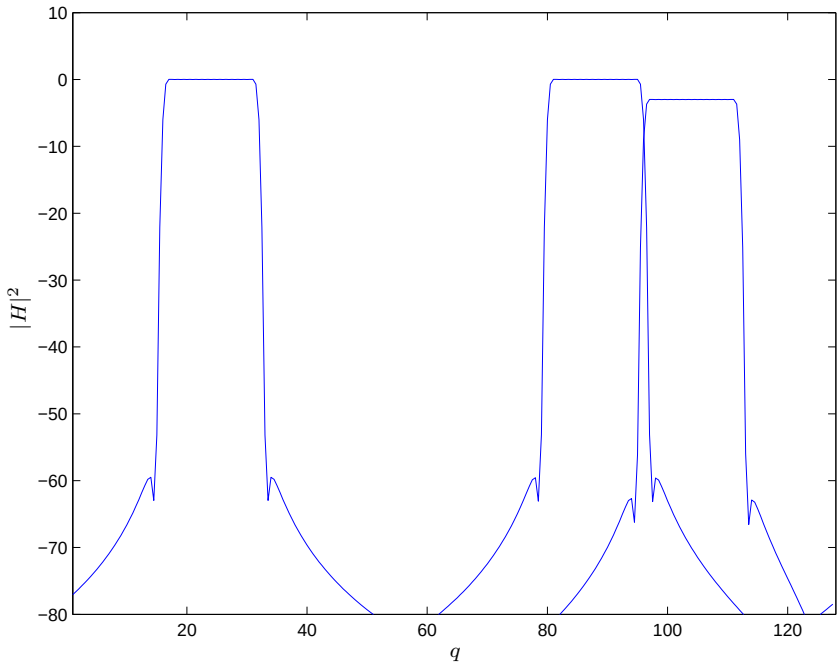

Figure 4.8: Squared magnitude of the signals adopted in the multiband scenario normalized to 0 dB. The higher frequency signal has a SNR drop of −3 dB.

nario. Here we consider that the fading attenuation is constant for all frequency bins and for the duration of the observation. With respect to the AWGN case we can see that fading has a big impact on the performance of the wideband algorithms, increasing the SNR value at which they reach a target probability of correct detection.

From the previous analysis it emerges that CAICF, CAIC2, and CAIC3 are the ITC algorithms that allows a better sensing performance allowing almost 1 probabilities of correct detection of the occupied bins set. Compared to simple ED strategies, the wideband ITC algorithms proposed allow a more accurate identification of the occupied bands.

4.5.2 Multiband sensing

In this section we analyze a multiband scenario in which three OFDM like signals are present in the observed bandwidth. The power spectral density (PSD) of the spectrum of the three signals is depicted in Fig. 4.8. In Fig. 4.9

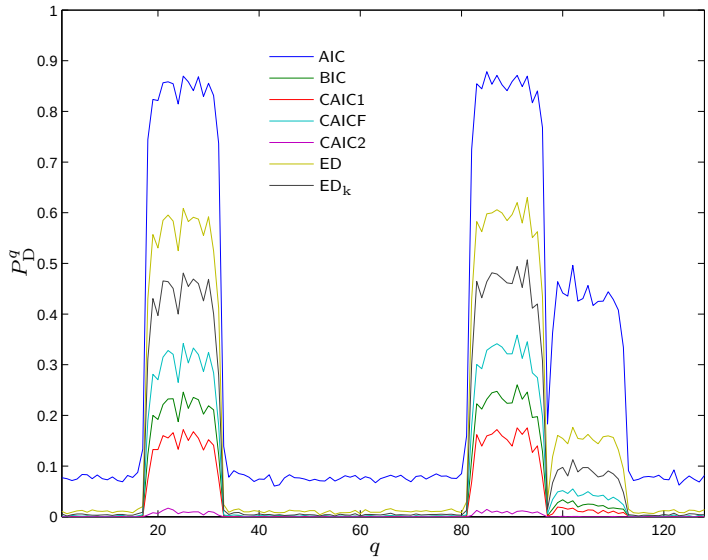

(a) $\mathsf{SNR} = -20\,\mathrm{dB}$

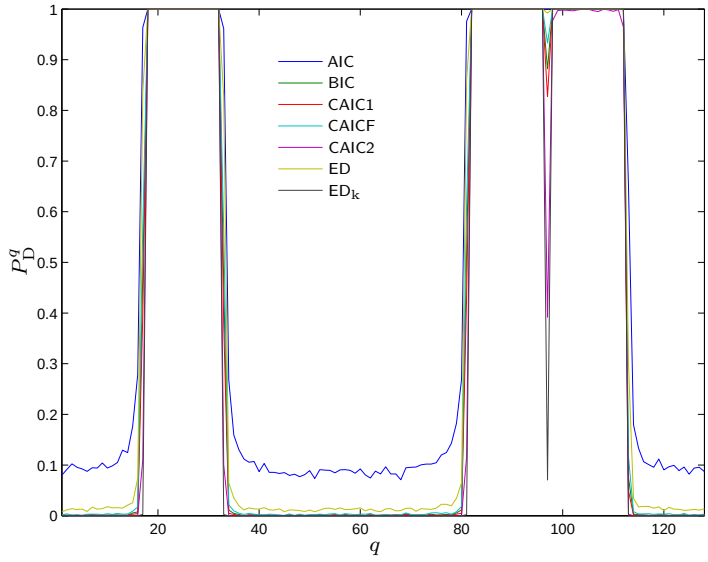

(b) $\mathsf{SNR} = -10\,\mathrm{dB}$

Figure 4.9: Probability of detection for each frequency bin when the DFT is adopted for the multi band scenario depicted in Fig. 4.8. $N_\mathrm{b} = 128$ and $N = 1000$.

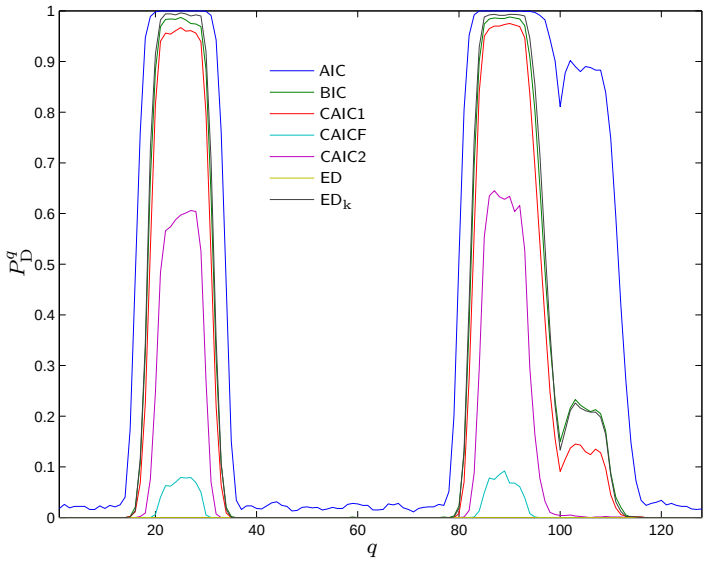

(a) SNR $= -20\,\mathrm{dB}$

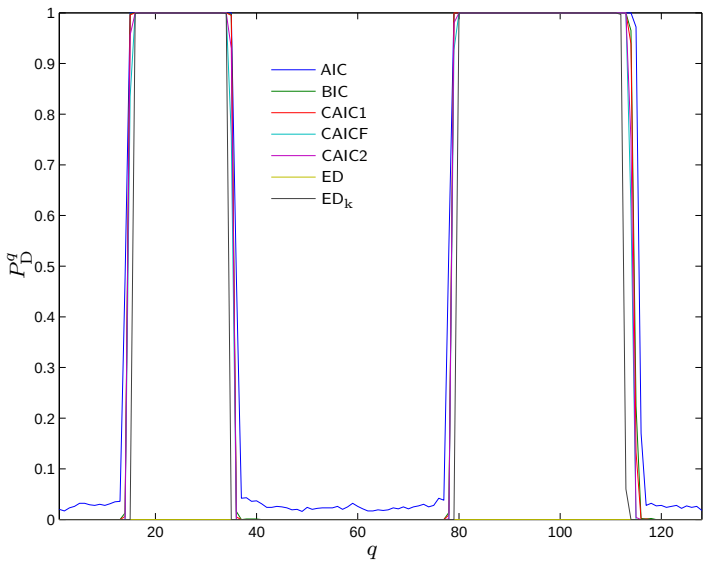

(b) SNR $= -10\,\mathrm{dB}$

Figure 4.10: Probability of detection for each frequency bin when a 128 points MTM spectrum estimate is adopted for the multi band scenario depicted in Fig. 4.8. $N = 1000$.

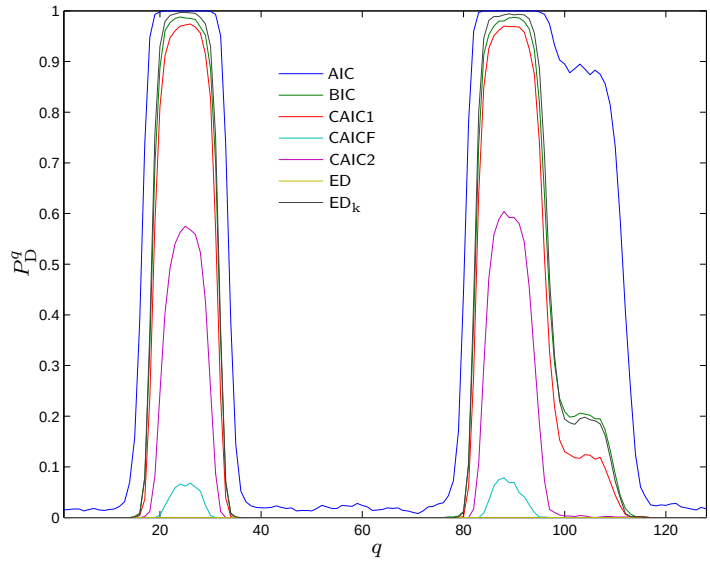

(a) SNR $= -20\,\mathrm{dB}$

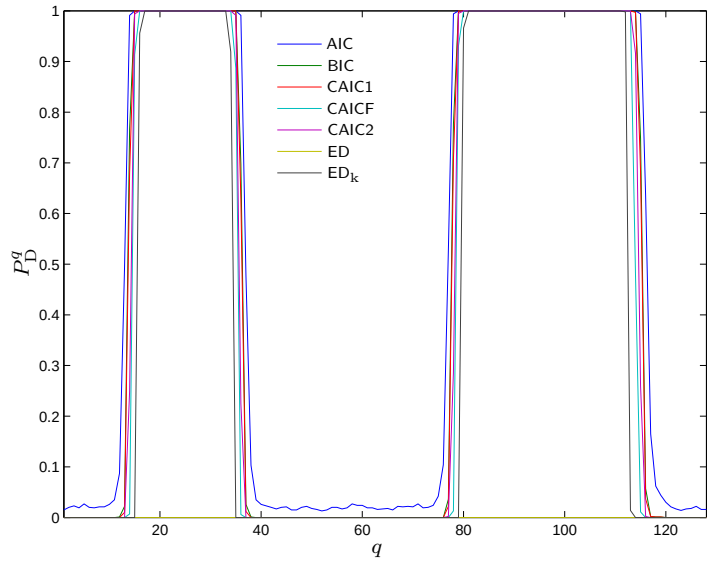

(b) SNR $= -10\,\mathrm{dB}$

Figure 4.11: Probability of detection for each frequency bin when a 128 points Welch spectrum estimate is adopted for the multi band scenario depicted in Fig. 4.8. $N = 1000$.

we show P_{D}^{q} when the wideband algorithm proposed in Section 4.4 is adopted. It is interesting to note that for very low SNR, such as $\mathsf{SNR} = -20\,\mathrm{dB}$, the algorithm that performs better is the AIC. In Section 4.5.1 we noted that generally AIC tends to overestimate the number of bins occupied, but this property turns to be an advantage at low SNR levels allowing a better probability to detect the presence of a signal. On the other hand AIC always lead to non negligible false alarms in unoccupied bins. From Fig. 4.9(b) we can see that in this case study all ITC performs well at $\mathsf{SNR} = -10\,\mathrm{dB}$.

ITC are conceived for being statistical approaches that chooses the model that best approximates data among a family of models. It is interesting therefore to analyze if this holds also when the true model that underlie the generation of the observation is not in the considered model set. This case has also an important impact on practical situations in which the exact statistical description of the collected data is not known or it is too complex to apply ITC in a rigorous way, and thus algorithms derived for simpler models are adopted. Here we consider the case in which the spectral representation used is a spectrum estimate derived using MTM or Welch periodogram, both with N_{b} points in frequency domain, and we apply the wideband ITC derived for the DFT analysis in Section 4.4. This can be considered an approximate based strategy in which these spectrum estimates, that in general are chi squared distributed, are approximated to Gaussian r.v.s[8] [162]. In Fig. 4.10 and Fig. 4.11 we can see that the MTM and Welch strategies provide a very good detection performance that outperforms the DFT based approach for low SNR levels. Then we can benefit from better spectrum estimates (DFT is a quite raw spectral representation) and apply anyway the wideband approach proposed in Section 4.4.

4.5.3 Correlated bins algorithms

In some practical applications, the signals collected present an non negligible spectral correlation. Some examples are provided in [163]. In this section we will show some numerical examples related to the wideband ITC approach described in Section 4.4.2. For simplicity we consider only AIC and BIC algorithms, and use the notation $\mathsf{AIC}^{\mathrm{i}}$, $\mathsf{BIC}^{\mathrm{i}}$ for denote the adoption of the independence based algorithm and $\mathsf{AIC}^{\mathrm{c}}$, $\mathsf{BIC}^{\mathrm{c}}$ for the correlated case.

To assess the performance of the algorithms we adopt a Gaussian signal sequence, generated as a simple autoregressive sequence in which consecutive samples has a correlation coefficient ρ. In Fig. 4.12 we show the probabilities

[8]Note that this approximation is valid when the chi squared distribution has a high number of degrees of freedom.

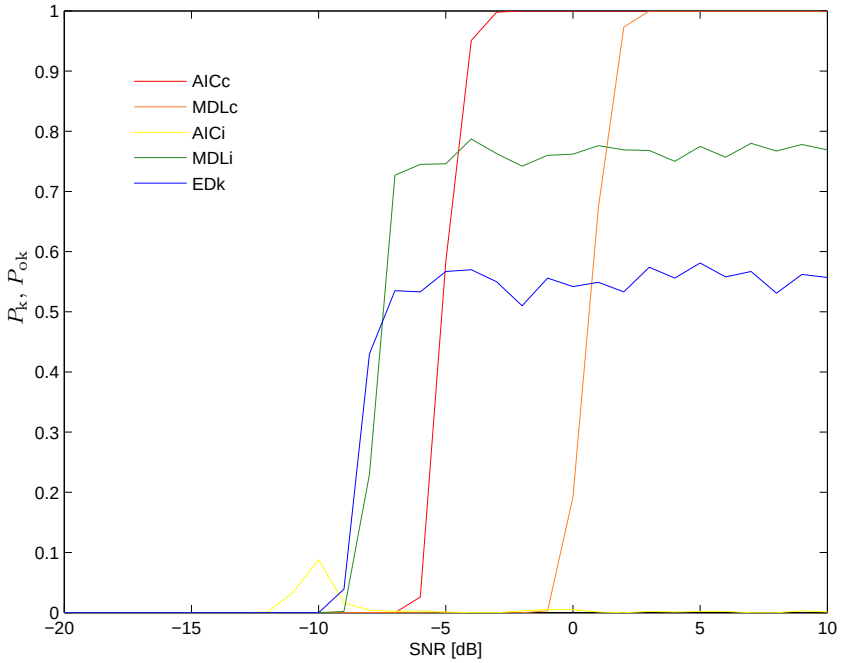

Figure 4.12: Probability to estimate the correct number of occupied bins (continuous line), and probability to detect the occupied frequency bins (dotted lines), as function of the SNR. The number of occupied bins is 64, $N_\mathrm{b} = 128$ and $N = 1000$.

of correct detection P_ok and P_k when $\rho = 0.8$, assuming $k^* = 64$, $N_\mathrm{b} = 128$ and $N = 1000$. For comparison we plot also the curves obtained with the ITC algorithm proposed in Section 4.4.1. Note that in this case the AIC is the algorithm that provides the better performance, reaching $P_\mathrm{ok} \sim 1$ at around $\mathsf{SNR} = -3\,\mathrm{dB}$.

The performance of the algorithms are also derived when the signal is a Gaussian random process with a root raised cosine shaped PSD with roll-off factor $\beta = 0.5$ and bandwidth (at $-3\,\mathrm{dB}$) equal to 32 bins, for a total excess bandwidth of around 48 bins. In Fig. 4.13 we show the probability of detection of the q-th frequency bin, P_D^q, when $\mathsf{SNR} = 10\,\mathrm{dB}$ for the AIC and BIC algorithms. Note that the adopting AIC^i and BIC^i generally underestimate the number of occupied bins,vwith respect to AIC^c and BIC^c. Thus the latter, allow to exploit the correlation among frequency bins to detect the frequency bins in which the PSD is lower. Similarly, Fig. 4.14 shows P_D^q,

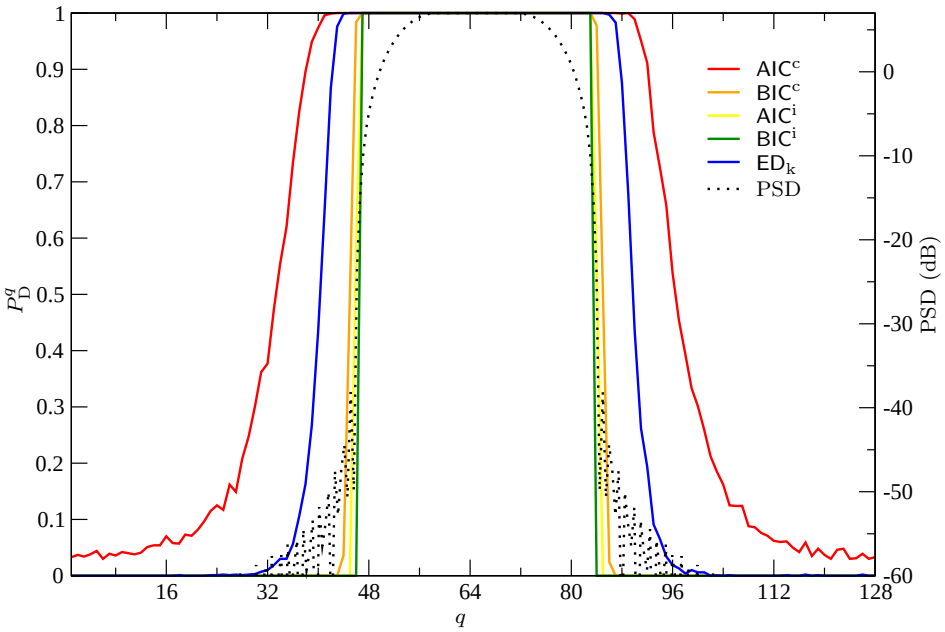

Figure 4.13: Detection probability for each bin, P_{D}^{q}, as function of the DFT frequency index, q, with parameters: $\mathsf{SNR} = 10\,\mathrm{dB}$, $N_{\mathrm{b}} = 128$, $N = 1000$. PSD represents the power spectral density of the signal to be detected.

when $\mathsf{SNR} = -10\,\mathrm{dB}$. In this case, due to the low SNR regime, the number of frequency bins detected is smaller that the real one. However $\mathsf{AIC}^{\mathrm{c}}$ performs better then $\mathsf{AIC}^{\mathrm{i}}$ and $\mathsf{BIC}^{\mathrm{c}}$, while $\mathsf{BIC}^{\mathrm{i}}$ has poor performance. The analysis above demonstrates that the $\mathsf{AIC}^{\mathrm{c}}$ generally has a better performance than $\mathsf{BIC}^{\mathrm{c}}$ in terms of number of frequency components identified. Anyway, these two new algorithms outperform $\mathsf{AIC}^{\mathrm{i}}$ and $\mathsf{BIC}^{\mathrm{i}}$ in presence of spectrally correlated signals.

4.6 Conclusions

In this chapter we proposed an ITC wideband spectrum sensing technique to distinguish between occupied and unoccupied frequency bands. We described a general approach that can be applied to any spectral representation and then focused on the simple DFT case. The proposed technique is completely blind since it does not require any knowledge about the noise power and characteristics of the signals present in the observed band. In particular, we showed that consistent ITC can reach an almost one probability to correctly identify the set of occupied bins, outperforming simple ED based approaches.

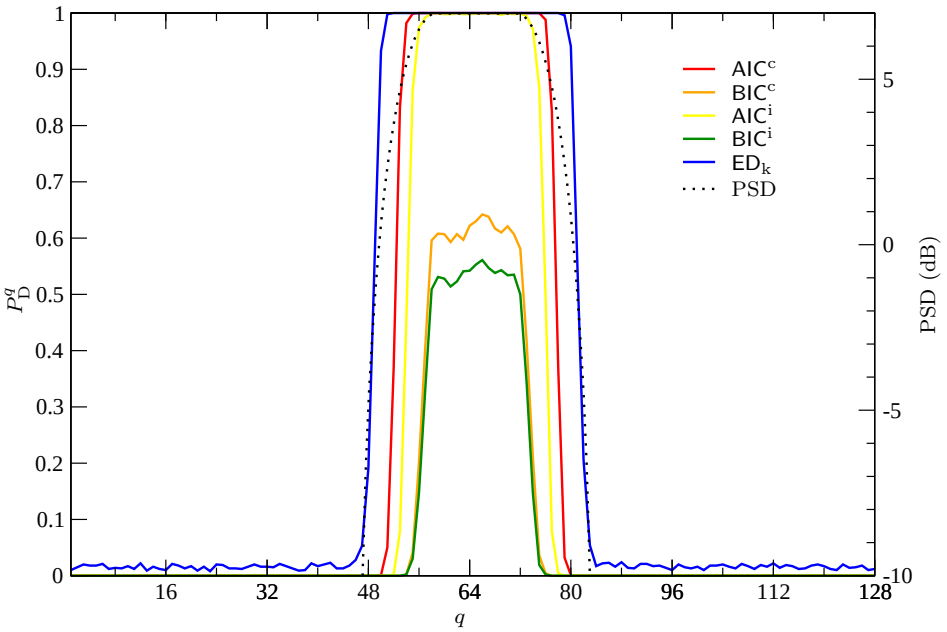

Figure 4.14: Detection probability for each bin, P_{D}^{q}, as function of the DFT frequency index, q, with parameters: $\mathsf{SNR} = -10\,\mathrm{dB}$, $N_{\mathrm{b}} = 128$, $N = 1000$. PSD represents the power spectral density of the signal to be detected.

Numerical results revealed that this wideband approach can be applied both with the independent and the correlated frequency components. In particular the derived DFT approach can be also applied in situations in which the exact distribution of the observation is unknown or too complex, such as advanced techniques like MTM spectrum estimation.

Chapter 5

Cooperative Weighted Centroid Localization

The localization information is important in particular when the PU considered is a low transmit power/low coverage area device (often called *small scale* PU [164]). This is the case, for example, of the PMSE devices that are allowed to transmit on DTV channels on a non interfering basis. Considering DTV as PU it is reasonable to assume that the SUs are located in an area with relatively smaller dimensions compared to the distance from the transmitter (*large scale* PU). It has been demonstrated that, in this scenario, cooperative algorithms can improve the sensing performance and allow to reduce the observation time. In order to sense the presence of small scale devices cooperation among the SUs is not an optional feature to improve the performance, but is an essential element for the fulfilment of the sensing task. In this case it is fundamental indeed to consider, besides fading and shadowing effects, also the path loss attenuation caused by the distance from the PU transmitter, that is different for each SU.[1] Cooperation therefore allows to reach a global network awareness of the radio environment exploiting the observations of the SUs that, due to their proximity, can sense the PU.

In this chapter we focus on cooperative localization algorithms for CR networks. We consider a CR scenario in which the PU is a PMSE device including noise and shadowing effects. We assume that each SU is equipped with a radiometer - that is a typical solution for detection purposes [92] - and focus on how the received power information can be exploited using WCL strategies [165–169]. These techniques have been proposed as coarse grained algorithms in the field of wireless sensor networks (WSNs), considering the

[1]For large scale PU scenarios the mean path loss from the transmitter is assumed to be the same for each SU.

requirement of maintaining a low computational complexity given cost and power constraints [165–168]. Centroid based techniques are very attractive also for CR systems, where we cannot assume any knowledge on the PU signal and low cost nodes implementation is a preferable feature. We propose different weighting functions and compare the relative performance in terms of RMSE. A common assumption in literature is that the PU is fixed in the center of the area [169]. We show that the performance of the algorithms can be strongly reduced if the PU moves away from this point and identify which weighting strategies are more robust to this effect. We also propose two SU selection strategies to reduce the localization error which result to be effective in harsh environments characterized by high path loss exponents.

5.1 System model

We consider a cooperative CR network composed by N SUs distributed in a $\mathcal{L} \times \mathcal{L}$ square area centered in the point $(0, 0)$. We assume that the i-th SU is located at the point with coordinates (x_i, y_i), with $i = 1, \ldots, N$, and that the positions of all the SUs are known. One PU is present and located at (x_0, y_0). We model the PU received power at the i-th SU location as

$$\mathrm{P}_i = \frac{\mathcal{K}_0 \mathrm{P}}{d_i^{\alpha}} S_i \tag{5.1}$$

where $1/\mathcal{K}_0$ is the path loss at the reference distance of 1 m,[2] P is the PU transmit power, d_i is the distance between the PU and the i-th SU, α is the power loss exponent and S_i is a r.v. that accounts for fading. Due to the presence of channel impairments such as fading and noise, we consider the estimation of the received power (5.1) as

$$\xi_i = \frac{1}{M} \sum_{j=0}^{M-1} \left| s_{i,j} + n_{i,j} \right|^2 \tag{5.2}$$

where M is the number of samples collected at the i-th SU receiver, $s_{i,j}$ is the j-th complex baseband received signal sample, and $n_{i,j}$ denotes the AWGN sample with power σ^2.[3]

[2] $\mathcal{K}_0$ may include the PU and SU antenna gains. Note that in the following we assume omnidirectional antennas and equal antenna gains at all SUs.

[3] Usually the receiver noise is neglected and fading is the sole channel impairment considered. As shown in the following, the effect of noise cannot be neglected since its impact is relevant in performance analysis as well as in the design of effective localization algorithms.

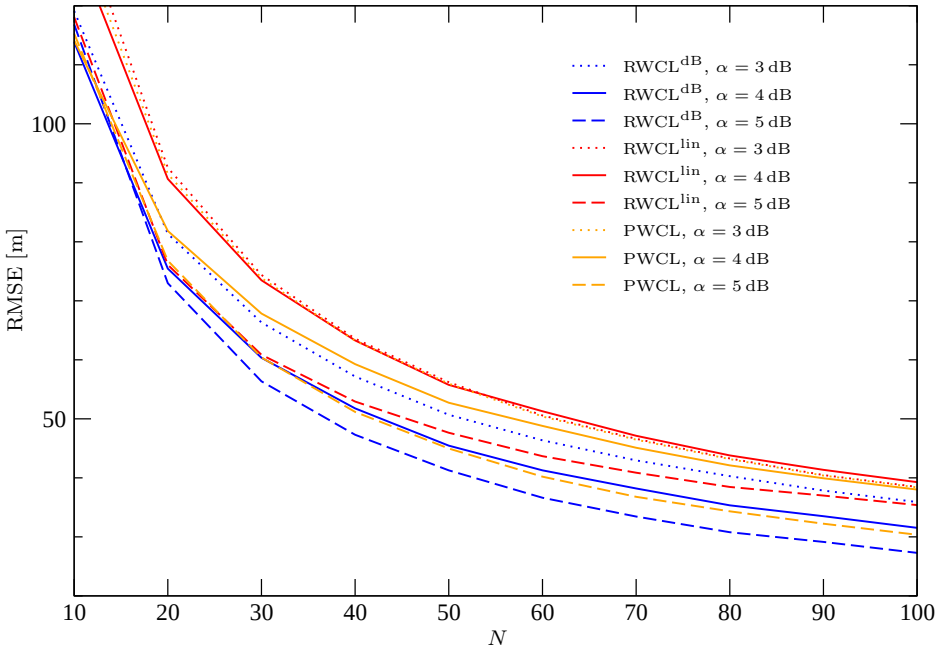

Figure 5.1: RMSE for the three WCL algorithms as function of the number of SUs for different values of α. The SUs are randomly distributed in a square area.

We set the scenario parameters according to the DTV frequency bands, in which PMSE can operate. The PMSE transmissions are allowed to operate in the 470-790 MHz band within the European Community [170] and in the 520-820 MHz band in Australia [171]. We choose the carrier frequency $f_0 = 600$ MHz, which can be also adopted in the United States [23]. We consider a PU transmit power P = 50 mW. The wireless channel considered is affected by log-normal shadowing with dB spread σ_{dB}, i.e. S_i in dB scale is a Gaussian r.v. with zero mean and variance $\sigma_{\text{dB}} \ln(10)/10$. In the following we consider $\sigma_{\text{dB}} = 5.5$ dB as reference value [172] and path loss exponents between 3 and 5, typical of urban/suburban environments [164].

Considering a CR scenario, having generally no particular spatial constraints, it is reasonable to assume that the SUs are randomly distributed in the area of interest. However in some case for analysis purposes it is useful to remove the effect of the randomness of the position of the SUs. For this purpose we will also consider a fixed SUs placement on the cross points of a square grid.[4]

[4]With reference to the $N = 100$ case we will consider the set of the SUs coordinates $(x_i, y_i) \in \{\pm 50, \pm 150, \pm 250, \pm 350, \pm 450\}$.

5.2 Weighted centroid localization

Generally in WSNs centroid based localization is adopted by a node that wants to localize itself exploiting a network of reference nodes, with known positions, that periodically transmit beacon signals. In CR we must consider a different scenario with respect to the WSNs. Indeed, in our case is the network of SUs that performs the localization of the PU transmitter which position is unknown. Since the localization process involves a collaboration of SUs, the WCL algorithms presented are cooperative.

5.2.1 Weighting strategies

The original formulation of the algorithm is the centroid localization (CL), which simply computes the PU location averaging the coordinates of the SUs [165]. Of course CL is a simple but very coarse technique. The more general formulation of CL, called WCL, has attracted a lot of interest due to its simplicity and robustness to changes in wireless propagation properties [166]. The WCL estimates (x_0, y_0) as

$$(\widehat{x}_0, \widehat{y}_0) = \left(\frac{\sum_{i=1}^{N} w_i \, x_i}{\sum_{i=1}^{N} w_i}, \frac{\sum_{i=1}^{N} w_i \, y_i}{\sum_{i=1}^{N} w_i} \right) \tag{5.3}$$

where w_i, with $i = 1, \ldots, N$, are the weighting coefficients.[5] Many techniques have been proposed in literature for the design of the coefficients. For example a distance based strategy has been proposed in [166] assuming that the estimates of the distances of the SUs from the PU are available. Alternatively, the choice of the coefficients can be based on the received energy at the SUs. Considering the path loss propagation effect it is indeed reasonable to assign an higher weight to the coordinates of the nodes that experience a higher received power, while distant nodes, which received signal power is lower, must be penalized. Assuming that the SUs are equipped with a radiometer for detection purposes, we can exploit the estimated power levels for weights calculation in WCL. We adopt in particular three reference models for the weighting coefficients. The first consists in the most intuitive choice of taking the weight of the i-th SU as

$$w_i = \xi_i. \tag{5.4}$$

We refer to this approach as power based WCL (PWCL). The second reference model is the relative span weighted centroid method, proposed in [168].

[5] Note that if $w_i = 1$, $\forall i$, we obtain the CL algorithm.

This criterion consists in a linear weighting of the received power levels in dB where the nodes with maximum and minimum ξ_i are assigned the weights 1 and 0, respectively. Then this weighting gives more emphasis on the difference among the received power levels at the SUs rather than on their actual values. For the i-th SU the corresponding weight is given by

$$w_i = \frac{\xi_i^{\mathrm{dB}} - \xi_{\min}^{\mathrm{dB}}}{\xi_{\max}^{\mathrm{dB}} - \xi_{\min}^{\mathrm{dB}}} \tag{5.5}$$

where $\xi_i^{\mathrm{dB}} = 10\log_{10}\xi_i$, $\xi_{\max}^{\mathrm{dB}} = \max_i \xi_i^{\mathrm{dB}}$ and $\xi_{\min}^{\mathrm{dB}} = \min_i \xi_i^{\mathrm{dB}}$. We refer to this approach as RWCL$^{\mathrm{dB}}$. We include in the analysis also a third weighting strategy that is a modification of the RWCL$^{\mathrm{dB}}$ where the ξ_i are expressed in linear scale. Then the weight of the i-th SU is expressed as

$$w_i = \frac{\xi_i - \xi_{\min}}{\xi_{\max} - \xi_{\min}} \tag{5.6}$$

where $\xi_{\max} = \max_i \xi_i$ and $\xi_{\min} = \min_i \xi_i$. We refer to this approach as RWCL$^{\mathrm{lin}}$.

5.2.2 WCL with node selection

In order to improve the localization performance of the WCL, with reference in particular to the dependency of the RMSE on the position of the PU, we investigate two possible techniques based on the selection of the SUs involved in the localization process. Similar approaches have been proposed in the field of WSNs to alleviate border effects [167].

The first technique, called two step WCL (TS-WCL) consists in two consecutive localization steps. The first is a simple WCL that provides the tentative estimate $\left(\widehat{x}_0^{\mathrm{I}}, \widehat{y}_0^{\mathrm{I}}\right)$. The second step estimates the PU location using only the SUs that are within a circle of radius R centered on $\left(\widehat{x}_0^{\mathrm{I}}, \widehat{y}_0^{\mathrm{I}}\right)$.

The second technique we propose consists in a simple SU selection based on the received power levels. In order to remove the contributions of the SUs with low received power (whose measurements mainly consist in noise) we select the nodes with $\xi_i > \eta$, where η is a threshold. We refer to this approach as energy based selection WCL (ES-WCL).

5.3 Localization Performance Analysis

The performance of the localization algorithm depends on many factors, such as the density of the SUs in the area, the transmission range, the path loss exponent and the position of the PU. In Fig. 5.1 we plot the RMSE on

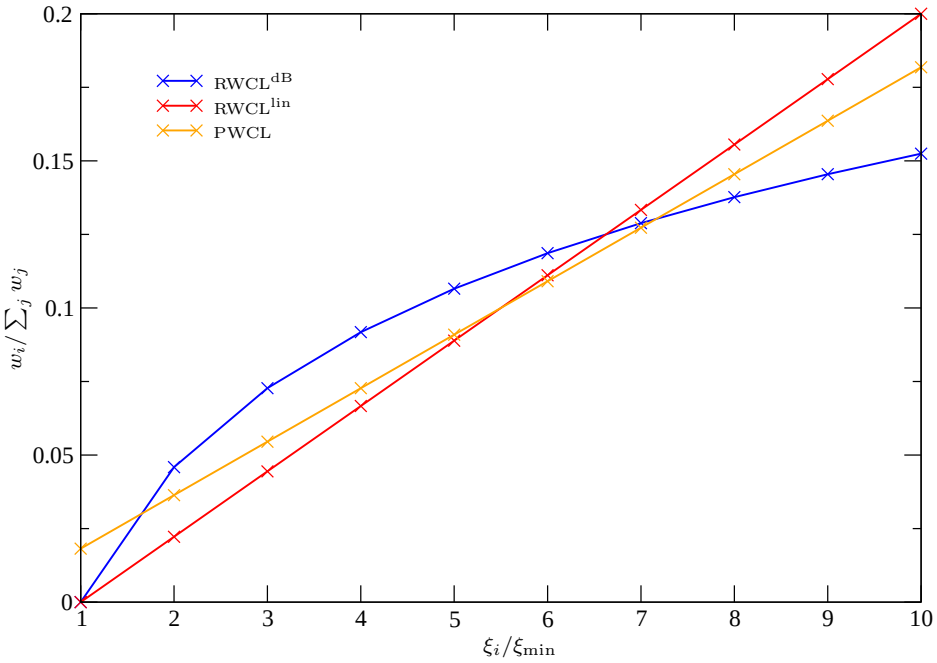

Figure 5.2: Example of WCL weighting coefficients. The reference power level set is $\{\xi_i\} = \{\xi_{\min}, 2\,\xi_{\min}, \ldots, 10\,\xi_{\min}\}$ and $\{w_i\}$ is the corresponding set of weights. $N = 100$.

the estimation of the PU position as function of N when $(x_0, y_0) = (0, 0)$, considering different values for the path loss exponent when the SUs are uniformly randomly distributed in the area. As expected we can see that the easiest way to improve the localization accuracy is simply to increase the number of secondary nodes. In the reminder of the section we analyze the dependence of the RMSE on the position of the PU when N is fixed. The number of received signal samples collected to perform power estimation is $M = 1000$.

All centroid based localization algorithms have in common that the effect of each SU in the localization process is to pull the estimate towards its own position [167]. The CL does this with the same strength for each node, while WCL acts the same with a strength that depends on the weight assigned to each SU. The corresponding overall network effect is that the estimate of the PU position is always pulled towards the center of mass of the network. This point therefore is a privileged point for the localization of the PU. In this sense we can say that the localizing network is *biased* towards its center of mass. The first consequence of this fact is that, considering the situation in which the PU is located in $(0, 0)$, surprisingly we have an improvement

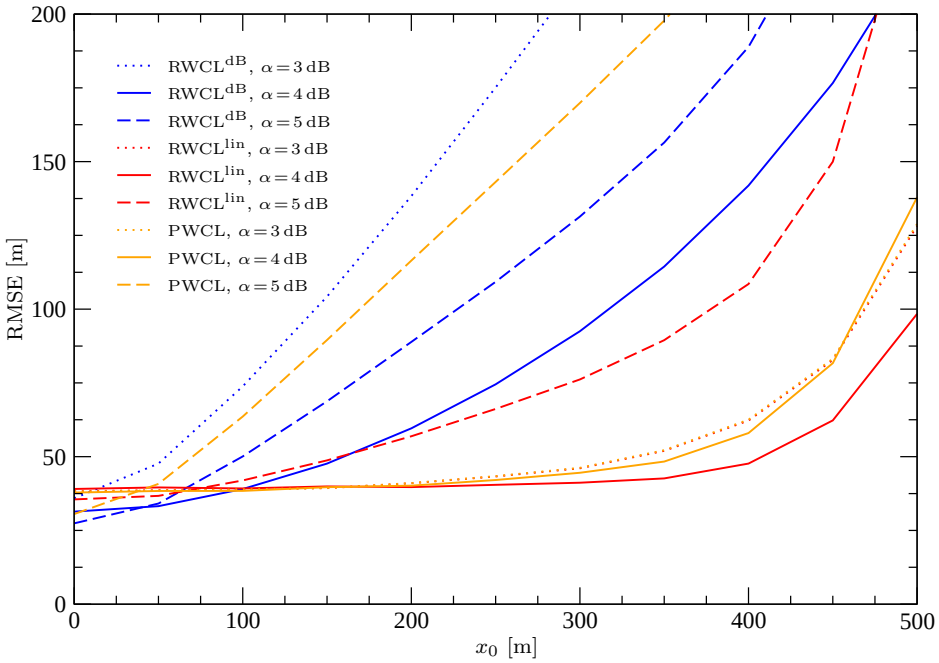

Figure 5.3: RMSE for the WCL algorithms as function of the x_0 coordinate of PU position for different values of α. The SUs are randomly distributed in a square area. $N = 100$.

in the RMSE when the path loss exponent increases (see Fig. 5.1). Indeed, reducing the transmission range increase the number of SUs which received power is mainly due to noise, whose impact on the estimation process is to reduce the RMSE due to the bias effect of the network. However if we move the PU away from the center of the network, the estimation error will be increased due to the natural tendency to localize the PU at the barycenter. In Fig. 5.3 we plot the RMSE on the PU localization as a function of the x_0 coordinate of the PU moved from the center ($x_0 = 0\,\mathrm{m}$) to the side of the area ($x_0 = 500\,\mathrm{m}$) for $N = 100$. We can see that the three different WCL algorithms described previously show a different dependence on the PU location. Indeed the RWCL$^{\mathrm{dB}}$, that gives low RMSE when the PU is at $(0, 0)$, rapidly degrades when it moves toward the border of the area. On the contrary, RWCL$^{\mathrm{lin}}$, that has a higher RMSE when the PU is at $(0, 0)$, maintains almost the same RMSE except for extreme PU positions on the edge of the area. This effect is simply due to the different weighting strategies applied. The RWCL$^{\mathrm{lin}}$ adopts a 'more selective' weighting, in the sense that the unbalance between higher and lower weights is bigger, while the RWCL$^{\mathrm{dB}}$ assigns higher weights to a large number of SUs. In Fig. 5.2 we

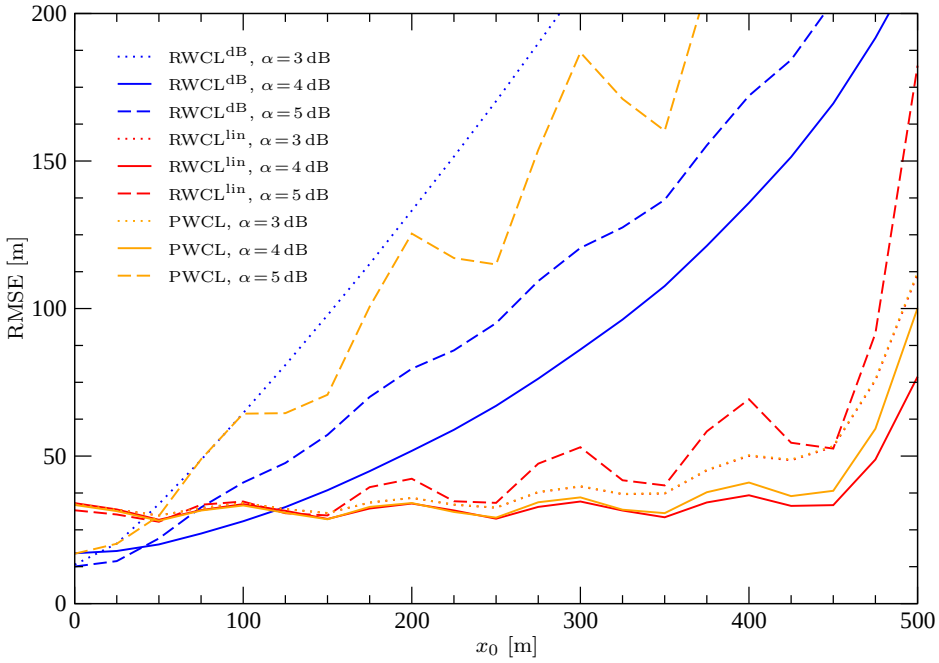

Figure 5.4: RMSE for the WCL algorithms as function of the number of the x_0 coordinate of the PU position for different values of α. The SUs are placed on a rectangular grid with equal spacing $\Delta = 100\,\mathrm{m}$. $N = 100$.

show an example of the weights corresponding to a test set of received power $\{\xi_i\} = \{\xi_{\min}, 2\,\xi_{\min}, \ldots, 10\,\xi_{\min}\}$. We can see that the difference between the higher and lower weights is bigger for the RWCL$^{\mathrm{lin}}$ than the RWCL$^{\mathrm{dB}}$, while the PWCL is in between. Moreover we can see that the RWCL$^{\mathrm{dB}}$ is 'less selective' because the weights are slowly decreasing for higher power levels, then the number of nodes that have high weights is greater for the RWCL$^{\mathrm{dB}}$. In this sense we can say that the number of nodes that effectively contribute in the weighting process is less for the RWCL$^{\mathrm{lin}}$ than the RWCL$^{\mathrm{dB}}$. Due to this difference the RWCL$^{\mathrm{dB}}$ benefits from the bias effect when the PU is at the center of mass of the network with distant nodes having relatively high weights. The RWCL$^{\mathrm{lin}}$ instead, that involves a smaller number of nodes, does not benefit from of the bias effect of the network but is much more robust to situations in which the PU is away from the center. To analyze the effect of the randomness of the SU positions, in Fig. 5.4 we plot the RMSE as a function of x_0 when the SUs are placed on a square grid. We can see that the localization error is reduced in particular for the RWCL$^{\mathrm{lin}}$ while performance of the RWCL$^{\mathrm{dB}}$ is less affected.The relative minima shown in

the curves correspond to the SU positions on the grid.

In Fig. 5.5 we show the RMSE for the three WCL algorithms using the TS-WCL approach. We can see that the selection strategy is not useful when the PU is in the center of the area. Indeed the selection of the nodes impedes the possibility to exploit the bias effect on the network. When the PU is at a different position ($x_0 = 200\,\mathrm{m}$ in Fig. 5.5) instead we can see that the $\mathrm{RWCL}^{\mathrm{dB}}$ presents a minimum that corresponds to the optimal R to be adopted, while the $\mathrm{RWCL}^{\mathrm{lin}}$ has a very weak improvement. For lower values of α however the gain provided by the TS-WCL is limited. Finding the optimal R is beyond the scope of this paper, although the performance sensitivity with respect to its value is quite low. In Fig. 5.6 we show the RMSE for the three WCL algorithms when the ES-WCL is adopted. We can see that, as for the TS-WCL, this selection does not provide improvements when the PU is in $(0, 0)$ and for low values of α. However for higher values of the path loss exponent, e.g. $\alpha = 5$ in Fig. 5.6(a), all the three WCL strategies present an optimal threshold value that allows to reduce the RMSE when the PU is in a different position ($x_0 = 200$ in Fig. 5.6). Finding the optimal η is beyond the scope of this paper, however it is interesting to note that in Fig. 5.6(a), when $\alpha = 5$, the optimum value of the threshold is approximatively $\eta \simeq \sigma^2$, which is a very simple rule of thumb.

5.4 Conclusions

In this paper we consider the problem of localizing the PU using WCL techniques based on the estimated received power at the SUs. We studied in particular three different weighting strategies and analyzed their performance in terms of RMSE and its dependence on the PU position within the area considered. The analysis reveals that the design of the WCL weights is crucial in determining the dependence between localization accuracy and PU position. The simulation results suggest that using 'more selective' weighting strategies (i.e. that emphasize the separation between high and low received power nodes), such as the $\mathrm{RWCL}^{\mathrm{lin}}$, reduces the effect of this dependence. Moreover we introduced two selection strategies that can be adopted to improve the localization accuracy in environments with high path loss exponents.

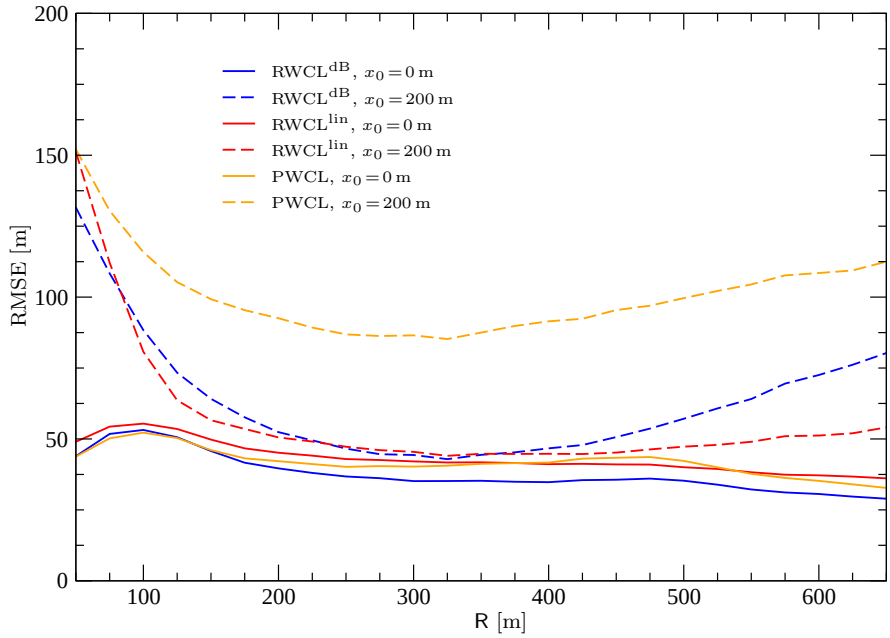

(a) $\alpha = 5$

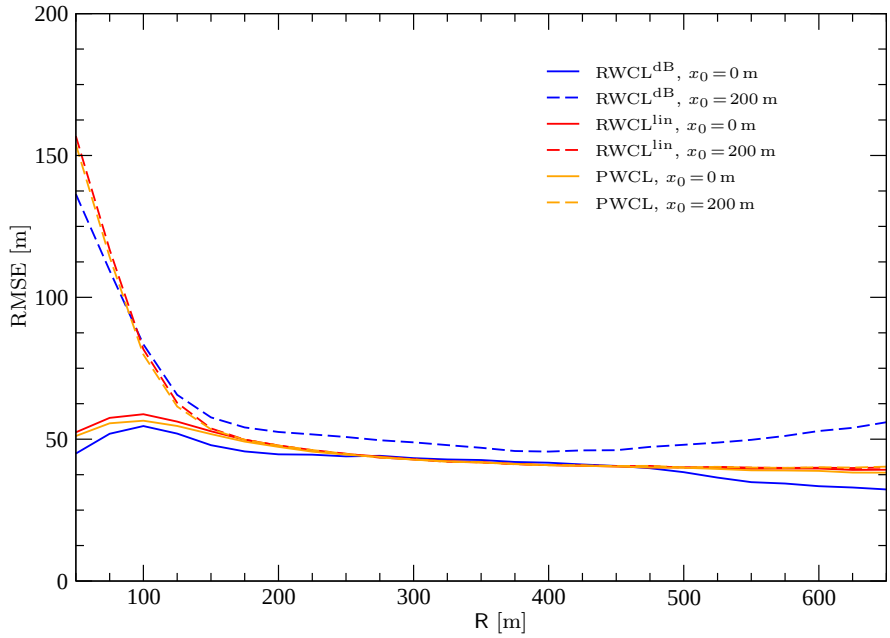

(b) $\alpha = 4$

Figure 5.5: RMSE for the WCL algorithms using the TS-WCL approach, as function of R. The SUs are randomly distributed in a square area. $N = 100$.

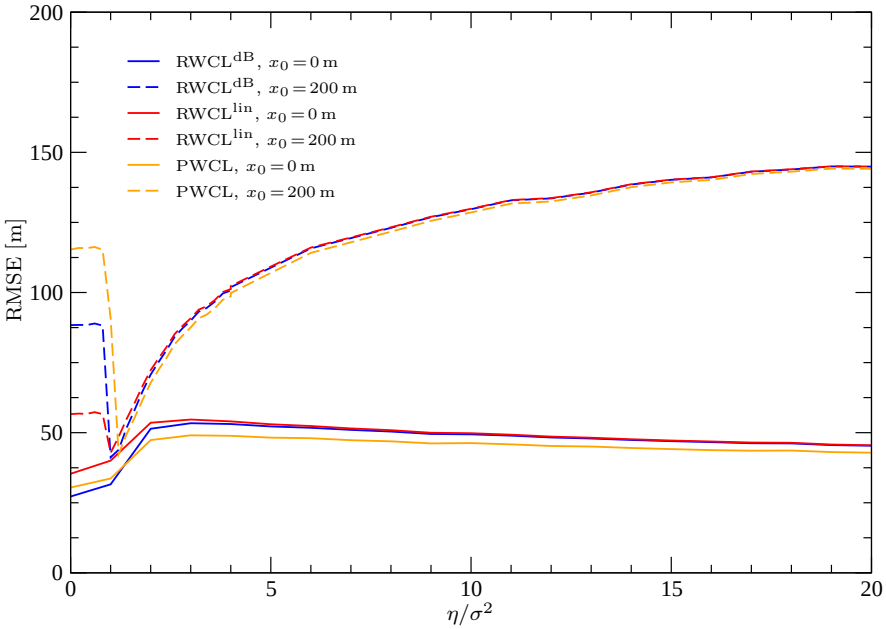

(a) $\alpha = 5$

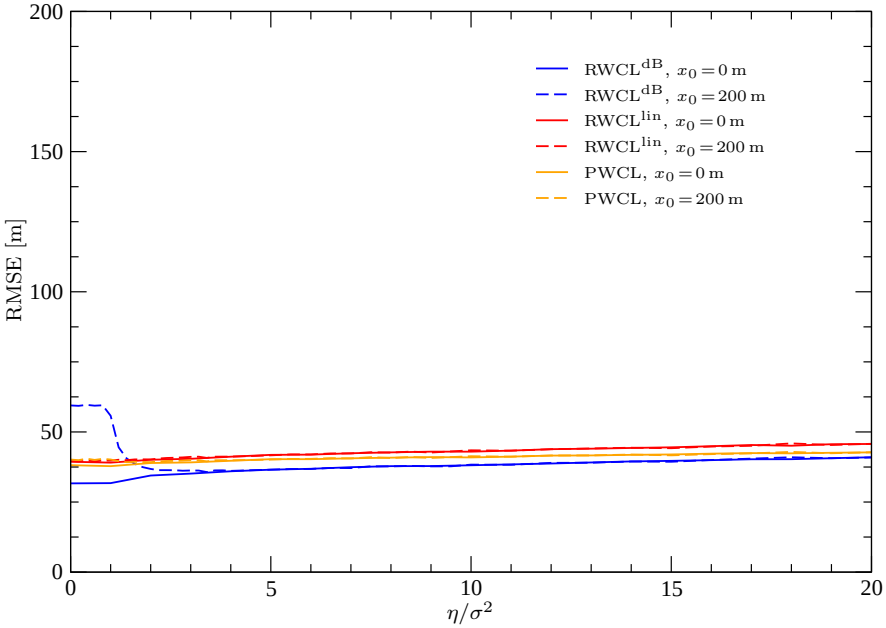

(b) $\alpha = 4$

Figure 5.6: RMSE for the WCL algorithms using the ES-WCL approach, as function of η. The SUs are randomly distributed in a square area. $N = 100$.

Chapter 6

Conclusions

In this dissertation we studied the problem of SS in CR wireless networks. We analyzed different sensing techniques, addressing algorithms from the different domains of SS, from simple energy detection, to cooperative strategies, to wideband sensing. Due to the fact the spectrum holes identification is the primary functionality of SS, we addressed in particular PU signal detection techniques.

We focused on the ED, which is the most popular sensing algorithm due to its simplicity of implementation, and its generality. The ideal ED also provide a good detection performance, that many feature detectors can attain only with a long observation time. The main problem of the ED is that an uncertain knowledge of the noise power level (noise uncertainty) can cause high performance losses, or even the rise of the SNR wall phenomenon, that makes impossible to detect the primary signal with arbitrary probabilities of detection and false alarm. Recent literature has emphasized this problem, in particular with the adoption of pessimistic uncertainty models, spreading the idea that the SNR wall phenomenon is an unavoidable problem in practical applications, since the estimated noise power always differs from the real noise power. Considering real implementations, the unknown noise power must be periodically estimated with a proper strategy. In this context we proved that noise estimation can avoid the SNR wall if the estimate is consistent with the observation interval. Then the SNR wall phenomenon is not caused by the presence of an uncertainty itself, but is rather due to the impossibility to refine the noise power estimation process while the observation time increases.

Within the context of cooperative SS we focused on eigenvalue based detection techniques, studying the GLRT in the most general case, i.e. making no assumptions on the covariance matrix of the received samples under the signal present hypothesis. When the noise power is the same for all the SUs, the GLRT is the sphericity test. However, in cooperative scenarios the most

proper assumption is that every node experiences a different noise power level. The GLRT in this case is the independence test. We addressed the statistical analysis of these tests, showing that both can be approximated as beta distributed r.v.s using a moment matching approach. This technique is a simple but effective strategy for situations in which exact distribution is unknown or has a complex form. It consists in using a simple distribution model, chosen among the most common ones, and setting its parameters using the exact moments of the tests under analysis. We focused in particular on the signal absent hypothesis providing easy to use expressions for the computation of the probability of false alarm and for setting the decision threshold under the NP approach.

Considering wideband observations of the spectrum, we studied a blind algorithm, based on ITC. This technique is based on the computation of a frequency representation of the spectrum (such as a spectral estimate or the output of a filter bank), followed by the adoption of ITC to discriminate between the noise only components from those that contain PU signals. We provided the general formulation of the problem and then we specialized the analysis for DFT, which is a simple frequency domain representation available in many receiver structures, such as OFDM receivers. The proposed technique is completely blind since it does not require any knowledge about the noise power and characteristics of the signals present in the observed band. Numerical results revealed that the wideband sensing algorithm proposed outperforms simple ED based strategies, and can be applied also when the statistical distribution of the observation is not known exactly.

In addition to PU detection for spectrum opportunities identification, the sensing functionality of CR includes any kind of technique that allows the SUs to collect information from the radio environment. In particular, information about the PU position plays an important role supporting higher level cognitive functionalities such as better spectrum resources allocation, avoiding and preventing harmful interference, aiding spectrum policy enforcement etc.. Therefore in this manuscript we also addressed the study of simple localization strategies, that can be adopted by SUs for estimating the PU position. We adopted in particular received power based WCL techniques, that are popular coarse grained algorithms developed in WSNs under computational complexity and power constraints. These strategies are also very attractive in CR contests, where we can not assume any knowledge on the PU and low cost nodes implementation is preferable. We studied in particular three different weighting strategies and analyzed their performance in terms of RMSE and its dependence on the PU position within the area considered. The analysis reveals that the design of the WCL weights is crucial in determining the dependence between localization accuracy and PU position.

The simulation results suggest that using 'more selective' weighting strategies (i.e. that emphasize the separation between high and low received power nodes) reduces the effect of this dependence. Moreover we introduced two selection strategies that can be adopted to improve the localization accuracy in environments with high path loss exponents.

List of Tables

List of Figures

Bibliography

[1] ITU, ICT Data and Statisics. [Online]. Available: http://www.itu.int/ITU-D/ict/statistics/.

[2] ——, Measuring the Information Society, Executive Summary, 2012. [Online]. Available: http://www.itu.int/ITU-D/ict/publications/idi/material/2012/MIS2012-ExecSum-E.pdf.

[3] CISCO, VNI Forecast Widget. [Online]. Available: http://www.ciscovni.com/vni_forecast/advanced.html.

[4] FCC, Mobile broadband: the benefits of additional spectrum, FCC Staff technical paper, Oct. 2010. [Online]. Available: http://download.broadband.gov/plan/fcc-staff-technical-paper-mobile-broadband-benefits-of-additional-spectrum.pdf.

[5] OFCOM, Real Wireless report, "Techniques for increasing the capacity of wireless broadband networks: UK, 2012-2030", Mar. 2012. [Online]. Available: www.ofcom.org.uk/static/uhf/realwireless-report.pdf

[6] CEPT, CEPT/ERC Report 25 The European table of frequency allocations and applications in the frequency range 9 kHz to 3000 GHz (ECA table), Feb. 2011.

[7] MIT Technology Review, Graphitis, Spectrum of Issues, Oct. 2010. [Online]. Available: www.technologyreview.com/graphiti/421421/spectrum-of-issues/

[8] EC, 2010/267/EU, EC Decision on harmonised technical conditions of use in the 790-862 MHz frequency band for terrestrial systems capable of providing electronic communications services in the European Union, May 2010.

[9] OFCOM, Securing long term benefits from scarce low frequency spectrum, UHF strategy statement, Nov. 2012.

[10] FCC, Spectrum Policy Task Force Report, ET Docket 02-135, Nov. 2002.

[11] A. Ghasemi and E. S. Sousa, "Spectrum sensing in cognitive radio networks: requirements, challenges and design trade-offs," *IEEE Commun. Mag.*, Apr. 2008.

[12] *IEEE Standard Definitions and Concepts for Dynamic Spectrum Access: Terminology Relating to Emerging Wireless Networks, System Functionality, and Spectrum Management*, IEEE Std. 1900.1-2008, Sep. 2008.

[13] J. Mitola III and G. Q. Maguire Jr., "Cognitive radio: making software radios more personal," *IEEE Personal Commun.*, vol. 6, no. 4, pp. 13–18, Aug. 1999.

[14] ITU-R, Definitions of Software Defined Radios (SDR) and Cognitive Radio Systems, Sept. 2009. [Online]. Available: http://www.itu.int/pub/R-REP-SM.2152.

[15] S. Filin, H. Harada, H. Murakami, and K. Ishizu, "International standardization of cognitive radio systems," *IEEE Commun. Mag.*, vol. 49, no. 3, pp. 82–89, Mar. 2011.

[16] S. Haykin, "Cognitive radio: brain-empowered wireless communications," *IEEE J. Sel. Areas Commun.*, vol. 23, no. 2, pp. 201–220, Feb. 2005.

[17] F. K. Jondal, "Software-defined radio - basics and evoluntion to cognitive radio," *EURASIP Journal on Wireless Communications and Networking*, vol. 3, pp. 275–283, 2005.

[18] I. Akyildiz, W.-Y. Lee, M. Vuran, and S. Mohanty, "A survey on spectrum management in cognitive radio networks," *IEEE Commun. Mag.*, vol. 46, no. 4, pp. 40–48, Apr. 2008.

[19] S. Kandeepan and A. Giorgetti, *Cognitive Radios and Enabling Techniques*. Boston, USA: Artech House Publishers, Nov. 2012.

[20] T. Yucek and H. Arslan, "A survey of spectrum sensing algorithms for cognitive radio applications," *IEEE Commun. Surveys Tuts.*, vol. 11, no. 1, pp. 116–130, 2009.

[21] P. Pawelczak, K. Nolan, L. Doyle, S. W. Oh, and D. Cabric, "Cognitive radio: Ten years of experimentation and development," *IEEE Trans. Commun.*, vol. 49, no. 3, pp. 90–100, Mar. 2011.

[22] D. Finn, L. Tallon, J.and DaSilva, P. Van Wesemael, S. Pollin, W. Liu, S. Bouckaert, J. Vanhie-Van Gerwen, N. Michailow, J. Hauer, D. Willkomm, and C. Heller, "Experimental assessment of tradeoffs among spectrum sensing platforms," in *in Proc. ACM Int. Workshop on Wireless Netw. Testbeds, Experimental Evaluation and Characterization (WiNTECH 2011)*, 2011, pp. 67–74.

[23] FCC, Report and order and further notice of proposed rulemaking 10-16, Jan. 2010.

[24] Industry Canada, Framework for the Use of Certain Non-broadcasting Applications in the Television Broadcasting Bands Below 698 MHz, Aug. 2011.

[25] B. Freyens and M. Loney, "Opportunities for white space usage in australia," in *in Proc. IEEE Int. Conf. on Wireless Commun., Veh. Technol., Inf. Theory and Aerosp. Electron. Syst. Technol. (Wireless VITAE 2011)*, Mar. 2011.

[26] H. Harada, Status report on usage of TV white space in Japan, 802.11-12/677r0, May 2012.

[27] *Ecma 392: MAC and PHY for Operation in TV White Spaces*, Ecma International Std., Dec. 2009, [Online]. Available: http://www.ecma-international.org/publications/standards/Ecma-392.htm.

[28] *Ecma 392: MAC and PHY for Operation in TV White Spaces, 2nd Edition*, Ecma International Std., Jul. 2012.

[29] *IEEE Standard for Information Technology - Telecommunications and information exchange between systems Wireless Regional Area Networks (WRAN) - Specific requirements - Part 22: Cognitive Wireless RAN Medium Access Control (MAC) and Physical Layer (PHY) Specifications: Policies and Procedures for Operation in the TV Bands*, IEEE Std. 802.22-2011, Jul. 2011.

[30] M. Mueck and D. Noguet, "TV white space standardization and regulation in Europe," in *in Proc. Int. Conf. on Wireless Commun., Veh. Technol., Inf. Theory and Aerosp. Electron. Syst. Technol. (Wireless VITAE 2011)*, Mar. 2011.

[31] M. Mueck, A. Piipponen, K. Kalliojaervi, G. Dimitrakopoulos, K. Tsagkaris, P. Demestichas, F. Casadevall, J. Péandrez-Romero, O. Sallent, G. Baldini, S. Filin, H. Harada, M. Debbah, T. Haustein, J. Gebert, B. Deschamps, P. Bender, M. Street, S. Kandeepan, J. Lota, and A. Hayar, "ETSI reconfigurable radio systems: status and future directions on software defined radio and cognitive radio standards," *IEEE Commun. Mag.*, vol. 48, no. 9, pp. 78–86, Sep. 2010.

[32] M. Matinmikko, "Spectrum sharing using cognitive radio system capabilities. methods to obtain and exploit knowledge of spectrum availability," Ph.D. dissertation, VTT Technical Research Centre of Finland, Nov. 2012.

[33] O. Tonelli, G. Berardinelli, A. F. Cattoni, T. B. Sørensen, and P. E. Mogensen, "Software architecture design for a dynamic spectrum allocation-enabled cognitive radio testbed," in *Proc. European Signal Process. Conf. (EUSIPCO 2011)*, Barcelona, Spain, 2011.

[34] A. Ghasemi and E. Sousa, "Spectrum sensing in cognitive radio networks: requirements, challenges and design trade-offs," *IEEE Commun. Mag.*, vol. 46, no. 4, pp. 32–39, Apr. 2008.

[35] FCC, Second memorandum opinion and order 10-147, Sep. 2011.

[36] OFCOM, Digital dividend: cognitive access. Statement on licence-exempting cognitive devices using interleaved spectrum, Jul. 2009.

[37] ECC, Report 159 Technical and Operational Requirements for the Possible Operation of Cognitive Radio Systems in the 'White Spaces' of the Frequency Band 470-790 MHz, Jan. 2011.

[38] ——, Draft Report 185 Complementaty Report to ECC Report 159 Further Definition of Technical and Operational Requirements for the Possible Operation of White Spaces Devices in the Band 470-790 MHz, Nov. 2011. [Online]. Available: www.cept.org/ecc/groups/ecc/wg-se/se-43/client/meeting-documents

[39] A. A. El-Sherif and K. J. R. Liu, "Joint design of spectrum sensing and channel access in cognitive radio networks," *IEEE Trans. Wireless Commun.*, vol. 10, no. 6, pp. 1743–1753, Jun. 2011.

[40] W.-Y. Lee and I. F. Akyildiz, "Optimal spectrum sensing framework for cognitive radio networks," *IEEE Trans. Wireless Commun.*, vol. 7, no. 10, pp. 3845–3857, Oct. 2008.

[41] H. Urkowitz, "Energy detection of unknown deterministic signals," *Proc. IEEE*, vol. 55, no. 4, pp. 523–531, April 1967.

[42] W. Saad, Z. Han, T. Basar, M. Debbah, and A. Hjorungnes, "Coalition formation games for collaborative spectrum sensing," *IEEE Trans. Veh. Technol.*, vol. 60, no. 1, pp. 276–297, Jan. 2011.

[43] H. Sarvanko, M. Mustonen, A. Hekkala, A. Mammela, M. Matinmikko, and M. Katz, "Cooperative and noncooperative spectrum sensing techniques using welch's periodogram in cognitive radios," in *in Proc. IEEE Int. Workshop on Cognitive Radio and Advanced Spectrum Management (CogART 2008)*, Feb. 2008.

[44] M. Mustonen, M. Matinmikko, and A. Mammela, "Cooperative spectrum sensing using quantized soft decision combining," in *in Proc. IEEE Int. Conf. on Cognitive Radio Oriented Wireless Netw. and Commun. (CROWNCOM 2009)*, Jun. 2009.

[45] H. Van Trees, *Detection, Estimation and Modulation Theory. Part I: Detection, Estimation, and Linear Modulation Theory.* New York, U.S.A.: Wiley, 1968.

[46] S. M. Kay, *Fundamentals of Statistical Processing: Estimation Theory.* Prentice-Hall Signal Processing Series, 1993, vol. 1.

[47] A. Sonnenschein and P. M. Fishman, "Radiometric detection of spread-spectrum signals in noise of uncertain power," *IEEE Trans. Aerosp. Electron. Syst.*, vol. 28, no. 3, pp. 654–660, Jul. 1992.

[48] R. Tandra and A. Sahai, "SNR walls for feature detectors," in *Proc. IEEE Int. Symp. on New Frontiers in Dynamic Spectrum Access Netw. (DySPAN 2007)*, Apr. 2007, pp. 559–570.

[49] ——, "SNR walls for signal detection," *IEEE Jour. on Selected Topics in Signal Proc.*, vol. 2, pp. 4–17, Feb. 2008.

[50] S. Chaudhari, V. Koivunen, and H. Poor, "Autocorrelation-based decentralized sequential detection of OFDM signals in cognitive radios," *IEEE Trans. Signal Process.*, vol. 57, no. 7, pp. 2690–2700, 2009.

[51] E. Axell and E. Larsson, "Optimal and near-optimal spectrum sensing of ofdm signals in AWGN channels," in *Proc. IEEE Int. Workshop on Cognitive Inf. Process. (CIP 2010)*, 2010, pp. 128–133.

[52] D. Danev, E. Axell, and E. Larsson, "Spectrum sensing methods for detection of DVB-T signals n AWGN and fading channels," in *Proc. IEEE Conf. on Personal, Indoor and Mobile Radio Commun. (PIMRC 2010)*, 2010.

[53] D. Cabric, A. Tkachenko, and R. Brodersen, "Spectrum sensing measurements of pilot, energy, and collaborative detection," in *Proc. IEEE Military Commun. Conf. (MILCOM 2006)*, Oct. 2006.

[54] W. A. Gardner, *Introduction to Random Processes with Applications to Signals and Systems*, 2nd ed. McGraw-Hill, 1990.

[55] W. Gardner, "Signal interception: a unifying theoretical framework for feature detection," *IEEE Trans. Commun.*, vol. 36, no. 8, pp. 897–906, Aug. 1988.

[56] A. Mariani, "Detection algorithms based on cyclic spectrum analysis for cognitive radio," Master's thesis, Second Faculty of Engineering, Alma Mater Studiorum University of Bologna, Cesena, Italy, 2009.

[57] M. Chiani, A. Giorgetti, A. Mariani, and M. Montanari, "Cognitive radio for defense scenarios Technical challenges and spectrum sensing issues," in *in Proc. SDR Italy'09 Workshop, Form Software Defined Radio to Cognitive Netw.*, Nov. 2009.

[58] J. Lunden, V. Koivunen, A. Huttunen, and H. Poor, "Collaborative cyclostationary spectrum sensing for cognitive radio systems," *IEEE Trans. Signal Process.*, vol. 57, no. 11, pp. 4182–4195, Nov. 2009.

[59] D. Cabric, "Addressing feasibility of cognitive radios," *IEEE Signal Process. Mag.*, vol. 25, no. 6, pp. 85–93, Nov. 2008.

[60] M. Chiani, M. Z. Win, and H. Shin, "MIMO networks: The effects of interference," *IEEE Trans. Inf. Theory*, vol. 56, no. 1, pp. 336–349, Jan. 2010.

[61] M. Chiani, M. Z. Win, and A. Zanella, "On the capacity of spatially correlated MIMO Rayleigh-fading channels," *IEEE Trans. Inf. Theory*, vol. 49, no. 10, pp. 2363–2371, Oct. 2003.

[62] A. Sibille, C. Oestges, and A. Zanella, *MIMO: From Theory to Implementation.* Academic Press, 2010.

[63] H. K. Bizaki, *MIMO Systems, Theory and Applications.* InTech, 2011.

[64] Y. Zheng and Y.-C. Liang, "Maximum-minimum eigenvalue detection for cognitive radio," in *in Proc. IEEE Int. Symposium on Personal, Indoor and Mobile Radio Commun. (PIMRC 2007)*, Sep. 2007.

[65] T. J. Lim, R. Zhang, Y. C. Liang, and Y. Zeng, "GLRT-based spectrum sensing for cognitive radio," in *Proc. IEEE Global Commun. Conf. (GLOBECOM 2008)*, Dec. 2008.

[66] F. Penna, R. Garello, and M. A. Spirito, "Cooperative spectrum sensing based on the limiting eigenvalue ratio distribution in Wishart matrices," *IEEE Commun. Lett.*, vol. 13, no. 7, pp. 507–509, Jul. 2009.

[67] M. Chiani and M. Z. Win, "Estimating the number of signals observed by multiple sensors," in *Proc. IEEE Int. Workshop on Cognitive Inf. Process. (CIP)*, Elba Island, Italy, Jun. 2010, pp. 156–161.

[68] R. Lopez-Valcarce, G. Vazquez-Vilar, and J. Sala, "Multiantenna spectrum sensing for cognitive radio: overcoming noise uncertainty," in *Proc. IEEE Int. Workshop on Cognitive Inf. Process. (CIP 2010)*, Elba Island, Italy, Jun. 2010, pp. 310–315.

[69] P. Wang, J. Fang, N. Han, and H. Li, "Multiantenna-assisted spectrum sensing for cognitive radio," *IEEE Trans. Veh. Technol.*, vol. 59, no. 4, pp. 1791–1800, May 2010.

[70] J. Mauchly, "Significance test for sphericity of a normal n-variate distribution," *The Annals of Mathematical Statistics*, vol. 11, no. 2, pp. 204–209, Jun. 1940.

[71] A. Leshem and A.-J. van der Veen, "Multichannel detection of gaussian signals with uncalibrated receivers," *IEEE Signal Process. Lett.*, vol. 8, no. 4, pp. 120–122, Apr. 2001.

[72] M. Wax and T. Kailath, "Detection of signals by information theoretic criteria," *IEEE Trans. Acoust., Speech, Signal Process.*, vol. 33, Apr. 1985.

[73] B. Zayen, A. Hayar, and K. Kansanen, "Blind spectrum sensing for cognitive radio based on signal space dimension estimation," in *Proc. IEEE Int. Conf. on Commun. (ICC 2009)*, Jun. 2009.

[74] R. Wang and M. Tao, "Blind spectrum sensing by information theoretic criteria for cognitive radios," *IEEE Trans. Veh. Technol.*, Oct. 2010.

[75] D. Thomson, "Spectrum estimation and harmonic analysis," *Proc. IEEE*, vol. 70, no. 9, pp. 1055–1096, Sep. 1982.

[76] T. Erpek, A. Leu, and B. Mark, "Spectrum sensing performance in tv bands using the multitaper method," in *Proc. IEEE Signal Process. and Commun. Applications Conf. (SIU 2007)*, Jun. 2007.

[77] Q. Zhang, "Theoretical performance and thresholds of the multitaper method for spectrum sensing," *IEEE Trans. Veh. Technol.*, vol. 60, no. 5, pp. 2128–2138, Jun. 2011.

[78] B. Farhang-Boroujeny, "Filter bank spectrum sensing for cognitive radios," *IEEE Trans. Signal Process.*, vol. 56, no. 5, pp. 1801–1811, May 2008.

[79] B. Farhang-Boroujeny and R. Kempter, "Multicarrier communication techniques for spectrum sensing and communication in cognitive radios," *IEEE Commun. Mag.*, vol. 46, no. 4, pp. 80–85, Apr. 2008.

[80] Z. Quan, W. Zhang, S. J. Shellhammer, and A. H. Sayed, "Optimal spectral feature detection for spectrum sensing at very low SNR," *IEEE Trans. Commun.*, vol. 59, no. 1, pp. 201–212, Jan. 2011.

[81] Z. Tian and G. B. Giannakis, "Compressed sensing for wideband cognitive radios," in *Proc. IEEE Int. Conf. on Acoustics, Speech and Signal Process. (ICASSP 2007)*, vol. 4, no. 4, Apr. 2007, pp. 1357–1360.

[82] P. Stoica and Y. Selen, "Model-order selection: a review of information criterion rules," *IEEE Signal Processing Magazine*, Jul. 2004.

[83] I. Akyildiz, B. Lo, and R. Balakrishnan, "Cooperative spectrum sensing in cognitive radio networks: A survey," *Physical Communication*, vol. 4, no. 1, pp. 40–62, 2011.

[84] J. Ma, G. Zhao, and Y. Li, "Soft combination and detection for cooperative spectrum sensing in cognitive radio networks," *IEEE Trans. Wireless Commun.*, vol. 7, no. 11, pp. 4502–4507, Nov. 2008.

[85] M. Chiani and A. Zanella, "Joint distribution of an arbitrary subset of the ordered eigenvalues of wishart matrices," in *Proc. IEEE Int. Symp. on Personal, Indoor and Mobile Radio Commun. (PIMRC 2008)*, 2008.

[86] O. A. Dobre, A. Abdi, Y. Bar-Ness, and W. Su, "Survey of automatic modulation classification techniques: classical approaches and

new trends," *IET Communications*, vol. 1, no. 2, pp. 137–156, Apr. 2007.

[87] A. Alaya-Feki, S. Ben Jemaa, B. Sayrac, P. Houze, and E. Moulines, "Informed spectrum usage in cognitive radio networks: Interference cartography," in *Proc. IEEE Int. Symp. on Personal, Indoor and Mobile Radio Commun. (PIMRC 2008)*, Cannes, France, Sep. 2008.

[88] A. Giorgetti, M. Chiani, D. Dardari, R. Piesiewicz, and G. Bruck, "The cognitive radio paradigm for ultra-wideband systems: The european project EUWB," in *Proc. IEEE Int. Conf. on Ultra-Wideband (ICUWB 2008)*, Sep. 2008, pp. 169–172.

[89] S. Kandeepan, S. Reisenfeld, T. Aysal, D. Lowe, and R. Piesiewicz, "Bayesian tracking in cooperative localization for cognitive radio networks," in *Proc. IEEE Veh. Technol. Conf. (VTC Spring 2009)*, Apr. 2009.

[90] A. Mariani, A. Giorgetti, and M. Chiani, "Energy detector design for cognitive radio applications," in *Proc. IEEE Int. Waveform Diversity & Design Conf. (WDD2010)*, Niagara, Canada, Aug. 2010, pp. 53–57, Invited Paper.

[91] ——, "SNR wall for energy detection with noise power estimation," in *Proc. IEEE Int. Conf. on Commun. (ICC2011)*, Kyoto, Japan, Jun. 2011.

[92] ——, "Effects of noise power estimation on energy detection for cognitive radio applications," *IEEE Trans. Commun.*, vol. 59, no. 12, pp. 3410–3420, Dec. 2011.

[93] ——, "Test of independence for cooperative spectrum sensing with uncalibrated receivers," in *Proc. of IEEE Global Commun. Conf. (GLOBECOM 2012)*, Anaheim, CA, USA.

[94] A. Giorgetti, A. Mariani, and M. Chiani, "Spectrum holes detection by information theoretic criteria," in *Proc. of Int. Conf. on Cognitive Radio and Advanced Spectrum Management*. ACM, 2011.

[95] A. Mariani, S. Kandeepan, A. Giorgetti, and M. Chiani, "Cooperative weighted centroid localization for cognitive radio networks," in *Proc. of IEEE Int. Symp. on Commun. and Inf. Technol. (ISCIT 2012)*, Oct. 2012.

[96] S. Kandeepan, A. Mariani, and A. Giorgetti, "Spectrum sensing and temporal detection with primary user transmission statistics," 2013, submitted to *IEEE Trans. on Wireless Commun.*

[97] EUWB D2.1.1 on "Spectrum Sensing and Monitoring", Mar. 2009.

[98] EUWB D2.2.1 on 'Interference Definition and Specification", Mar. 2009.

[99] EUWB D2.2.2 on "Interference Identification Algorithms", Mar. 2010.

[100] EUWB D2.2.3 on "Interference Classification", Mar. 2010.

[101] EUWB D2.4.2 on "Interference Mitigation Techniques Algorithms", July 2010.

[102] EUWB D2.5.2 on "Networking co?operation and negotiation algorithms", Oct. 2010.

[103] CORASMA D3.2.1, Intermediate Report 1 for Task 3.2, Sensing, May 2011.

[104] CORASMA D3.2.2, Intermediate Report 2 for Task 3.2, Sensing, Nov. 2011.

[105] CORASMA D3.2.3, Intermediate Report 3 for Task 3.2, Sensing, May 2012.

[106] CORASMA D3.2.4, Intermediate Report 4 for Task 3.2, Sensing, Nov. 2012.

[107] SELECT D2.2.1, Signal processing techniques: interim report, July 2011.

[108] SELECT D2.2.2, Signal processing techniques: final report, Apr. 2012.

[109] M. Abramowitz and I. A. Stegun, Eds., *Handbook of Mathematical Functions with Formulas, Graphs, and Mathematical Tables.*, National Bureau of Standards Applied Mathematics Series 55, Washington, D. C.: U. S. Government Printing Office, 1964.

[110] M. Chiani, D. Dardari, and M. K. Simon, "New exponential bounds and approximations for the computation of error probability in fading channels," *IEEE Trans. Wireless Commun.*, vol. 2, no. 4, pp. 840–845, Jul. 2003.

[111] M. Wellens and P. Mahonen, "Lessons learned from an extensive spectrum occupancy measurement campaign and a stochastic duty cycle model," in *Proc. IEEE Int. Conf. Testbeds and Research Infrastructures for the Develop. of Netw. and Communities*, Washington, DC, USA, Apr. 2009.

[112] D. Torrieri, *Principles of Spread-Spectrum Communication Systems*. Springer, 2005.

[113] R. Mills and G. Prescott, "A comparison of various radiometer detection models," *IEEE Trans. Aerosp. Electron. Syst.*, vol. 32, no. 1, pp. 467–473, Jan. 1996.

[114] S. Kandeepan, A. Giorgetti, and M. Chiani, "Periodic spectrum sensing performance and requirements for detecting legacy users with temporal and noise statistics in cognitive radios," in *Proc. IEEE Globecom Broadband Wireless Access Workshop*, Honolulu, HI, USA, Nov./Dec. 2009, pp. 1–6.

[115] D. Torrieri, "The radiometer and its practical implementation," in *Proc. IEEE Military Commun. Conf. (MILCOM 2010)*, Oct.-Nov. 2010, pp. 304–310.

[116] R. Tandra and A. Sahai, "Fundamental limits on detection in low SNR under noise uncertainty," in *Proc. IEEE Int. Conf. on Wireless Netw., Commun. and Mobile Computing*, Maui, HI, USA, Jun. 2005, pp. 464–469.

[117] S. M. Mishra, A. Sahai, and R. W. Brodersen, "Cooperative sensing among cognitive radios," in *Proc. IEEE Int. Conf. on Commun. (ICC 2006)*, Istanbul, Turkey, Jun. 2006, pp. 1658–1663.

[118] B. Shen, L. Huang, C. Zhao, Z. Zhou, and K. Kwak, "Energy detection based spectrum sensing for cognitive radios in noise of uncertain power," in *Proc. IEEE Int. Symp. on Commun. and Inf. Technol. (ISCIT 2008)*, Vientiane, Lao PDR, Oct. 2008, pp. 628–633.

[119] C. Cordeiro, K. Challapali, and D. Birru, "IEEE 802.22: an introduction to the first wireless standard based on cognitive radios," *Journal of Communications*, vol. 1, no. 1, pp. 38–47, Apr. 2006.

[120] C. Stevenson, G. Chouinard, Z. Lei, W. Hu, S. Shellhammer, and W. Caldwell, "IEEE 802.22: The first cognitive radio wireless regional

area network standard," *IEEE Commun. Mag.*, vol. 47, no. 1, pp. 130–138, Jan. 2009.

[121] S. Shellhammer and G. Chouinard, "Spectrum sensing requirements summary," IEEE P802.22-06/0089r1, Tech. Rep., Jun. 2006.

[122] G. Ko, A. A. Franklin, S.-J. You, J.-S. Pak, M.-S. Song, and C.-J. Kim, "Channel management in IEEE 802.22 WRAN systems," *IEEE Commun. Mag.*, vol. 48, no. 9, pp. 88–94, Sep. 2010.

[123] D. A. Shnidman, "Radar detection probabilities and their calculation," *IEEE Trans. Aerosp. Electron. Syst.*, vol. 31, no. 3, pp. 928–950, Jul. 1995.

[124] J. J. Lehtomaki, M. Juntti, and H. Saarnisaari, "CFAR strategies for channelized radiometer," *IEEE Signal Process. Lett.*, vol. 12, issue 1, pp. 13–16, Jan. 2005.

[125] F. Digham, M.-S. Alouini, and M. Simon, "On the energy detection of unknown signals over fading channels," in *Proc. IEEE Int. Conf. on Commun. (ICC'03)*, Anchorage, AK, USA, May 2003, pp. 3575–3579.

[126] M. K. Simon, *Probability distributions involving Gaussian random variables: A handbook for engineers and scientists.* Kluwer Academic Publishers, 2002.

[127] W. Gifford, M. Win, and M. Chiani, "Diversity with practical channel estimation," *IEEE Trans. Wireless Commun.*, vol. 4, no. 4, pp. 1935–1947, Jul. 2005.

[128] S. J. Shellhammer, "Spectrum sensing in IEEE 802.22," in *Proc. IAPR Work. on Cognitive Inf. Process., (CIP 2008)*, Santorini, Greece, Jun. 2008.

[129] S. S. Wilks, "Certain generalizations in the analysis of variance," *Biometrika*, vol. 24, 1932.

[130] A. Giorgetti and M. Chiani, "A new approach to time-of-arrival estimation based on information theoretic criteria," in *Proc. IEEE Int. Conf. on Ultra-Wideband (ICUWB 2011)*, Bologna, Italy, Sep. 2011, pp. 460–464.

[131] M. Abramowitz and I. A. Stegun, *Handbook of Mathematical Functions wih Formulas, Graphs, and Mathematical Tables.* Washington, D.C.: United States Department of Commerce, 1970.

[132] T. W. Anderson, *An introduction to multivariate statistical analysis*, 3rd ed. New York: Wiley, 2003.

[133] D. Cochran, H. Gish, and D. Sinno, "A geometric approach to multiple-channel signal detection," *IEEE Trans. Signal Process.*, vol. 43, no. 9, pp. 2049–2057, Sep. 1995.

[134] M. D. Springer and W. E. Thompson, "The distribution of products of beta, gamma and gaussian random variables," *SIAM Journal on Applied Mathematics*, vol. 18, no. 4, pp. 712–737, Jun. 1970.

[135] B. N. Nagarsenker and M. M. Das, "Exact distibution of sphericity criterion in the complex case and its percentage points," *Communications in statistics*, vol. 4, no. 4, pp. 363–374, 1975.

[136] D. Cabric, S. Mishra, and R. Brodersen, "Implementation issues in spectrum sensing for cognitive radios," in *Proc. Asilomar IEEE Conf. on Signals, Systems and Computers*, vol. 1, Nov. 2004, pp. 772–776.

[137] I. Akyildiz, W.-Y. Lee, M. Vuran, and S. Mohanty, "Next generation/-dynamic spectrum access/cognitive radio wireless networks: A survey," *Communication Networks Journal (Elsevier)*, Sep. 2006.

[138] N. Krasner, "Efficient search methods using energy detectors–maximum probability of detection," *IEEE J. Sel. Areas Commun.*, vol. 4, no. 2, pp. 273–279, Mar. 1986.

[139] S. Kandeepan, R. Piesiewicz, T. C. Aysal, A. R. Biswas, and I. Chlamtac, "Spectrum sensing for cognitive radios with transmission statistics: Considering linear frequency sweeping," *EURASIP J. on Wirel. Commun. and Netw.*, 2010.

[140] H. Sun, W.-Y. Chiu, J. Jiang, A. Nallanathan, and H. V. Poor, "Wideband spectrum sensing with sub-Nyquist sampling in cognitive radios," *IEEE Trans. Signal Process.*, vol. 60, no. 11, pp. 6068–6073, Nov. 2012.

[141] Z. Quan, S. Cui, A. Sayed, and V. Poor, "Optimal multiband joint detection for spectrum sensing in cognitive radio networks," *IEEE Trans. Signal Process.*, vol. 57, no. 3, pp. 1128–1140, Mar. 2009.

[142] A. Taherpour, S. Gazor, and M. Nasiri-Kenari, "Invariant wideband spectrum sensing under unknown variances," *IEEE Trans. Wireless Commun.*, vol. 8, no. 5, May 2009.

[143] A. Coulson, "Blind detection of wideband interference for cognitive radio applications," *EURASIP J. Advances Signal Process.*, pp. 1–12, 2009.

[144] ——, "Blind spectrum sensing using Bayesian sequential testing with dynamic update," in *Proc. IEEE Int. Conf. on Commun. (ICC 2011)*, Kyoto, Japan, Jun. 2011.

[145] J. Font-Segura, G. Vazquez, and J. Riba, "Multi-frequency GLRT spectrum sensing for wideband cognitive radio," in *IEEE Int. Conf. on Commun. (ICC 2011)*, Kyoto, Japan, Jun. 2011.

[146] M. Rashidi, K. Haghighi, A. Owrang, and M. Viberg, "A wideband spectrum sensing method for cognitive radio using sub-nyquist sampling," in *Proc. IEEE Int. Digital Signal Process. and Signal Process. Education Workshop (DSP/SPE 2011)*, Jan. 2011.

[147] S. Liu, J. Shen, R. Zhang, Z. Zhang, and Y. Liu, "Information theoretic criterion-based spectrum sensing for cognitive radio," *IET Communications*, vol. 2, no. 6, pp. 753–762, Feb. 2008.

[148] M. Fujii and Y. Watanabe, "A study on interference detection scheme using AIC for UWB MB-OFDM systems," in *Proc. Int. Workshop on Multi-Carrier Systems Solutions (MC-SS), 2011*, May 2011.

[149] T. Sato and M. Umehira, "A new spectrum sensing scheme using overlap FFT filter-bank for dynamic spectrum access," in *Proc. Int. ICST Conf. on Cognitive Radio Oriented Wireless Netw. and Commun. (CROWNCOM 2011)*, 2011.

[150] H. Akaike, "Information theory and an extention of the maximum likelihood principle," in *Proc. Int. Symp. on Inf. Theory*, 1972, pp. 267–281.

[151] G. Schwarz, "Estimating the dimension of a model," *The annals of statistics*, vol. 6, no. 2, pp. 461–464, 1978.

[152] K. Burnham and D. Anderson, *Model selection and multi-model inference: a practical information-theoretic approach.* Springer, 2002.

[153] J. Rissanen, "An introduction to the mdl principle," 2004. [Online]. Available: www.mdl-research.org

[154] H. Bozdogan, "Akaike's information criterion (AIC): The general theory and its analytical extensions," *Psychometrica*, vol. 52, no. 3, pp. 345–370, 1987.

[155] H. Akaike, "On newer statistical approaches to parameter estimation and structure determination," in *Int. Federation of Automatic Control*, vol. 3, 1978, pp. 1877–1884.

[156] R. Nishii, "Maximum likelihood principle and model selection when the true model is unspecified," *Journal of Multivariate Analysis*, vol. 27, no. 2, pp. 392–403, 1988.

[157] L. C. Zhao, P. R. Krishnaiah, and Z. D. Bai, "On detection of the number of signals when the noise covariance matrix is arbitrary," *Journal of Multivariate Analysis*, vol. 20, no. 1, pp. 26–49, 1986.

[158] A. Giorgetti and M. Chiani, "Time-of-arrival estimation based on information theoretic criteria," *IEEE Trans. Signal Process.*, accepted for publication.

[159] M. H. Hansen and B. Yu, "Model selection and the principle of minimum description length," *Journal of the American Statistical Association*, vol. 96, no. 454, pp. 746–774, 2001.

[160] R. A. Horn and C. R. Johnson, *Matrix analysis*. Cambridge University Press, 1990.

[161] J. G. Proakis, *Digital communications*, 4th ed. New York: McGraw-Hill, 2001.

[162] D. B. Percival and A. T. Walden, *Spectral analysis for physical applications*. Cambridge University Press, 1993.

[163] A. J. Coulson, "Do wireless data signals exhibit spectral autocorrelation?" in *Proc. of IEEE Australian Commun. Theory Workshop (AusCTW 2008)*, 2008.

[164] S. M. Mishra, R. Tandra, and A. Sahai, "The case for multiple sensing," in *Proc. IEEE Annual Allerton Conf. on Commun. Control and Computing*, Sep. 2007.

[165] N. Bulusu, J. Heidemann, and D. Estrin, "GPS-less low-cost outdoor localization for very small devices," *IEEE Personal Commun.*, vol. 7, no. 5, pp. 28–34, Oct. 2000.

[166] J. Blumenthal, R. Grossman, F. Colatowski, and D. Timmermann, "Weighted centroid localization in Zigbee-based sensor networks," in *Proc. IEEE Symp. on Intelligent Signal Process. (WISP 2007)*, Oct. 2007.

[167] R. Behnke, J. Salzmann, R. Grossmann, D. Lieckfeldt, D. Timmermann, and K. Thurow, "Strategies to overcome border area effects of coarse grained localization," in *Proc. IEEE Workshop on Positioning, Navigation and Commun. (WPNC 2009)*, Mar. 2009, pp. 95–102.

[168] C. Laurendeau and M. Barbeau, "Centroid localization on uncooperative nodes in wireless networks using a relative span weighting method," *EURASIP Journal on Wireless Commun. and Networking*, Sep. 2010.

[169] J. Wang, P. Urriza, Y. Han, and D. Cabric, "Weighted centroid localization algorithm: theoretical analysis and distributed implementation," *IEEE Trans. Wireless Commun.*, vol. 10, no. 10, pp. 3404–3413, Oct. 2011.

[170] CEPT, ERC/REC/(70)03 Relating to the use of short range devices (SRD), Aug. 2011.

[171] ACMA, Radiocommunications (Low Interference Potential Devices) Class Licence 2000, Jan. 2009.

[172] S. J. Shellhammer, S. Shankar N, R. Tandra, and J. Tomcik, "Performance of power detector sensors of DTV signals in IEEE 802.22 WRANs," in *Proc. Int. Workshop on Technol. and Policy for Accessing Spectrum (TAPAS'06)*, no. 4. New York, NY, USA: ACM, 2006.